Dissertation

Submitted to the

combined Faculties for the Natural Sciences and for Mathematics

of the Ruperto-Carola University of Heidelberg, Germany

for the degree of

Doctor of Natural Sciences

presented by

MRes in Neuroscience	Evangelia Tasouri
born in	Potamia, Cyprus

Oral examination 20.10.2015

Analysis of the role of primary cilium in the dopaminergic neurogenesis in mouse embryonic midbrain

Referees: Prof. Dr. Hilmar Bading

Prof. Dr. Kerry Lee Tucker

1 Acknowledgements

I would like to take this opportunity to thank first of all my PhD advisor Professor Kerry Lee Tucker for being my mentor these four and a half years. I joined his laboratory at a relatively young age for a PhD degree but he believed in me, he supported me and patiently guided me. Throughout our day to day relationship I grew as a scientist but as a person too. I have truly appreciated that Kerry offered me the chance to co-author reviews and a book chapter with him, and for this I thank him. As the project described in this thesis was a collaborative work, I thank PD Dr. Sandra Blaess and her team at the University of Bonn for the fruitful collaboration and Dr. Christian Gojak for assisting me with the scanning electron microscope. I would also like to thank my doktorvater Prof. Dr. Bading and my two referees, Prof. Dr. Müller and Prof. Dr. Wölfl for taking the time to be members of my PhD committee. I would also like to thank Prof. Dr. Kirsch who offered me to stay in the department also after Kerry had moved away.

I would like to send my heartfelt thanks to my amazing fellow PhD students and post-doc, with whom I have not only shared an office for almost the entire duration of our PhDs but with whom we have built strong friendships. They always knew how to lighten up the atmosphere after an experiment went wrong yet again, how to cheer for me when finally something worked or was published or when I had a good hair day. They were always present when I needed to talk to someone and always happy to share thoughts on science and beyond. Denise, Sabrina and Aline I cannot thank you enough! Richard thanks for being always ready to jump in a philosophical, political, football discussion with me and even though we were usually reaching a dead-end, the trip was more than pleasant and exciting! Thank you for being so tall and kind to help me with the perfusion device and for all the knowledge you tried to push in my little head! I would also like to thank two previous students from our lab, Marc and Kathrin who made my entry in the lab and the german reality very pleasant, but also the last two students of the lab Kang and Rasem for bringing life in the lab when Kerry moved to the US. Many thanks also to Rosanna, who I admire for her positivity, for supporting me whether I needed scientific advice, equipment, or advice for the future.

The fourth floor of the INF 307 was a fun place to work at, with really nice colleagues. I would like to thank Andrea, who was always happy to answer questions, help, provide me her wonderful hippocampal cultures and be present every time I approached her – and there were

many times! As there were too many people that made my everyday life in the lab enjoyable but if I start listing names I will definitely forget someone, I would just like to thank everyone who was a member of the 4th floor, for sharing a hello on the corridor or for always being happy to share equipment and consumables.

My warmest thanks go to my new family, my husband, who even though far away from the biological community, he supported me all the way when I had to spend weekends in the lab, when I was stressing with experiments and writing or when during our dinners I talked about science.

Last but not least, I would like to thank my wonderful family, my brothers and sister-in-law, but especially my parents. Because of them I am where I am today, because of them I am the person who I am, and without them standing by my side throughout every difficulty I encountered and cheering for me for every success, I would have not managed to come so far. I hope I have become a person that they can be proud of.

2 Zusammenfassung

Bei primären Zilien handelt es sich um peitschenartige Strukturen mit einer durchschnittlichen Länge von 1-3 µm, die von der Zellmembran von beinah allen Säugetierzellen in die extrazelluläre Matrix herausragen. In den letzten Jahrzehnten wurde die Tatsache aufgedeckt, dass primäre Zilien unverzichtbar für ein fehlerfreies Funktionieren des Hh- Signalweg sind. Diese Tatsache zeigt weiterhin an, dass primäre Zilien somit auch eine wichtige Rolle in Entwicklungsprozessen spielen.

Dopaminerge Neurone des Mittelhirns sind für die Regulation von sowohl bewussten Bewegungen, als auch für kognitive Funktionen wie Emotionen und Belohnung verantwortlich. Studien haben gezeigt, dass mDA Neurone in einer Anzahl von neuropsychiatrischen als auch neurodegenerativen Krankheiten dysfunktional sind. Es ist heutzutage weithin bekannt, dass der Hh- Signalweg für die Bildung/ Generierung und Spezifizierung der mDA Neurone im ventralen Mittelhirn notwendig ist.

Diese Thesis beschäftigt sich, in Zusammenarbeit mit PD Dr. Sandra Blaess und Ihren Kollegen an der Universität Bonn, mit der Untersuchung der Rolle von primären Zilien bei der Entwicklung der mDA Neurone unter Nutzung zweier Mausmutanten. Diese weisen Defekte in den Genen *Ift88* bzw. *Kif3a* auf, welche wichtig sind für die Bildung und Aufrechterhaltung der primären Zilien. Dies ist das erste Mal, dass die Rolle von primären Zilien in der Schaffung/Erzeugung von mDa betrachtet wird.

Die Untersuchung der konditionellen Inaktivierung von *Ift88* nach E9.0 zeigte sowohl einen fortschreitenden Verlust der primären Zilien an, der bei E10.5 vollendet war, als auch eine signifikante Reduzierung von mDa Vorläuferzellen und mDa Neuronen in späteren Stadien. Dies wurde durch immunohistochemische Färbungen gegen TH- einem typischen Marker für dopaminerge Neurone- und gegen FoxA2, einem Transkriptionsfaktor, der durch Shh induziert und gewöhnlich als ein Marker für die Bodenplatte benutzt wird, gezeigt. Diese Beobachtungen zeigen, dass voll funktionsfähige primäre Zilien für die Strukturierung des ventralen Mittelhirns notwendig sind.

Zusätzlich deckten ISH für *Gli1* und *Gli3* auf, dass im ventralen Mittelhirn von *Ift88* cko Mutanten der Shh- Signalweg inaktiviert war, was auf den Verlust der primären Zilien zurückgeführt wurde. Des Weiteren zeigte die Verwendung eines Mausmodels, in dem Smoothened konstitutiv aktiv war, dass die konstitutive Aktivierung des Shh- Signalweges in diesen Mäusen zu einer Ausweitung der mDa Vorläuferdomäne führte. In der Abwesenheit

von Ift88, und somit in der Abwesenheit von primären Zilien war dies jedoch nicht der Fall. Dies weist darauf hin, das Smo nachgeschaltet von Ift88 aktiv ist.

Überraschenderweise rief die konditionelle Inaktivierung von *Kif3a* einen ähnlichen Phänotyp der mDa hervor. Die Ursache dafür kann möglicherweise darin liegen, dass der Verlust der primären Zilien und die damit verbundene Inaktivierung des Shh- Signalweges in *Kif3a* cko im Vergleich zu *Ift88* cko leicht verzögert ist.

Zusammengefasst decken die Resultate die Bedeutung der Beziehung zwischen primären Zilien und des Shh- Signalweges auf und bestimmen zugleich zum ersten Mal ein wichtiges Fenster, bei welchem beide entscheidend sind für die Induzierung der mDa Neurone.

3 Summary

Primary cilia are whip-like structures, usually 1-3μm long, protruding from the cell membrane of almost all mammalian cells. During the last decades, it has been uncovered that primary cilium is crucial for Hedgehog (Hh) signalling. Its involvement in the appropriate function of Hh signalling pathway indicated by extension its importance in developmental processes.

Midbrain dopaminergic neurons are responsible for the regulation of voluntary movements, as well as for cognitive functions such as emotion and reward. Studies have revealed that midbrain dopaminergic (mDA) neurons are dysfunctional in a number of neuropsychiatric or neurodegenerative diseases. Nowadays it is also widely known that Hh signalling is necessary for the generation and specification of dopaminergic (DA) neurons in the ventral midbrain. This thesis, through a collaboration with PD Dr. Sandra Blaess and her colleagues at the University of Bonn, investigates the role of primary cilia in the development of mDA neurons by using two mouse mutants defective in intraflagellar transport protein 88kDA (*Ift88*) or kinesin family member 3a (*Kif3a)*, two genes important for the genesis and maintenance of the primary cilium. This is the first time that the role of primary cilia in the generation of mDA is examined.

Study of conditional inactivation of *Ift88* after embryonic day (E) 9.0 resulted in a progressive loss of primary cilia that was completed by E10.5 and a significant reduction of both mDA progenitors and mDA neurons at later stages, as observed by immunostainings against tyrosine hydroxylase (TH) – a typical marker for dopaminergic neurons and forkhead box A2 (FoxA2), a transcription factor induced by Sonic hedgehog (Shh) and commonly used as a floor plate marker. These observations show that functional primary cilia are necessary for the patterning of the ventral midbrain. Additionally, *in situ* hybridizations for glioma-associated oncogene 1 and -3 (*Gli1* and *Gli3*) revealed that in the ventral midbrain of *Ift88* knock-down (cko) mutants Shh signalling was inactivated. Shh pathway inactivation was attributed to the loss of primary cilia. Moreover, employment of a mouse model in which *Smoothened* (*Smo*) was constitutively active demonstrated that the constitutive activation of Shh signalling in these mice led to the expansion of the mDA precursor domain. However, this was not the case in the absence of *Ift88*; hence in the absence of primary cilia. This indicates that Smo acts downstream of Ift88 and by extension of primary cilia in Shh signalling. Surprisingly, conditional inactivation of *Kif3a* did not produce a similar phenotype

of the mDA neurons. However, this could be attributed to the slightly delayed loss of primary cilia and the delayed inactivation of Shh signalling in *Kif3a* cko in comparison to *Ift88* cko. Taken together, these results uncover the importance of the relationship between primary cilia and Shh signalling and identify for the first time a crucial window at which the two are critical for the induction of mDA neurons.

4 Table of Contents

5 List of Abbreviations

ADPKD	Autosomal dominant polycystic kidney disease
Aldh1a	Aldehyde dehydrogenase 1a
A/P	Anterior / Posterior
APC	Adenomatous polyposis coli protein
Arl13b	ADP-ribosylation factor-like 13B
ARPKD	Autosomal recessive polycystic kidney disease
BDNF	Brain-derived neurotrophic factor
bHLH	Basic helox-loop-helix
BLBP	Brain Lipid-Binding Protein
BSA	Bovine Serum Albumine
Cbs	cobblestone
cDNA	Copy DNA
CNS	Central Nervous System
cRNA	Copy RNA
DA	Dopaminergic
DAPI	4‘, 6‘- diamidino-2-pheylindol
DAT	Dopamine transporter
D/V	Dorsal / Ventral
DMSO	Dimethylsulfoxide
DNA	Deoxyribonucleic acid
dNTP	Deoxyribonucleotide-triphosphate
Dvl	dishevelled
DTT	dithiothreitol

Dync2h1	Dynein cytoplasmic 2 heavy chain 1
E	Embryonic day
EDTA	Ethylendiamine-tetraacetate
En-1,2	Engrailed -1, -2
ENU	N-ethyl-N-nitrosoura
EtBr	Ethidium Bromide
FGF8	Fibroblast growth factor 8
FoxA2	Forkhead box A2
GAPDH	Glyceraldehyde 3-phosphate dehydrogenase
Gli1, 2, 3	Glioma-associated oncogenes family members 1, 2, 3
$Gli3X^t$	Gli3 extra toes
GSK3β	Glycogen synthase kinase 3β
Hh	Hedgehog
IFT	Intraflagellar transport
IFT88	Intraflagellar transport protein of 88 kDA
Ihh	Indian Hedgehog
Inv	Inversin
JBTS	Joubert-Boltshauser syndrome
KAP-3	Kinesin-associated protein 3
Kif3a	Kinesin-like protein 3a
Lmx1a/b	Lim-homeodomain factor a / b
LRP5	Low density lipoprotein receptor-related protein 5
mDA	Midbrain dopaminergic
MEFs	Mouse embryonic fibroblasts

MRI	Magnetic Resonanse Imaging
mRNA	Messenger Ribonucleic Acid
Msx1	Msh homeobox 1
MTS	Molar Tooth Sign
Ngn2	Neurogenin 2
Nkx6.1	Homeobox protein Nkx6.1
Nurr1	Nuclear receptor related protein 1
O/N	Overnight
Otx2	Orthodenticle homeobox 2
PBS	Phosphate buffered saline
PC-1	Polycystin-1
PC-2	Polycystin-2
PCP	Planar cell polarity
PCR	Polymerase chain reaction
PD	Parkinson’s disease
PDGF	Platelet-derived growth factor
PFA	Paraformaldhehyde
PIPES	Piperazine-N, N‘- bis (2-ethanesulfonic acid)
Pitx3	Paired-like homeodomain 3
PKA	Protein kinase A
PKD	Polycystic kidney disease
RRF	Retrorubral field
RT	Room Temperature
SDS	Sodium dodecyl sulfate

SEM	Scanning electron microscopy
Shh	Sonic Hedgehog
Smo	Smoothened
SNc	Substantia nigra pars compacta
TAE	Tris-acetic acid EDTA-buffer
TEMED	Tetramethylethylenediamine
TH	Tyrosine hydroxylase
Tris	Trimethylsilylsilan
Triton-X	Polyethylene glycol p-(1,1,3,3-tetramethylbutyl)-phenyl-ether
Tween-20	Polyoxyethylen(20)-sorbitan-monolaurate
UV	Ultraviolet
VM	Ventral mesencephalic
VTA	Ventral Tegmented Area
VZ	Ventricular zone
Wnt	Wingless/ Integrated
Wnt 1/ 5a/ 7a	Wingless-related MMTV integration site 1/ 5a/ 7a

6 INTRODUCTION

6.1 Dopaminergic system

6.1.1 Neuroanatomy

Dopamine, a neurotransmitter of the catecholamine family, is present in several areas of the central nervous system (CNS). Classification of dopaminergic (DA) cell groups followed the nomenclature A1-A7 used for the noradrenergic system; hence the DA cell groups followed a classification of A8-A17 (Dahlstrom and Fuxe, 1964). Areas of the hypothalamus such as the posterior hypothalamus, the arcuate nucleus, the zona inserta and the para- and periventricular hypothalamic nucleus consist of DA cell groups. DA neurons also reside in the amacrine cells of the retina and the superficial tufted cells of the olfactory bulb. However, about 75% of all DA neurons in the adult CNS are found in the ventral midbrain (Wallen and Perlmann, 2003). In the human ventral midbrain reside about 400,000 to 600,000 DA neurons whereas in the ventral midbrain of the mouse which is the animal model used in this thesis about 20,000-30,000 can be found (German et al., 1983; Pakkenberg et al., 1991). Studies have shown that these DA neurons are being generated during embryonic development in the floor plate region (Ono et al., 2007), a structure located on the ventral midline of the embryonic neural tube, and they would essentially lead to the formation of three functionally different groups of DA neurons in the mesencephalon known as the A8, A9 and A10 groups. The ventral tegmental area, VTA, is developed from the A10 group whereas the retrorubral field (RRF), which is situated caudal to the VTA as seen in Fig.1, rises from the A8 group. Their neurons play a role in the regulation of emotion and reward as they innervate the ventral striatum and the prefrontal cortex through the mesocorticolimbic system (Tzschentke and Schmidt, 2000). Additionally, it has been shown that abnormal neurotransmission of the mesocorticolimic DA system is linked to the development of drug addiction, depression but also schizophrenia (Robinson and Berridge, 1993; Meyer-Lindenberg et al., 2002). The A9 cluster develops into the substantia nigra pars compacta (SNc) located lateral to the VTA (Fig.1). Neurons from SNc project to the dorsal striatum through the nigrostriatal pathway and their loss is the main pathological hallmark of Parkinson's disease (PD) as their main innervations targets are the basal ganglia controlling motor function, which is impaired in PD patients (Lees et al., 2009; Toulouse and Sullivan, 2008).

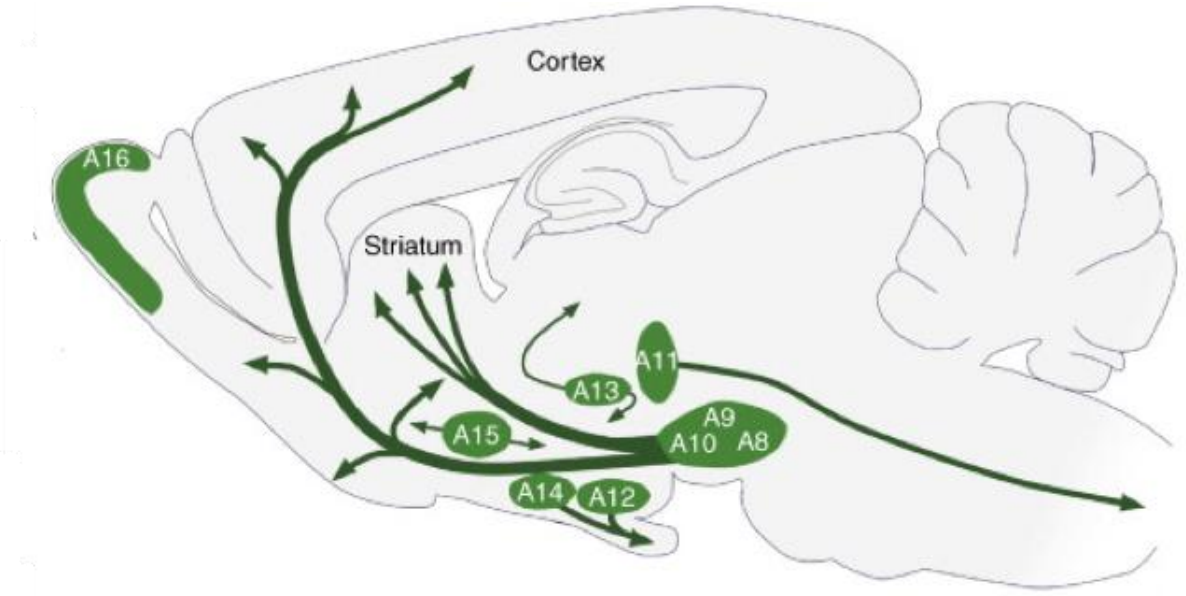

Figure 1. Illustration of the distribution of the DA cell groups A8-A16 and their projections in the adult mouse brain. A8, A9 and A10 give rise to the retrorubral field (RRF), the substantia nigra pars compacta (SNc) and the ventral tegmental area (VTA) respectively. A8 and A10 prject to the prefrontral cortex while neurons from SNc project to the dorsal striatum. (Björklund, A. & Dunnett, S. B., 2007).

The three populations of the DA neurons present in the ventral midbrain have, besides their anatomical and functional differences, also obvious sensitivity differences as for example the SNc DA neurons have been found to be more susceptible to cell death in comparison to the other two groups of mDA populations (Betarbet et al., 2000; McNaught et al., 2004; Alavian et al., 2008). This type of diversity among the DA neuronal populations is most likely due to developmental differences from very early on, but even nowadays the exact molecular mechanisms to which these variabilities can be attributed to are not well known. Furthermore, the only neuronal group out of the three that has been the subject of extensive studies to decipher the molecular mechanisms underlying its development is the SNc DA neurons, due to its involvement in PD. However, even the information generated by these efforts is important for the identification of molecular pathways that may have key roles in the development of not only the SNc DA neurons but of RRF and VTA ventral midbrain neurons as well.

6.1.2 Patterning of ventral mesencephalon

The involvement of midbrain dopaminergic neurons in PD but also other psychiatric disorders has turned the attention of the scientific community to this group of neurons making them the subject of intensive studies the last decades. This has led to the basic understanding of the development of mDA which is done in a timely manner consisting of three major transitions during their generation in the ventricular zone until their migration towards the marginal zone of the neural tube. The first course of events is described by a regionalisation i.e. the appropriate placement of the midbrain within the neural tube in order to give rise to mDA precursors, occurring from around E8.5 to E10.5 in the mouse. This is then followed by the second step, the cell fate determination phase taking place from approximately E10.5 to E12.5 in the mouse and lastly the third phase where the mDA precursors will undergo their final differentiation in which they will acquire their mature mDA neurons phenotype from E12.5 onwards. (Prakash and Wurst, 2006a; Gale and Li, 2008). After this time point, cells that have undergone the final specification step are restricted to that distinct cell fate which will accordingly provide them with a series of unique features such as neuronal and electrophysiological characteristics.

Studies have shown that during gastrulation, signals coming from the Speamann organiser guide the dorsal ectoderm towards a neural fate (Hemmati-Brivanlou and Melton, 1997, Harland, 2000, Liu and Niswander, 2005). As a result of dorsal ectoderm's response to these signals, the neural plate forms with its domains and then closes to form the neural tube (Simon et al., 1995, Puelles, 2001). Gene expression patterns received from both anterior-posterior (A/P) and dorso-ventral (D/V) axes will then direct the ventral mesencephalic (VM) region towards its proper development. Importantly, regulation of these patterns of gene expression and thus organization of the VM area relies on two signaling centers, the midbrain floor plate and the isthmus organizer. Naturally the main characteristic of a signaling center is to be able to reach a certain group of cells through a diffusible signal, which once received will activate transcription of cell-specific genes. From approximately E8.5, Shh protein secreted by the notochord initiates the induction of the floor plate, a structure found along the length of the neural tube (Echelard et al., 1993; Hynes et al., 1995, Mavromatakis et al., 2011). Shh also induces the expression of *FoxA2* from the floor plate, and FoxA2 in its turn acts as a regulator for *Shh* expression in the floor plate (Mavromatakis et al., 2011). It has been recently shown that Shh expression at the VM contributes to all three groups of DA neurons in this region. An 'early medial pool' contributes predominantly to DA neurons in

the VTA, and only few in SNc, whereas a 'later intermediate pool' gives rise mainly to SNc DA neurons as well as the other two DA groups (Joksimovic et al., 2009). Analysis of the factors needed for the induction of mDA done in both human embryonic stem cells and induced pluripotent stem cells from PD patients demonstrated that fibroblast growth factor 8 (FGF8), wingless-type MMTV integration site family member 1 (Wnt1) and Shh alone were essential for this process (Cooper et al., 2010). Shh in cooperation with the transcription factor FoxA2 induce not only the cell fate of mDA neurons but also of other neuronal types present in the ventral midbrain such as motor neurons forming the oculomotor nucleus and neurons consisting the red nucleus. Generation and analysis of Shh null mutant clearly shows the significance Shh signaling has in the induction of the ventral midbrain and its distinct neuronal populations (Chiang et al., 1996). Lack of Shh in these mutants leads to the non-induction of the ventral midbrain and subsequently to the complete abolishment of neurons that would normally be positive for the dopamine marker tyrosine hydroxylase (TH) (Blaess et al., 2006). Moreover, in the same study, conditional inactivation of *Smoothened* (Smo), a receptor that is a component of the Hh signaling, at E9.0 leads to the significant reduction of mDA neurons (Blaess et al., 2006). In addition, it has been shown that Hes1, a transcription factor of the bHLH (basic helix-loop-helix) family, can regulate the number but also the patterning of mDA neurons by suppressing proneural gene expression and also by inducing cell cycle exit (Baek et al., 2006; Ono et al., 2010). Despite the fact that the null Hes1 mutants demonstrated severe defects in neurogenesis, mDA in the ventral midbrain of these mutants were increased in number between E11.5 and E12.5 in comparison to the wild type. However, this transient increase but also the fiber density of mDA neurons was then followed by dramatic reduction from E13.5 and onwards (Kameda et al., 2011).

The second key signaling center, the isthmus organizer, is basically separating the midbrain from the hindbrain. In combination with extrinsic signals from the mesoderm and endogenous regional patterning genes, the isthmus affects the development of both midbrain and hindbrain as it induces specification of the neuronal populations flanking the two brain regions (Liu and Joyner, 2001; Rhinn and Brad, 2001). Expression of two opposing homeodomain transcription factors, Otx2 and Gbx2 defines the position of the isthmus at the midbrain-hindbrain boundary (Martinez-Barbera et al., 2001). At around E8 the isthmus secretes FGF8 which is important for the establishment of the anterior-posterior axis of the brain (Fig.2) (Martinez, 2001). Even though FGF8 is not expressed in the midbrain, an *FGF8* conditional inactivation approach led to the absence of both midbrain and cerebellum at the age of E17.5 (Chi et al., 2003). The same study has shown that this loss was caused by

ectopic cell death in the mesencephalon and metencephalon (Chi et al., 2003). In addition, Crossley et al. had used tissue graft from the isthmus to the caudal forebrain of the chick. Following this, the caudal forebrain mirrored a normal midbrain and FGF8 protein induced ectopic expression of genes that are normally expressed by the isthmus, in the forebrain (Crossley et al., 1996). These two observations together suggest that obviously an isthmus-like center induced in the forebrain influenced the formation of the ectopic midbrain seen at the caudal forebrain and secondly the fact that FGF8 is expressed at the isthmus makes it a molecule of great importance for midbrain development. Furthermore, it has been shown that Otx2 and Gbx2 are not only required for the determination of the correct positioning of the isthmic organizer, they are also necessary for the right positioning of the expression domains of *FGF8* and of other genes expressed at the isthmus organizer but they do not play a role in their induction (Liu and Joyner, 2001; Brodski et al., 2003). Gbx2 and Otx2 are expressed caudally and rostral to the boundary between midbrain-hindbrain, respectively (Joyner et al., 2000). The role of *Otx2* in the right positioning of the expression domains mentioned above and consequently its importance on the regional identity of the midbrain has been stressed by a number of studies demonstrating that ectopic *Otx2* expression in the hindbrain results in a caudal shift of the isthmus-organizer's position. After this caudal shift, the number of mDA neurons was increased. In the same sense, depletion of Otx2 in the midbrain led to a shift towards the rostral neural tube and in this case a decrease in the number of mDA was observed (Brodski et al., 2003). Both findings reveal that Otx2 is also a regulator of the size of the midbrain and show the crucial role of the isthmus organizer (Brodski et al, 2003).

While both Otx2 and Gbx2 help to determine the borders of the isthmus organizer, several transcription factors are secreted from the same signaling center that are also of major importance for the regional specification of the ventral midbrain. This group of transcription factors includes the glycoprotein Wnt1 which is expressed around an area that will later form the caudal midbrain as seen in Fig.2 (Wilkinson et al., 1987; Crossley and Martin, 1995; Adams et al., 2000), the lim-homeodomain factor Lmx1b (Smidt et al., 2000), the two homeodomain transcription factors Engrailed-1 (En1) and -2 (En2) (Davis and Joyner, 1988) and the paired box genes *Pax2* and *Pax5* (Urbanek et al., 1997; Schwarz et al., 1997). It has been demonstrated that Wnt1 together with En1, Otx2 and Gbx2 work to sharpen the boundaries of the expression domain of FGF8 at the isthmus. In the meantime, Pax2 is important for the induction of this domain (Ye et al., 2001). Analyses of either a heterozygous deletion of *En1* (Le Pen et al., 2008) or of *En1* and *En2* double mutants (Liu and Joyner, 2001; Simon et al., 2001) demonstrated significant defects in the ventral midbrain

of these mice as well as a complete loss of mDA neurons. Moreover, the Parkinson-like phenotype observed in these mice was attributed to the cell death of the mDA neuronal population (Le Pen et al., 2008). Most importantly the solid evidence demonstrating that all the transcription factors expressed at the isthmus organizer mentioned above are required for the appropriate specification of the ventral midbrain results from the analyses of mutant mice for *Pax2/Pax5* (Schwarz et al., 1997) and *En1/En2* (Liu and Joyner, 2001; Simon et al., 2001) double mutants, *Wnt1* (Prakash et al., 2006), *Lmx1b* (Smidt et al., 2000) and *Otx2* (Acampora et al., 1995; Ang et al., 1996). These mutant mice exhibit defects in the specification of ventral midbrain as well as partial or even complete loss of mDA neurons. In a more recent study, En1 and En2 have been shown to be necessary for the proliferation of mDA progenitors but also for the later survival of mDA neurons (Alves dos Santos and Schmidt, 2011).

6.1.3 Induction and specification of ventral midbrain dopaminergic neural progenitors

The involvement of mDA neurons in PD has brought them into the focus of several research groups working towards a therapy for this chronic neurodegenerative disorder. Their future potential use in cell replacement therapies has led to the rigorous study of the developmental patterns leading to the correct specification of their identities (Toulouse and Sullivan, 2008; Morizane et al., 2008). Despite the fact that the origin of mDA neural precursors remained for many years uncertain, studies were introducing different brain regions as potential candidates such as the isthmus (Marchand and Poirier, 1983), later on the midbrain basal plate (Hynes et al., 1995a, 1995b) and more recently the diencephalon (Marin et al., 2005). It was not until less than a decade ago that a study parted from the notion that the floor plate consists of non-neurogenic glial type cells (Jessell, 2000; Placzek and Briscoe, 2005) and demonstrated that the floor plate cells in the ventral midbrain have actually neurogenic activity and that mDA neurons originate from these cells (Ono et al., 2007). On the other hand, the same study revealed that the caudal floor plate cells did not seem to share the neurogenic potential of their ventral counterparts. In addition, by ectopically expressing *Otx2* in caudal floor plate cells the authors showed that *Otx2* is not only important for the positioning of the isthmus organizer as thought so far, but it also has a crucial role in determining the anterior identity that would grand the floor plate cells with the neurogenic activity (Ono et al., 2007). Studies

working towards deciphering the specific floor plate cell type which acts as an mDA neural precursor showed that these precursor cells were radial-glial cells in the mouse floor plate and they demonstrated radial glial characteristics as they expressed brain lipid-binding protein (BLBP), a marker expressed by radial glial, and exhibited radial morphology (Bonilla et al., 2008; Hebsgaard et al., 2009). Even though this finding could be considered surprising or strange, it resurfaces the controversial topic of the existence of different identities between the radial glial cells and the radial neuroectodermal stem cells as a recent publication proposes that these two are essentially the same cell type (Kriegstein and Alvarez-Buylla, 2009).

The first step in establishing the appropriate identities of mDA neural precursors occurs with the expression of two transcription factors which act as determinants of mDA neurons, the lim-homeodomain *Lmx1a* and the *msh homeobox 1* (*Msx1*) (Alavian et al., 2008). This step happens at approximately E9.0 in the ventricular zone of the ventral midbrain of the mouse and it begins with the expression of *Shh* that subsequently causes the induction of Lmx1a. Lmx1a in its turn induces the expression of *Msx1*, a homeobox-containing transcription factor which is its downstream effector (Andersson et al., 2006). It has been also shown by overexpressing Lmx1a in the anterior ventral midbrain that ectopic mDA neurons are formed, whereas in the reverse paradigm reduction in Lmx1a expression leads to the loss of mDA in the ventral midbrain (Andersson et al., 2006). Surprisingly expression of Msx1 is only restricted to mDA neural precursors whereas Lmx1a expression is present also in post-mitotic mDA in almost 6-month old mice (Andersson et al., 2006; Zou et al., 2009). Furthermore, Msx1 complements Lmx1a expression by inducing the expression of a proneural gene, namely *Neurogenin 2* (*Ngn2*) that belongs to a family of helix-loop-helix transcription factors, and basically contributing in this way to mDA neurogenesis and consequently to neuronal differentiation. Ngn2 involvement in mDA neurogenesis is supported from studies where *Ngn2* null mutants are characterized by a substantial decrease of mDA as showed by the reduced expression of markers such as Nurr1 and TH (Kele et al., 2006). In addition to this observation, overexpression of *Ngn2* in the dorsal midbrain or in cell cultures resulted in increased levels of neurogenesis, proposing that *Ngn2* plays a proneural role through which it is responsible for providing the generic neuronal characteristics to mDA progenitors but is not necessary for their terminal differentiation (Andersson et al., 2006a; Kim et al., 2007). Analysis of Ngn2 expression levels in mice where *Otx2* was conditionally ablated showed loss of its expression in mDA neural precursors (Vernay et al., 2005). This is in line with the knowledge that *Otx2* induces *Lmx1a* expression in the floor plate, thus it illustrates that the

loss of *Ngn2* expression in *Otx2* mutant mice is an indirect effect that can be attributed to the failure of Lmx1a induction leading to the suppression of *Msx1* expression (Ono et al., 2007). Another homeodomain protein induced by Shh is Nkx6 homeobox 1 (Nkx6.1), whose expression domain lays lateral to the Lmx1a domain, and it is widely expressed in ventral progenitor cells (Vallstedt et al., 2001). Expression of *Nkx6.1* by neural precursor cells will eventually form the cells comprising two nuclei, the oculomotor and the red nucleus (Prakash et al., 2009). Nkx6.1 at E9.0 is co-expressed with Lmx1a but already from E9.5 its expression begins to gradually diminish. At the same time *Msx1* starts to be expressed and basically acts as a repressor for Nkx6.1 at the level of the midline in order to avoid the fusion of midbrain progenitors (Andersson et al., 2006). Moreover, Nurr1, a nuclear receptor of the superfamily of steroid-thyroid hormone activated transcription factors (Law et al., 1992) that is also indirectly induced by Lmx1a- seems to be crucial in the development of mDA neurons. This was supported by studies using *Nurr1* null mutants in which the mDA progenitors, even though initially born, are abolished possibly due to apoptosis. It is also important to note that *Nurr1* is expressed at E10.5 in the ventral midbrain, about one day before TH expression begins (Zetterstrom et al., 1996) and is constantly expressed till adulthood (Backman et al., 1999). It was shown that mDA progenitors that express *Nurr1* are located at the intermediate zone of the ventral midbrain and that by ectopically expressing *Lmx1a* one can expand this Nurr1-expressing area demonstrating that Lmx1a acts as an activator for downstream genes (Andersson et al., 2006). Additionally, *Nurr1* null mutants present halted transcription of genes that are important for the genesis of dopamine such as TH, or for neurotransmission such as the dopamine transporter Dat, suggesting that Nurr1 could act as a transcriptional activator of these genes involved in providing mDA neurons their unique properties (Sakurada et al., 1999). The effects that Nurr1 has on the expression of genes mentioned above such as *TH* or *Dat* are enhanced by an interaction that forms between Nurr1 and the activated form of β-catenin. Through this interaction, transcriptional repressors affecting transcription of these genes are dissociated whereas transcriptional co-activators are recruited (Kitagawa et al., 2007). Pitx3 is a bicoid-related transcription factor that is under the control of Wnt1, and together with Nurr1, has a major role in the differentiation of mDA progenitors. Its expression in the ventral midbrain of the mouse begins from E11.5, even though mDA neurons only begin to express *Pitx3* at a later point once they reach their final ventral destination (Smidt et al., 1997; Smidt et al., 2004). A study showed that Pitx3 could be regulating the expression of *TH* in a subset of mDA neurons since in its absence about half of mDA neurons located at the SN and the VTA are lost (Maxwell et al., 2005). However, this

was contradicted by another publication reporting that in the absence of Pitx3, mDA neurons of the SNc did not express TH whereas mDA neurons of the VTA did (Korotkova et al., 2005). In addition to this, it was also reported that Pitx3 expression is six fold higher in VTA DA neurons than in the ones of SNc (Korotkova et al., 2005). Furthermore, even though Nurr1 and Pitx3 act synergistically, conditional knockout of *Nurr1* results in abolishment of *TH* expression in mDA neurons despite the fact that *Pitx3* and *Aldehyde dehydrogenase 1 family member A1* (*Aldh1a1*), encoding an enzyme involved in synthesis of retinoic acid, were still expressed (Wallen et al., 1999). Another sign of the contribution of both Nurr1 and Pitx3 in mDA differentiation is the finding that they induce the expression of dopamine transporter Dat, one of the traditional markers for mature mDA neurons (Hwang et al., 2009; Jacobs et al., 2009). However, it is worth noting that in *Pitx3* null mutant mice, which lack Pitx3 due to deletions in the *Pitx3* gene, the development of mDA neurons at the ventral midbrain is normal until E12.5. Only at this time point the defects are observed in the lateral population of the ventral mDA that would later form the SNc (Hwang et al., 2003; Nunes et al., 2003; Smidt et al., 2004). Interestingly, the group of DA neurons of the VTA is mostly not affected leading to the assumption that different developmental plans for DA neurons in the SNc and the VTA might exist. Also, it seems that the loss of TH-positive neurons observed in the ventral midbrain is due to neuronal loss instead of an abolished expression of TH mRNA (Hwang et al., 2003; Nunes et al., 2003; Smidt et al., 2004). This could be explained by the notion mentioned in the current literature that suggests that SNc mDA show higher sensitivity to neurodegeneration than those found in the VTA region. Recently, Pitx3 was reported to induce expression *of brain-derived neurotrophic factor* (*BDNF*) in the mDA neurons of the SNc and that lack of BDNF expression in *Pitx3* null mice is linked to the loss of neurons laying in the SNc region (Peng et al., 2011). A few years back, a study reported also a link between *BDNF* and *Nurr1*, as the former has been identified as a target gene of the latter (Volpicelli et al., 2007). Taken together, all these data demonstrate that Nurr1 and Pitx3 act cooperatively by controlling the expression of genes involved in DA neurotransmission and of neurotrophic factors such as BDNF, in order to ensure the survival of DA neurons of the ventral midbrain and the establishment of the appropriate mature DA neurotransmitter phenotype.

A pathway that has been long known to be implicated in the induction of mDA is the Shh signalling as observed in Fig.2. Shh signalling, as aforementioned, induces the expression a *FoxA2* – a transcriptional regulator and a widely used floor plate marker. Gli1, a downstream effector is basically the modulator of FoxA2 expression since Gli1 is essentially also a

readout for the activation of Shh signalling. In response to Shh signaling, Gli2A (Gli2 activator) promotes up-regulation of Gli1 which is necessary for the neurogenesis of mDA neurons. At the same time, Gli3R (Gli3 repressor) is being suppressed by Shh, hence it can act as a readout for inactivation of Shh signalling.

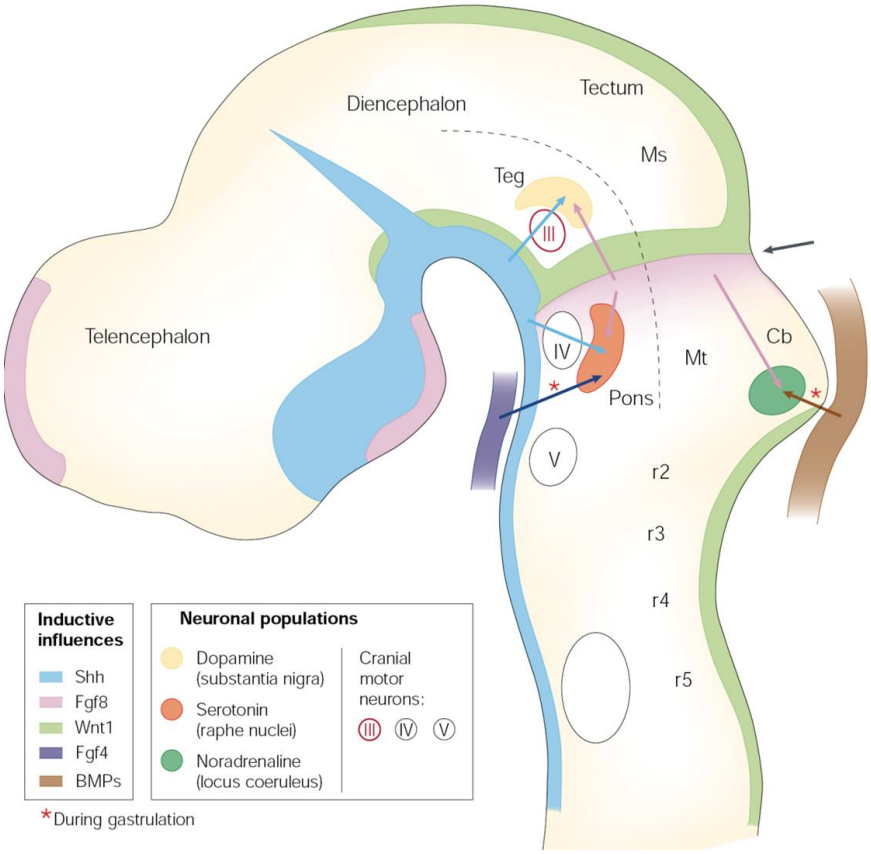

Figure 2. Sagittal view of E11.5 mouse neural tube. Anterior is to the left and the top arrow on the right side indicates the midbrain/hindbrain borders. Expression of Shh, Fgf8, Wnt1, Fgf4 and BMPs and their inductive influences in the developing mouse brain are shown in blue, pink, green, dark blue and brown respectively (Wurst W. & Bally-Cuif L., 2001).

In addition, suppression of Gli3R enables as well the relief of the repression of expression of *FGF8* (Blaess et al., 2006). The key role that Gli2 has in inducing ventral phenotypes is clearly demonstrated through the *Gli2* homozygous null mutants that exhibit defective neurogenesis of mDA in the ventral midbrain and also through the double *Gli1/Gli2* mutants who display an even more dramatic phenotype (Park et al., 2000). FoxA2 in its part has been reported to act as a regulator for *Ngn2* expression but also to have a role in the maintenance of *Lmx1a* and *Lmx1a* expression levels, which consequently promotes DA neurogenesis in the ventral midbrain. Both *FoxA1* and *FoxA2* are expressed in the ventral midbrain and during development their expression can also be detected in DA neurons undergoing

differentiation (Ferri et al., 2007; Lin et al., 2009). FoxA2 is believed to be a regulator of Shh expression in the ventral neural tube as its expression begins earlier than that of Shh, thus establishing a back and forth feedback relationship between the two (Echelard et al., 1993). The crucial role that FoxA2 has is highlighted in a recent study suggesting that in fact Shh is required for the generation of the lateral floor plate, whereas FoxA2 is essential for the specification of the entire floor plate, medial and lateral, in a Shh-dependent and independent manner (Bayly et al., 2012). FoxA2 induction by Shh functions together with Lmx1a and Lmx1b for the generation of DA neurons from the ventral floor plate, which was expected as it was already known that both Shh and FoxA2 act as positive regulators of the expression of these two lim-homeodomain containing transcription factors (Nakatani et al., 2010). Unfortunately, the study of *FoxA2* mutant mice in order to decipher the exact roles that FoxA2 has and its significance in DA induction, cannot be concluded as these mutant mice do not survive later than E9.5 due to their defective floor plate and notochord development (Ang and Rossant, 1994; Sasaki and Hogan, 1994).

Another family of proteins that play a role in the induction of DA neurons has been more recently recognized, and its exact involvement is under the scope of many research groups, is the Wnt family of secreted glycoproteins. As mentioned earlier in this section *Wnt1* is expressed in the isthmus organizer (Fig.2), hence *Wnt1* null mice lack most of the midbrain and its DA neurons (McMahon and Bradley, 1990), at approximately E9.5 in mice but is also present during the later development of the midbrain (Wilkinson et al., 1987), as are also other Wnt-family members (Rawal et al, 2006; Andersson et al., 2008). An *in vitro* study found that expression of *Wnt1*, *-3a* and *-5a*, was differentially regulated during midbrain development. Wnt1 was reported to increase the proliferation of mDA neural precursors and subsequently to increase the number of DA neurons resulting from these. Wnt5a seemed to be important for the acquisition of the appropriate DA phenotype necessary to increase the number of DA neurons and even though Wnt3a promoted proliferation of mDA neural precursors, it later inhibited their final differentiation into DA neurons (Castelo-Branco et al., 2003). Wnt5 has also been suggested to be responsible for the mediation of the DA inductive activity of the glia at the region of the ventral midbrain (Castelo-Branco et al., 2006). In support of these data, a study demonstrated *in vivo* that Wnt5 is involved in the attainment of the DA phenotype in mDA neural precursors (Andresson et al., 2008) and a second report proposed that its implication in the process of mDA neurons differentiation is facilitated through Rac1 guanosine exchange factor, T-cell lymphoma invasion and metastasis 1 (Tiam 1) (Cajanek et al., 2013). A more recent investigation of *Wnt1* null mice revealed that mDA

neural precursors are developed in the midbrain of these mice, however these precursors they neither proliferate nor differentiate as they are expected. The few DA neurons that manage to complete their final differentiation step are subsequently lost (Prakash et al., 2006). In addition to these three members of the Wnt family, the generation of *Wnt2* null mutants identifies Wnt2 as another regulator of the proliferation of mDA neural precursors in the ventral midbrain since these mutants exhibit reduced DA neurogenesis (Sousa et al., 2010). Even more indications highlighting the key role of Wnt signalling in DA neurogenesis arise from the study of Wnt receptors low density lipoprotein receptor-related protein 6 (LRP6), Frizzled3 and -6. Loss of these receptors results in the best situation in developmental abnormalities similar to the ones observed in *Wnt1* null mice, or in an almost completely structurally impaired midbrain (Pinson et al., 2000; Castelo-Branco et al., 2010; Stuebner et al., 2010). Moreover, specific inactivation of β-catenin, a protein acting as an intracellular signal transducer necessary in the canonical Wnt signalling, also mirrors the phenotype observed in *Wnt1* mutants where the midbrain-hindbrain boundary is defective (Chilov et al., 2010). This finding clearly suggests that Wnt1 possibly functions through β-catenin during development of both midbrain and hindbrain. Another mutant demonstrating similar phenotype at the ventral midbrain with the one observed in *Wnt1* null mutants, is the *En1/En2* double knockout mouse, proposing that loss of *En* expression may be responsible for the phenotype of *Wnt1* mutants (McMahon et al., 1992). A later study confirmed this relationship between *En* expression and Wnt1 by using solely En1 to rescue the defective midbrain phenotype seen in *Wnt1* null mutants (Danielian and McMahon, 1996). It was already known that expression of both *En1* and *En2* begins approximately at E8.0, hence around the same time as *Wnt1* expression begins in the ventral mesencephalon, and that by E12 expression of all three domains is restricted (Davis and Joyner, 1988). The study of Danielian and McMahon revealed that a knock-in of *Wnt1* into the *En1* expression domain can expand the *Wnt1* expression in ventro-rostral but also ventro-caudal direction (Danielian and McMahon, 1996). This expansion of *Wnt1* expression leads to the subsequent expansion of the DA population of the most ventral-rostral region (Panhuysen et al., 2004), which is the one giving rise to the SNc. Therefore, these observations conclude that the most influenced by Wnt1 DA cell group is the SNc. Taking into consideration that FGF8 has also been involved in the regulation of *En1* expression in the ventral midbrain (Lahti et al., 2012) one could hypothesise that this could be done by Wnt1 induction. Additional results published recently describe a link between FGF8 and Wnt signalling (Chilov et al., 2010), adding to the speculation that an autoregulatory loop could possibly exist in which *En1/En2* expression is

induced by Wnt1, which was previously induced by FGF8. The transcription factors Lmx1a and Lmx1b could be involved in this loop as by regulating *Wnt1* expression they essentially affect the proliferation of mDA neural precursors of the ventral midbrain (Yan et al., 2011).

6.1.4 The antagonizing relationship of Shh and Wnt signalling pathways

Not long ago, a study was published describing interplay between Shh and Wnt signalling pathways which occurs through an antagonizing relationship between the two. The authors proposed that Wnt/β-catenin signalling is necessary for antagonizing Shh and through that enabling the induction of DA progenitor markers and hence the promotion of dopaminergic neurogenesis (Joksimovic et al., 2009b). Even though initially one of the findings of this study- i.e. Shh has an inhibitory role in the production of DA neurons and proliferation, was unexpected, the authors went on to explain that by proposing that Shh is necessary early on for the formation of the mDA neural precursor pool, they indicate that once this pool has been formed Wnt/β-catenin comes into play by suppressing Shh expression levels, in order to allow DA neurogenesis to occur. Moreover, this study also demonstrated that Wnt signalling is important for the induction of both Otx2 and Lmx1a (Joksimovic et al., 2009b). In addition to the speculation discussed above regarding the existence of an autoregulatory loop between Wnt1, FGF8 and En1/En2, recent evidence argues about another autoregulatory loop being present during mDA neurogenesis- this time between Wnt1 and Lmx1a- which regulates Otx2 expression through β-catenin (Chung et al., 2009). Additionally, another publication demonstrated that Otx2 by regulating Wnt1 manages to affect the proliferation of mDA neural precursors (Omodei et al., 2008); hence suggesting that an additional feedback loop could exist between these proteins. However, the whole topic of Shh and Wnt signalling acting in an antagonistic way is still a controversial one among the scientific community. Another publication contradicts this antagonistic role of Wnt signalling by suggesting that in fact the Wnt1-Lmx1a and Shh-FoxA2 loops regulate mDA neurogenesis in a synergistic way (Chung et al., 2009). A year later another paper (Tang et al., 2010) emerged supporting the theory that Joksimovic et al. (2009b) first proposed regarding the antagonistic relationship between the two pathways. Moreover, the importance of the Wnt/β-catenin signalling was also shown by studies showing that a stable β-catenin in the neural precursors, after the suppression of GSK3β, of the ventral midbrain correlated with an increased differentiation of mDA (Castelo-Branco et al., 2004; Tang et al., 2009). All these findings indicate the role that

Wnt signalling has in inducing mDA but also highlight the significance of the interplay between Wnt and Shh signalling for mDA neurogenesis.

6.1.5 Clinical implications

The main reason why so much focus has been thrown into researching the development of the midbrain dopaminergic system in the last decades, is the involvement of this system in several diseases, with the most widely known being PD. Identification of the exact role of the midbrain DA system in neurological and psychiatric disorders such as PD, schizophrenia and addiction will open new horizons in the search of new drug targets but also in novel therapies such as the use of stem cells.

6.1.5.1 Parkinson's disease

PD is a chronic neurodegenerative disorder characterized by tremor, bradykinesia, rigidity and postural instability that gradually worsen as the disease progresses (Pankratz et al., 2009). Even though PD is a disease predominantly linked with problematic body movements, non-motor symptoms are also present such as gastrointestinal complications, sleep difficulties, anxiety and depression (Olanow and Tatton, 1999). It is estimated that approximately seven to ten million people worldwide are affected by PD, with about 1.5 million people in Europe alone. The average age of onset is around 55 years and as the world population ages the incidence of PD is expected to increase in the recent decades. Due to the nature of this devastating disease, the patients need constant care as the PD manifestations worsen and their living standard is severely affected. The economic consequences and social burden that the societies have to cope with are considerable. Although PD has been and still is extensively studied its exact etiology is not entirely decoded and consequently a cure is still not available. Additionally, there is only a limited number of drugs used to ameliorate the symptoms but none of them halts the progression of the disease.

The main pathological feature of PD is the loss of dopaminergic neurons in the SNc that accounts for the subsequent reduction of the dopaminergic population in the striatum. Nowadays, the fast growing knowledge and usage of stem cell therapy is a promising approach in the search for a cure. The theory behind the work of many groups working towards this goal is to transform fibroblasts collected from PD patients into induced

pluripotent stem cells in order to be able to differentiate them *in vitro* into DA neurons that would later be transplanted into the same patient to replace the degenerated neurons of the SNc (Kim et al., 2011; Pang et al., 2011). The difficulties this kind of research is facing lie in the identification of the necessary factors that would enable induction of pluripotency that would let proper differentiation into mDA neurons to occur.

6.2 Cilia: The cell's antennae

6.2.1 Ultrastructure of motile and primary cilia

Cilia are short, usually 1-3μm but sometimes up to 10μm long and 250 nm wide, microtubule-based organelles protruding from the plasma membrane of unicellular organisms, from almost all cells in vertebrates and to a very limited extent from plants and fungi. Etymologically, the word 'cilium' originates from latin and means eyelid or by association an eyelash, perfectly fitting not only to the hair-like structure that cilia have but also to their wave-like movement (Tucker, K. L. and Caspary T. 2013). Even though an organelle is traditionally bound by a plasma membrane and cilia lack this feature, they are considered as one since they form a spatially distinct compartment keeping their contents separated from the rest of the cell. Primary cilia consist of the basal body, which originates from the mother centriole that functions as microtubule-organizing center underneath the plasma membrane, and a microtubule-based structure called the axoneme (Davenport and Yoder, 2005). Recent studies have reported involvement of primary cilia in cell proliferation and differentiation during development due to its association with the centrosome and in projection with cell cycle (Pan and Snell, 2007, Pugacheva et al., 2007, Spektor et al., 2007). In addition, it has been also shown that primary cilia have the ability to sense extracellular signals that regulate brain development (Eggenschwiler and Anderson, 2007, Gerdes et al., 2009).

According to their ultrastructure and function, cilia can be divided into two classes which share basic features but significantly differ in both areas. Both classes of cilia have a centrosome, also known as the basal body which acts as a ciliary anchor within the cytoplasm (Davis et al, 2006). Motile cilia bear a '9+2' microtubule-based axoneme, in which nine microtubule doublets are arranged in a circular pattern surrounding a central doublet as seen

in the scheme of Fig.3. Protein-protein interactions between the central and the outer doublets facilitate the characteristic wave-like movement that cilia exhibit.

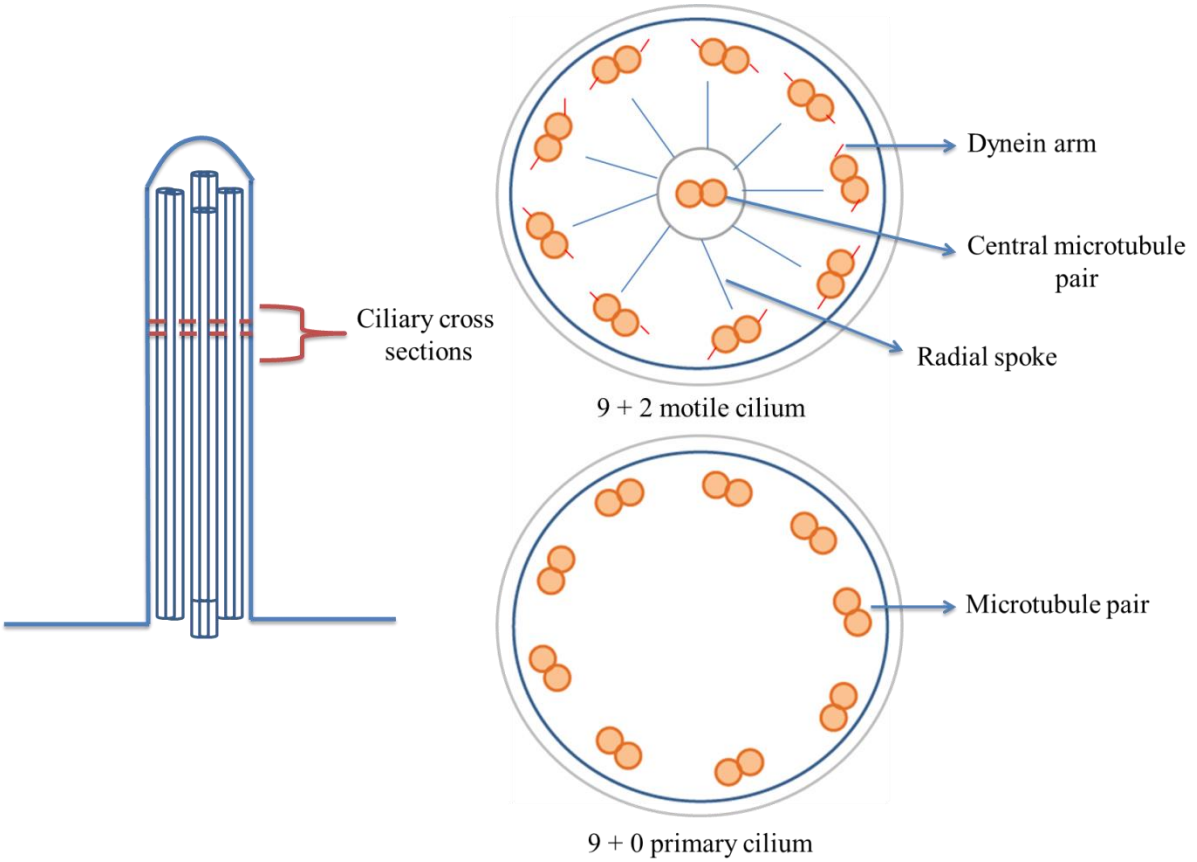

Figure 3. Ciliary cross sections demonstrating the ultrastructure of 9+2 motile cilium and 9+0 primary cilium axoneme. The noticeable structural differences determine the nature of each cilium as the motile cilium (top right) consists of a central microtubule pair surrounded by another 9 pairs of microtubules (9+2). Primary cilium (bottom right) lacks the central microtubule doublet (9+0), as well as the dynein arms seen in the motile cilium.

In areas such as the trachea, bronchi, brain ventricles, oviduct and paranasal sinuses this beating of cilia generates a rhythmic current of overlying fluid or mucus. On the other hand, primary cilia seen in the lower scheme of Fig.3 - which comprise the second class of cilia- have a '9+0' arrangement, as they lack the central doublet. As a result, primary cilia were thought until recently to be completely non-motile. However, it has been shown not long ago that although primary cilia are not characterized by the 'whip-like' beating, they do generate a rotatory movement at the embryonic node leading in liquid flow over short distance (Nonaka et al, 1998). Furthermore, this fluid movement in the embryonic node has a critical role for left-right asymmetry (Essner et al., 2002; McGrath et al., 2003; Essner et al., 2005).

6.2.2 Primary cilia and Intraflagellar Transport (IFT)

Both ciliary categories depend upon a microtubule-based system, namely intraflagellar transport (IFT) for maintenance of the axoneme but also for transport of protein cargo in and out of the cilium (Scholey, 2003). Not unlike axonal transport, IFT utilizes kinesin-II-based and dynein motors depicted in Fig.4 for anterograde and retrograde protein transport, respectively. Kinesin-II is a heterotrimeric motor composed of two distinct motor subunits, Kif3a and Kif3b, and an accessory 'KAP-3' (Kinesin-associated protein 3) subunit (Scholey, 1996). Dynein motor on the other hand consists of light Dync2l1 and heavy Dync2h1 chains (Scholey et al., 2003). Interaction between the transport motors and the protein cargo is facilitated by IFT scaffolding proteins which are named after their protein sizes as shown in Fig.4, e.g. Ift88, Ift172. IFT proteins are divided into two classes, A and B, associated with retro- and anterograde transport, respectively (Scholey, 2003). These proteins are necessary for the assembly and maintenance of the cilium. As the cilium itself lacks the machinery needed for protein synthesis, they are synthesized in the cell body and from there transported into the cilium.

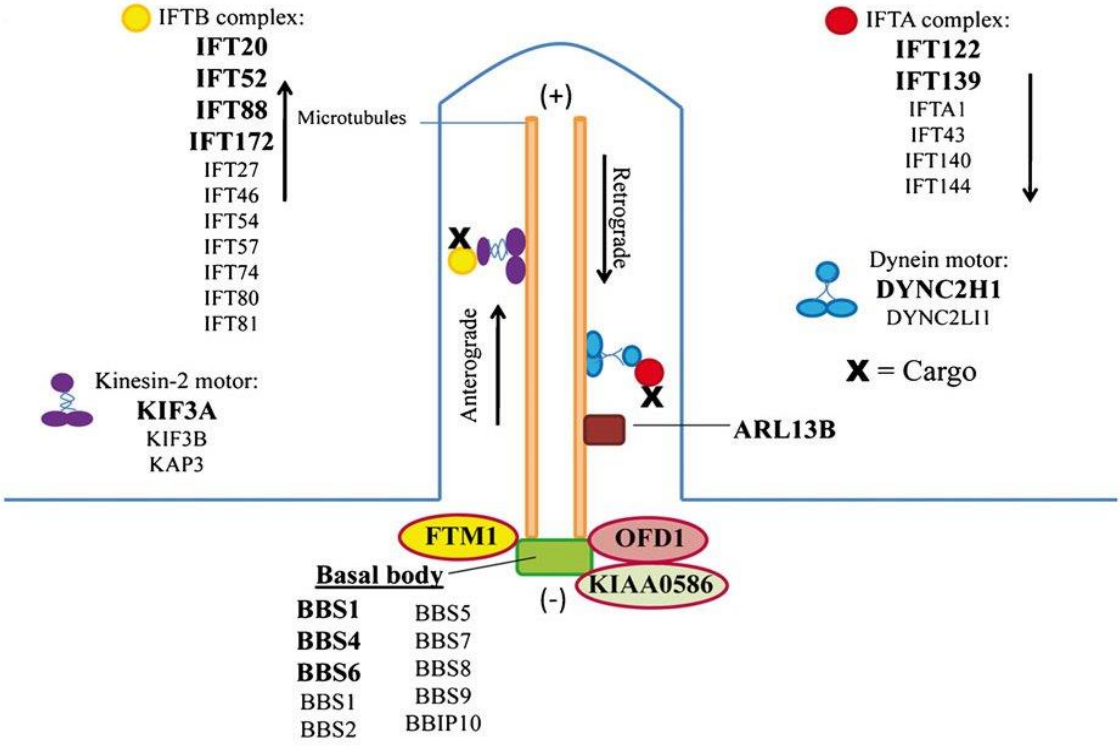

Figure 4. Distribution of proteins localized to the axoneme and/or basal body of the primary cilium. Ciliary proteins members of the IFTA and IFTB complexes are listed respectively. Protein members of kinesin-2 and dynein motors involved in anterograde and retrograde transport

respectively are also listed. Interaction between the protein cargo and the kinesin-2 and dynein motors occurs through the respective IFT scaffolding protein members of the IFTA and IFTB complexes. (Tasouri and Tucker, 2011).

Defects in anterograde transport caused by mutations in protein members of the IFTB complex lead to loss of primary cilia (Follit et al., 2009). On the contrary, mutations on proteins of the IFTA complex disrupt retrograde transport and result in the swelling of primary cilia as the protein cargo accumulates in the cilium (Ocbina and Anderson, 2008). Once the protein cargo reaches the tip of the cilium, a remodeling of the IFT complex occurs through which dynein motor now enters the IFT complex and transports the cargo to the base of the cilium. A study showed that Ift20, an IFT protein member of the IFTB complex, is also found at the Golgi apparatus suggesting that this could reveal the link between the assembly of cilia and vesicle trafficking (Follit et al., 2006).

6.2.3 Hedgehog (Hh) signaling

A plethora of papers in the last decade reveal the importance of primary cilia, especially during developmental processes. This came as a surprise as until then primary cilia were considered ‘vestigial organelles’ because they lacked the central doublet forbidding them to have the characteristic wave-like beat that motile cilia exhibit. Nowadays, primary cilia have been found to be involved in the development of organs of the central nervous system, skeletal system, circulatory system, of the liver, the pancreas and ovaries to name a few (for a detailed review see (Tasouri and Tucker, 2011). Furthermore, several medical syndromes now grouped under the name ‘ciliopathies’ have been linked to proteins found in the cilium or at its basal body, such as Joubert, Bardet-Biedl, Meckel-Gruber syndromes and polycystic kidney disease (PKD) (Badano et al. 2006).

The significance of primary cilia became solid in the scientific community when it was uncovered that all three ligands of the Hh family, namely Sonic Hedgehog (Shh), Indian Hedgehog (Ihh) and Desert Hedgehog (Dhh) bind to the same receptor called Patched1 (Ptch1) which is found inside the primary cilium. In the absence of an Hh ligand, Ptch1 is localized to the primary cilium and represses localization of its co-receptor, Smoo, to the membrane (Fig.5A). As the glioma-associated oncogenes (Gli) are essential mediators in the Shh signaling cascade, inhibition of Smoothened results in the proteolytic cleavage of Gli family member Gli3. Gli3R transcriptional repressor is formed inhibiting the transcription of

Shh target genes. Another Gli family member, namely Gli2, is proteolytically cleaved to a repressor form, but to a lesser extent.

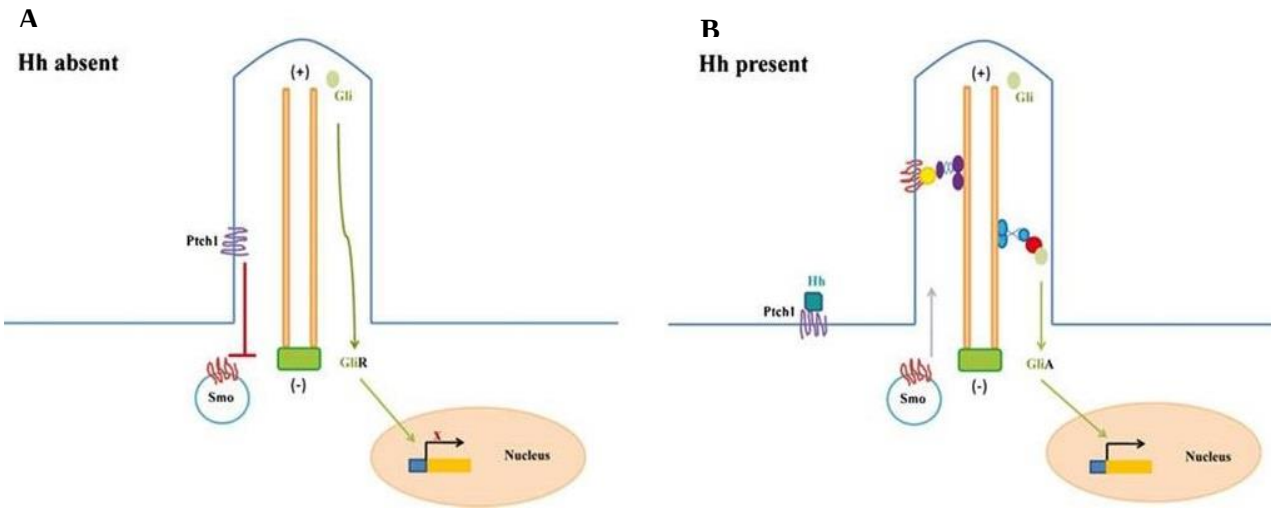

Figure 5. The relationship between primary cilium and Hh signaling. **A.** Distribution of proteins in the absence of Hh signaling. In the absence of Hh ligand, Patched1 (Ptch1) suppresses its co-receptor Smoothened (Smo). **B.** Distribution of proteins in the presence of Hh signaling. In the presence of Hh ligand, Ptch1 relieves the suppression of Smo which then moves into the primary cilium and activates a signaling cascade. (Tasouri and Tucker, 2011).

Upon ligand binding, Patched1 translocates out of the cilium therefore relieving inhibition of Smoothened. Smoothened can then enter the primary cilium and activate a signaling cascade that promotes the formation of Gli2 activator, Gli2A, and to a lesser extent Gli3A, while inhibiting formation of the repressor forms (Fig.5B). Gli2A then enters the nucleus where it interacts with DNA through its zinc-finger DNA-binding motif, resulting in the transcription of Shh target genes such as *Gli1*. Gli1 lacks the N-terminal repression domain and therefore it can only function as a transcriptional activator making it an indicator of Shh signaling levels. If Gli1 levels are high, Shh pathway is active (Hui and Angers, 2011).

A number of studies done in mouse and chick spinal cord have identified Hh signaling as a morphogen of vertebrate nervous system as its ligands bear the characteristics of a morphogen. Shh, expressed by the notochord and the ventral floor plate exhibits all the features of a morphogen, namely: it acts through a concentration-dependent fashion at a distance from the source but it can also directly act on the recipient cells in order to specify different cellular identities (Echelard et al. 1993; Krauss et al. 1993; Roelink et al. 1994). It has been shown that Shh plays a major role in the appropriate patterning (Dessaud et al., 2008) of various tissues during embryonic development and in the formation of digits in the limb bud (Echelard et al., 1993; Roelink et al., 1995). Studies have also revealed that Hh

signaling in zebrafish is also dependent on functional IFT as zebrafish lacking maternal and zygotic *Ift88* display abnormal signaling in the neural tube and somites (Huang et al., 2009). However, patterning defects observed showed differences between the two different models. In zebrafish *Ift88* mutants only the cell fates of e.g. V3 interneuron progenitors that need high levels of Hh were affected, whereas the somites and cell types in the neural tube underwent specification and were expanded as they only require low levels of Hh (Huang et al., 2009).

Generally, loss of genes encoding proteins involved in Shh signaling lead to dramatic morphological phenotypes such as holoprosencephaly, cyclopia and defective axial skeleton, while as expected the floor plate cannot be established due to low or no levels of Shh expression. As a result of the abnormal morphology of the floor plate, induction of the ventral cell types fails resulting in an entirely dorsalized neural tube (Chiang et al., 1996). In the ventral midbrain, but also in ventral spinal cord, Shh affects induction of floor plate and the expression of *FoxA2* (Blaess et al., 2011). Additionally, an examination of *Smo* mutant embryos showed that their phenotype was worse than the one observed in *Shh* mutant embryos as both Shh and Indian hedgehog pathways were inactivated (Zhang et al., 2001).

Forward genetic screens, such as ENU-mutagenesis screen, led to the identification of several mutants exhibiting morphological and patterning phenotypes due to defective Hh signaling, such as loss of the ventral types in the neural tube that their specification is normally dependent upon high level of Shh (Huangfu et al., 2003). These mutants demonstrated mutations in genes encoding proteins involved in the IFT, including protein members of the IFT-B complex responsible for the anterograde transport of protein cargo inside the primary cilium. *Ift172* and *Ift88* were two of the genes found to be disrupted in this study (Huangfu et al., 2003; Huangfu and Anderson 2005). Double mutants for one of the IFT-B proteins, such as *Ift88*, and one of the components of the Shh signaling such as *Smo*, show similar phenotypes to the ones observed in single IFT mutants. This observation demonstrates the importance of primary cilia in Shh signaling pathway. A number of studies showed that in the absence of primary cilia, Gli3R and Gli2A cannot form (Liu et al., 2005; Huangfu and Anderson, 2005; Obcina and Anderson, 2008). In addition, disruption of genes encoding motors implicated in IFT such as Kinesin-2 in *Kif3a* mutants resulted in patterning defects attributed to abnormal Shh signaling caused by the loss of primary cilia (Huangfu et al., 2003; Zhou et al., 2009). Furthermore, detailed analysis of *cobblestone* (*cbs*) mutant- a hypomorphic allele of the *Ift88* gene uncovered by an ENU-mutagenesis screen- showed a pleiotropic phenotype including defects in forebrain development such as defects in the formation of dorsomedial telencephalic structures and relaxation of both dorsal-ventral and

rostral-caudal compartmental boundaries (Willaredt et al., 2008). These mutants were characterized by the formation of rosette-shaped heterotopias from which the name cobblestone derived. The authors also showed that targets of Shh signaling were disturbed in the forebrain of *cbs* mutants but also that phenotypes such as polydactyly mirrored the ones observed in *Gli3X*^{t} mutants (Willaredt et al., 2008).

6.2.4 Wnt signaling

As the importance of primary cilia in Hh signaling has been highlighted in the last decades, interest was raised in their possible involvement in other signaling pathways as well. Most of the research focus was thrown into deciphering the relationship between primary cilia and Wnt signaling but despite the considerable work done so far it still remains unresolved. β-catenin-dependent Wnt pathway acts as a regulator of cell fate and proliferation in the nervous system (Angers and Moon, 2009), while planar cell polarity (PCP) Wnt signaling is responsible for the correct orientation of cell sheets by controlling for example the cell movements during convergent extension in order to facilitate the appropriate closure of the neural tube (Tissir and Goffinet, 2010).

Using a number of knock-down of different proteins associated with cilia in culture and in zebrafish embryos, many research groups have observed an upregulation of canonical Wnt signaling while non-canonical Wnt signaling pathway seemed to be disrupted (Ross et al., 2005; Wiens et al., 2010). This finding led the scientists to believe that primary cilium could function as a molecular switch between canonical and non-canonical Wnt signaling pathways. More specifically it has been suggested that inversin acting in the cilium (Watanabe et al., 2003) suppresses canonical Wnt (Fig.6B) signaling during kidney morphogenesis (Simons et al., 2005). Other publications report that mice deficient in *Ift88* or *Kif3a* displayed up-regulation of Wnt signaling (Corbit et al., 2008), while studies in zebrafish and cell culture revealed that proteins implicated in the Bardet-Biedl Syndrome (BBS) stabilized b-catenin causing an increase in the expression of canonical Wnt pathway target genes (Gerdes et al., 2007). Moreover, mouse models in which IFT proteins are mutated do not exhibit the characteristic phenotypes observed in Wnt pathway mutants such as abnormal gastrulation and early patterning defects (Barrow et al., 2007). Reports on non-canonical Wnt signaling mutants show failure of the neural tube closure whereas the IFT mutants are characterized by a fairly normal neural patterning (Greene et al., 1998; Curtin et

al., 2003). Additionally, even though zebrafish mutants lacking both maternal and zygotic *Ift88* were characterized by defective Hh signaling pathway, the same mutants do not demonstrate any disruption in processes linked to abnormal non-canonical Wnt signaling, such as the convergent extension (Huang and Schier, 2009). Moreover, the authors of this study proposed that the two structures that form the primary cilium, the axoneme and the basal body, might not function together regarding the regulation of both canonical and non-canonical Wnt pathway as in both *Ift88* and *Kif3a* mutants in which non-canonical Wnt signaling activity is normal the basal body is still present (Corbit et al., 2008). Interestingly these findings have been questioned as *in vivo* studies of canonical Wnt activity in mouse models that were mutant for proteins found in the primary cilium such as *Ift88, Ift172, Kif3a* or *Dync2h1* reported no changes in the levels of Wnt expression (Ocbina et al., 2009). Another study examining mouse embryos lacking the IFT-A protein, Tct21b or Ift139 came to the same conclusion, since the embryos displayed phenotypes coinciding with an active Hh signaling but did not exhibit any alterations in canonical Wnt signaling (Stottmann et al., 2009).

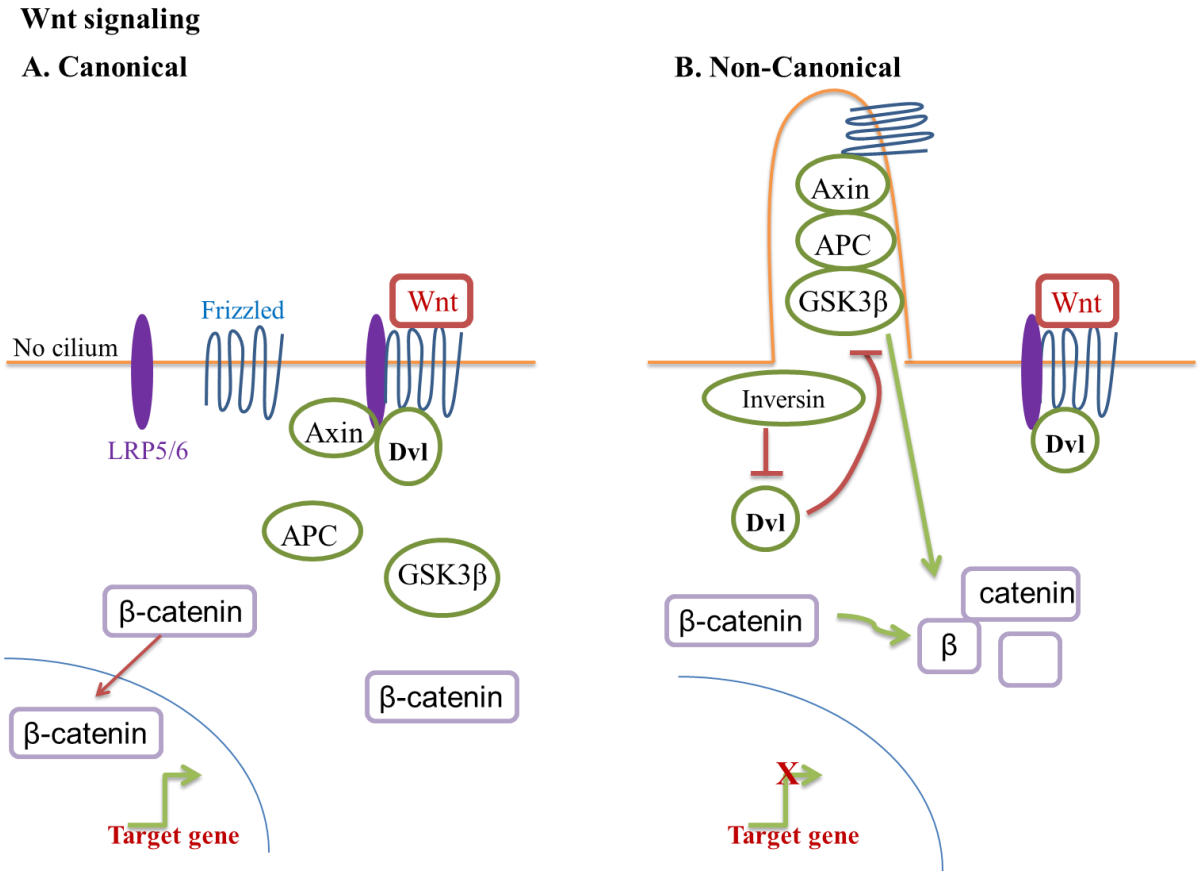

Figure 6. Proposed cilia involvement in Wnt signaling. Left panel: Canonical Wnt signaling. Binding of Wnt ligand to Frizzled and LRP5/6 receptors leads to an accumulation of β-catenin in the

cytoplasm and its subsequent translocation into the nucleus to affect transcriptional activation of transcription factors. **Right panel: Non-canonical Wnt signaling.** Wnt ligand binds to Frizzled and LRP5/6 receptors but inversin, a protein defective in ciliopathies, inhibits Dvl (Disheveled). Dvl in its turn suppresses the dissociation of Axin/APC/GSK3β complex which then degrades the cytoplasmic β-catenin.

Whether these disparate results can be truly explained by the suggestion that, even in the absence of the axoneme, the basal body is enough for normal mediation of Wnt signaling remains to be elucidated. However, primary cilia might have another association with Wnt signaling through PCP signaling.

6.2.5 Planar Cell Polarity signaling

PCP, or as it was earlier known tissue polarity, describes the polarization of epithelial tissues and organs within the plane of the epithelium. The components of PCP signaling have been discovered by genetic screens done in *Drosophila*, while later studies in vertebrates demonstrated that the corresponding pathways are evolutionary conserved (Simons and Mlodzik, 2008). Recent studies, such as the one in hair cells in the cochlea, propose that a close link among cilia positioning and factors of the PCP signaling exist. In the organ of Corti, the mammalian auditory sensory organ present in the cochlea, the primary cilium located on the mechanosensory hair cells is called kinocilium and its position is important for the orientation of stereocilia that are found on the hair cell. Several reports demonstrate that components of the PCP pathway are necessary for the polarity of these hair cells (Montcouquiol et al., 2003; Wang et al., 2005; Wang et al., 2006). Conditional deletion of *Ift88* mimics the phenotype observed in non-canonical Wnt mutants where polarity of the hair cells is defective suggesting that the kinocilium is indeed involved in orientating stereocilia in the appropriate way and is crucial for the organization of hair cells. This finding added to the idea that primary cilia are involved in regulation of the non-canonical Wnt pathway in the cochlea. However, polarity of proteins involved in PCP signaling is not altered in the hair cells of *Ift88* mutants suggesting that cilia are not necessary for the PCP signaling activity in cochlea in contrast to their importance in early embryonic stages. Nevertheless, non-canonical Wnt signaling functions as a regulator of the basal body positioning, while findings suggest that Ift88 plays a role in repositioning the basal body to a polarized position (Jones et al., 2008).

Reports examining motile cilia on the epidermis of the *Xenopus* embryos indicate that the polarity and organization of cilia is dependent on components of the PCP pathway. The cells of the epidermis bear multiple cilia that have the same polarity (Park et al., 2008). Disheveled (Dvl), a PCP protein, is present on the basal bodies of the epidermal cells and Dvl morphants (embryos treated with morpholinos in order to knock down expression of the target gene) are characterized by a decrease in the number of short cilia. In addition, disruption of Dvl affects polarity of the cilia on the epidermis (Park et al., 2008). These two observations indicate that cilia formation is possibly dependent on Dvl and perhaps also other factors of the PCP signaling.

Recent work on two downstream effectors of the non-canonical Wnt signaling in *Xenopus*, Inturned or Fuzzy, revealed that their knockdown using morpholinos leads to the disruption of ciliogenesis as well as defects on the apical actin network (Park et al., 2006). Both Inturned and Fuzzy morphants have defective PCP signaling as seen by the failure to undergo normal convergent extension. Surprisingly, these morphants also demonstrate phenotypes that are attributed to the loss of Shh signaling (Park et al., 2006). The mouse mutants *Fuz* and *Inturned* further support these findings as they show short cilia and a defective Hh signaling as well (Gray et al., 2009; Heydeck et al., 2009).

Taken together, all these findings indicate that factors of the PCP signaling could have an important role in the formation and polarity of cilia although until nowadays no evidence involving other PCP components in ciliogenesis exist. Therefore, it remains to be seen whether implication of Fuzzy and Inturned in cilia formation is truly related to non-canonical Wnt signaling.

6.2.6 PDGF signaling

In addition to the signaling cascades discussed above, primary cilium acts also as a mediator for the platelet-derived growth factor (PDGF) signaling which is crucial for cell proliferation, survival and migration. *In vivo* study showed that PDGF receptor alpha (PDGFRa) is localized on the primary cilium in neural stem cells of the subventricular zone of adult rats (Danilov et al., 2009). In mouse embryonic fibroblasts (MEFs) PDGF homodimers activate the PDGFRa and this subsequently leads to the activation of two other signaling pathways, the AKT and Erk1/2 (Schneider et al., 2005), whereas MEFs mutant for *Ift88* show no response to active PDGF signaling (Schneider et al., 2010) highlighting the role of primary

cilia in PDGF pathway. Already more than a decade ago reports demonstrated that PDGFRa signaling is fundamental for the development of later tissues such as oligodendrocytes, though in earlier embryonic stages loss of the pathway does not lead in any severe phenotypes (Soriano et al., 1997; Klinghoffer et al., 2002). As PDGF and Shh are both chemoattractant for cultured fibroblasts (Albrecht-Buehler, 1977) and precursor cells (Hammond et al., 2009) respectively, it has been challenging to dissect the relationship between PDGF and primary cilia. Therefore, further work is necessary to decipher the exact link between the two.

6.2.7 Ciliopathies

Nowadays, this tiny organelle that had been long neglected by the scientific community has been linked to several human disorders. The term ciliopathies is now used to cover a spectrum of diseases, such as the autosomal dominant polycystic kidney disease (PKD) and disorders such as Joubert syndrome, Meckel syndrome and Bardet-Biedl syndrome, associated with genetic mutations that lead to defects in cilia formation or in proteins that are normally localized at the cilium. Most of these disorders are characterized by features such as polydactyly, renal disease, retinal degeneration and cerebral anomalies. These disease manifestations can be attributed to defective Hh signalling which is dependent upon primary cilia, hence highlighting the latter as a major player in these human diseases.

6.2.7.1 Polycystic kidney disease

PKD consists of a group of disorders which have a common hallmark, the formation of kidney cysts mostly in the kidney and liver. These cysts usually form already during foetal life and can still be present through adulthood. PKD can be inherited both as an autosomal dominant (ADPKD) and a recessive disease (ARPKD). The vast majority of ADPKD patients have mutations in the *PKD1* gene that encodes polycystin-1 (PC-1), whereas a small group of patients has mutation in *PKD2* encoding polycystin-2 (PC-2). Studies on homozygous *Pkd1* null mice show that these mutants cannot survive past E16.5 and they display characteristic cystic appearance in both the kidneys and pancreas (Lu et al., 1997). In a report where the authors conditionally inactivate Pkd1 at a later time point, specifically after postnatal day 13, the mice exhibit a milder phenotype (Piontek et al., 2007). The question arising is whether

kidney cysts develop as a result of misregulated developmental pathways dependent on functional cilia. However, it is worth mentioning that even though Hh signalling is necessary during kidney development (Gill and Rosenblum, 2006), in mutants where this pathway is disrupted there have been no reports stating the presence of kidney cysts (Yu et al., 2002; Hu, 2006). In contrast, data suggest that Wnt signalling is regulated by primary cilia in the kidney (Benzing et al, 2007). Examination of mice that carried a mutation at the *inversin* (*inv*) gene, whose protein product can bind to microtubules and is found at the basal body of the cilium, revealed the presence of renal cysts (Philips et al., 2004). Additionally, human patients of kidney disease also carried mutations in *inv* gene (Otto et al., 2003). Studies done in cell culture but also using knock-down experiments have proposed that since *inv* can interact with Dvl, it could function as a switch between canonical and non-canonical Wnt signalling (Simons et al., 2005). Nevertheless, overexpression experiments in mice showed that elevated levels of Wnt signalling led to the formation of kidney cysts while in mouse mutants lacking primary cilia nuclear β-catenin in the cystic kidney tubules was increased (Saadi-Kheddouci et al., 2001; Lin et al., 2003). In addition to these observations, mice mutant in Jouberin, a protein found at the cilium that is mutated in Joubert syndrome, exhibit cystic kidneys as well as a reduction in Wnt signalling and nuclear β-catenin (Lancaster et al., 2009). Therefore, further work is essential in order to identify the exact role that Wnt signalling and by extension primary cilia have in PKD.

6.2.7.2 Joubert syndrome

Joubert syndrome (JBTS) is a rare autosomal recessive ciliopathy characterized by neurodevelopmental phenotypes such as malformations of the cerebellum and the brainstem, vermis hypoplasia or even complete aplasia (Louie and Gleeson, 2005; Brancati et al., 2009). These features are responsible for the characteristic ‘molar tooth sign’ (MTS) that one can observe on a cranial magnetic resonance imaging (MRI) scan of JBTS patients as the one shown in Fig.7c. Other features include polydactyly, ataxia, sleep apnea, abnormal breathing patterns and hypotonia. Until now, 16 genes have been identified to be involved in JBTS and all of them encode a protein found on the basal body of the primary cilium (Sang et al., 2011; Novarino et al., 2011; Garcia-Gonzalo et al., 2011; Lee et al., 2012). This alone is strong evidence that primary is implicated in the clinical pathology of this disorder. However, there is still a long way until the mechanisms, through which defects in primary cilium result in the

malformations observed in JBTS patients can be fully understood. Interestingly, recently a study using neuroimaging findings from 75 JBTS patients revealed that structures localized in the midbrain of some of the patients had abnormalities such as failure of the superior cerebellar peduncles to decussate (Poretti et al., 2011). This finding was supported by a later neuroimaging study where the authors also reported deformities in the substantia nigra in two post-mortem JBTS patients (Juric-Sekhar et al., 2012). Other observations seen in most of the subjects used in this particular study included enlarged arcuate nuclei, hypoplastic medial lemnisci and disorganization of the dorsal spinal cord, leading the authors to propose that primary cilium is in fact a crucial organelle in the developing human brain (Juric-Sekhar et al., 2012). Naturally, the necessity of more in depth studies addressing the mechanisms behind these pathological conditions, the midbrain defects present in ciliopathies and the involvement of primary cilia is still fundamental.

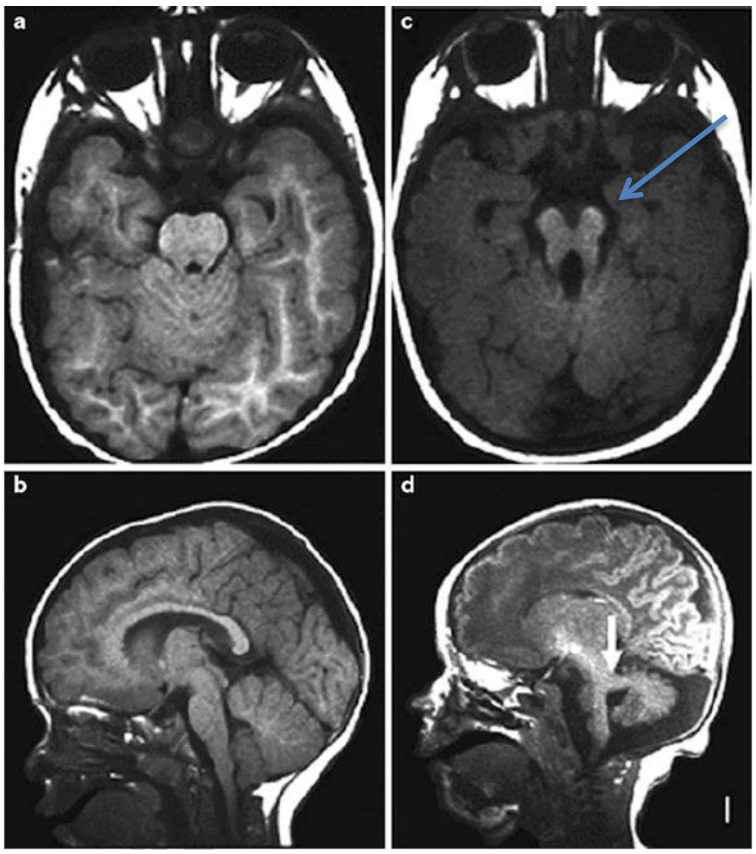

Figure 7. Comparison of MRI of a control and a Joubert patient. Left column (a,b) shows the MRI of a control, with a normal cerebellar vermis and superior cerebellar peduncles. **Right column (c,d)** shows the MRI of a Joubert patient showing cerebellar vermis hypoplasia and thickened superior cerebellar peduncles indicated by the white arrow. (Sattar and Gleeson, 2011). MRI in c clearly shows the characteristic 'molar tooth sign', indicated by the blue arrow, observed in the majority of Joubert patients.

7 AIMS OF THE STUDY

Primary cilia are short, microtubule-based organelles protruding from the cell membrane of almost all mammalian cells. Even though in the past they have been considered a vestigial organelle, work done in the last decades has reintroduced them to the scientific community as an important player in Hh signalling and therefore a possible regulator in embryonic development among other functions. In this current study, the role of primary cilia in midbrain development was looked at through the scope of a conditional knock-out mouse for Ift88, a protein involved in the anterograde transport of protein cargo along the axonemal structure of the cilium and therefore important for its maintenance. Moreover, it is worth mentioning that earlier studies have looked extensively into the role that Hh signaling pathway plays in the development of dopaminergic neurons. However, this particular study is the first to look into the role, and its extent, of primary cilium in the importance that Hh has for midbrain development. This investigation therefore is very relevant as nowadays more and more publications discuss the idea of a non-canonical Hh signaling that could be possibly not entirely dependent on primary cilium for the activation of its components.

Previous work done in our laboratory uncovered a hypomorphic allele of *Ift88*, namely the *cobblestone* mutant, by an ENU (*N*-ethyl-*N*-nitrosourea) screen. Characterization of the *cobblestone* mutant showed pleiotrophic phenotype including, among others, defects in the formation of dorsomedial telencephalic structures and relaxation of both dorsal-ventral and rostral-caudal compartmental boundaries (Willaredt et al., 2008). However, my colleagues had also observed midbrain defects such as floor plate dismorphogenesis in which the floor plate marker FoxA2 was mostly absent from its regular ventral domain in a mosaic pattern. Labelling of dopaminergic neurons with TH in the midbrain of the *cobblestone* mutant revealed that they failed to form in comparison to the dopaminergic neurons in wild-type littermate. These observations raised the question whether the midbrain defects observed in *cobblestone* mutants could be accounted to the loss of Ift88 and therefore whether they were dependent on primary cilia.

The logic behind using an area-specific conditional inactivation of *Ift88* was to be able to answer this question in a clearer system than the one the *cobblestone* mutant could provide, as it has been shown that in this mutant primary cilia were not completely lost even though the Ift88 mRNA and protein levels were reduced by 70-80% (Willaredt et al., 2008).

Therefore, mutant lines deficient in proteins that are necessary for the maintenance and the function of primary, namely the Ift88 and the kinesin motor protein Kif3a, were used in order to strengthen the proof that whatever finding would be observed would be attributed to the loss of primary cilia. Crossing *Ift88*^{flox} or *Kif3a*^{flox} mice to a mouse with a Cre recombinase knock-in at the *Engrailed1* (*En1*) gene allowed the generation of mice in which *Ift88* or *Kif3a* was inactivated in the midbrain from around E8.5. Using these two mouse genetic models as main model systems in this study, the aims were:

1) To identify the impact of primary cilia function in the neurogenesis of mDA neurons in the ventral midbrain of the developing murine brain

2) To dissect through which signalling pathway, Shh or Wnt signalling, primary cilia are involved in the generation of mDA and to which extent

3) To investigate whether primary cilia are important for the specification of mDA

8 MATERIALS AND METHODS

8.1 General Reagents

Acetone	Zentrallager INF 367 (Heidelberg, Germany)
Acrylamide	BioRad (München, Germany)
Agarose (elctrophoresis grade)	Roth (Karlsruhe, Germany)
Aquatex Mounting Medium	Merck (Darmstadt, Germany)
ß-Mercaptoethanol	Sigma-Aldrich (St. Louis, USA)
Boric acid	AppliChem (Darmstadt, Germany)
Bovine serum albumine (BSA)	Roth (Karlsruhe, Germany)
DAB	Sigma-Aldrich (St. Louis, USA)
DMSO	Acros Organics (Geel, Belgium)
DNA Polymerase DreamTaq	Fermentas (Waltham, USA)
DNA Polymerase DreamTaq Mastermix	Fermentas (Waltham, USA)
DTT	AppliChem (Darmstadt, Germany)
EDTA	AppliChem (Darmstadt, Germany)
Ethanol absolut puriss.	Sigma-Aldrich (St. Louis, USA)
Ethidium bromide	Fluka (Buchs, Switzerland)
Glacial acetic acid	Sigma-Aldrich (St. Louis, USA)
Glutaraldehyde (25% solution)	Merck (Darmstadt, Germany)
Glycerol	Sigma-Aldrich (St. Louis, USA)
Glycine	Sigma-Aldrich (St. Louis, USA)
ImmEdge Pen	Vector Laboratories (Burlingame, USA)
Methanol	Merck (Darmstadt, Germany)
Paraformaldehyde	Sigma-Aldrich (St. Louis, USA)
Phenol/Chloroform/Isoamylalcohol, pH 7.5-8.0	Roth (Karlsruhe, Germany)
PIPES	AppliChem
2-Propanol	AppliChem (Darmstadt, Germany)
Protease inhibitor tablets,	Roche (Penzberg, Germany)

Complete, EDTA-free	
Proteinase K	Roth (Karlsruhe, Germany)
Oligo(dT)12 – 18 primer	Invitrogen (Carlsbad, USA)
Orange G	Sigma-Aldrich (St. Louis, USA)
Random hexamer primer	Applied Biosystems (Darmstadt, Germany)
Sodium chloride	Sigma-Aldrich (St. Louis, USA)
Sodium citrate dihydrate	Sigma-Aldrich (St. Louis, USA)
Sodium dodecyl sulfate (SDS)	Serva (Heidelberg, Germany)
Sodium tetraborate decahydrate	Sigma-Aldrich (St. Louis, USA)
Sucrose	Sigma-Aldrich (St. Louis, USA)
TEMED	Sigma-Aldrich (St. Louis, USA)
Tissue freezing medium	Jung (Nussloch, Germany)
Tris	Roth (Karlsruhe, Germany)
Tris ultrapure	Applichem (Darmstadt, Germany)
Triton X-100	Merck (Darmstadt, Germany)
Trypan blue	Sigma-Aldrich (St. Louis, USA)
Tween-20	Roth (Karlsruhe, Germany)
Xylene cyanol	Sigma-Aldrich (St. Louis, USA)
Xylol	AppliChem (Darmstadt, Germany)

8.1.1 Equipment

ABI PRISM 7000 Sequence Detection System	Applied Biosystems
Autoclave Fedegari FVA3	Integra Biosciences GmbH
Tpersonal Thermal Cycler	Biometra, Goettingen
Centrifuge MIKRO 20	Hettich, Tuttlingen
CO2 incubator, HERA cell 150	Kendro laboratory product GmbH, Thermoscientifc
CPD 030 Critical Point Dryer	BAL-TEC, Wetzlar
Cryostat CM3050 S	Leica Microsystems, Nussloch
Digital Camera COOLPIX 5000	Nikon, Japan

Electophoresis chamber	Feinmechanikwerkstatt, Uni Heidelberg
Fine forceps & Scissors	Fine Science Tools, Germany
Fluorescent confocal laser scanning microscope A1	Nikon Instrument, Europe B.v.
Precision Balance 440-33N	Kern und Sohn (Balingen, Germany)
Potter S Homogenizer	Sartorius Stedim Biotech
Spectrophotometer Ultrospec 3100 pro	Amersham Biosciences, Amersham, UK
Sterile Hood, LaminAir model 1.2	Holten, Denmark
Vortex Genie 2 G-560E Mixer	Bender and Hobein, Switzerland
Waterbath	Memmert, Schwabach

8.1.2 Disposables

Autoclave bags CPP clear	Nerbe Plus, Winsen Germany
Amersham Hyperfilm ECL	GE Healthcare
Cellstar Culture Dishes and Plates	Greiner Bio-One GmbH
Coverslips (24 x 60mm)	Roth, Karlsruhe
Cell scraper	Greiner Bio-One GmbH (Kremsmüster, Austria)
Cell strainer 100um	Millipore, Billerica USA
Conical tubes, 15ml and 50ml	Greiner Bio-One GmbH
Filtered pipette tips	Sarstedt, Nümbrecht Germany
Gloves Nitrile Small	VWR (Radnor, USA)
Gloves pH soft Small	Hartmann, Heidenheim
Injection Needles	BD Microlance, San Jo José, USA
Kimwipes	Kimberly Clark, Roswell USA
Microscope Slides Super Frost	Roth, Karlsruhe
Microscope Slides Super Frost Ultra Plus	Roth, Karlsruhe
Microtome Blades	Leica Microsystems, Wetzlar Germany
Optical Adhesive Film Kit	Applied Biossystems
Parafilm	Pechiney, Akron USA
Pasteur Capillary Pipettes	WU Mainz
PCR cup (G002/G003	G. Kisker GbR

Petri dishes 10cm	Zentrallager, INF 367 Heidelberg
Pipette tips	Greiner Bio-One GmbH
Plastic cuvettes 1mL	Sarstedt (Numbrecht, Germany)
Safe-Lock tubes (1.5mL / 2.0 mL)	Eppendorf
Sterile pipettes	Gibco, Invitrogen
Tissue freezing medium	Jung, Leica, Nussloch
Tissue freezing molds	Polysciences Europe, Eppendorf
Tubes (1.5mL / 2.0mL)	Sarstedt, Germany
96-well optical bottom plate polymerBase	Nunc

8.1.3 Software

4D Client	4D, San Jose, USA
ABI Prism 7000	Applied Biosystems, Darmstadt
Adobe Acrobat/Photoshop/Illustrator	Adobe Systems, San Jose, USA
ImageJ	Wayne Rasband, NIH

8.1.4 Molecular Weight Markers

GeneRulerTM100 bp ladder	Fermentas
1 kb bp ladder	NEB, Ipswich USA
λ/Hind III ladder	Fermentas

8.1.5 Kits

BCA Protein Assay Kit	ThermoScientific
Bradford-Assay	BioRad, München
GenElute HP Plasmid Midiprep Kit	Sigma-Aldrich
Rneasy Mini Kit	Qiagen
SuperScript® II First-Strand Synthesis	Invitrogen, Carlsbad USA

8.1.6 Primers

8.1.6.1 Primers for genotyping

The following primers were ordered from the website of Themo Fisher Scientific. Once delivered, they were centrifuged and the appropriate amount of distilled H_2O was then added. Before they were used, they were diluted to a final concentration of 10ul/ug.

Ift88$^{tm1.1Bky}$

Ift88 common 5' primer	5'–GCC TCC TGT TTC TTG ACA ACA GTG-3'
Ift88 3' flox and wild type allele primer	5'-GGT CCT AAC AAG TAA GCC CAG TGT T-3'
Ift88 3' delta allele primer	5'-CTG CAC CAG CCA TTT CCT CTA AGT CAT GTA-3'

Kif3a

Kif3a 5' flox allele	5'– TCT GTG AGT TTG TGA CCA GCC -3'
Kif3a common 5' primer	5'- AGG GCA GAC GGA AGG GTG G -3'
Kif3a 3' delta allele primer	5'- TGG CAG GTC AAT GGA CGC AG -3'

En1::CRE

En1WT-F	5'– CAC CGC ACC ACC AAC TTT TTC -3'
En1WT-R	5'- TCG CAT CTG GAG CAC ACA AGA G -3'

R26SMO

R26SMO YFP_F	5'– CCT CGT GAC CAC CTT CG -3'
R26SMO YFP_R	5'- TTG ATG CCG TTC TTC TGC -3'

8.1.6.2 Primers for testing cDNA quality

These primers were used to test quality of the cDNA before proceeding to use it for Real Time Quantitative PCR.

G3PDH F	5'– AAC ACA GTC CAT GCC ATC AC -3'
G3PDH R	5'- TCC ACC CTG TTG CTG TA -3'

8.1.6.2.1 Primers for RT-qPCR

The following TaqMan Gene Expression Assays were ordered from Applied Biosystems and used for qPCR:

Gene	Assay Number	Species
GAPDH	Mm99999915_g1	Mouse
Ift88	Mm01313467_m1	Mouse
Axin2	Mm01265783_m1	Mouse
Wnt1	Mm01300555_g1	Mouse
Wnt5a	Mm00437347_m1	Mouse
Wnt7a	Mm00437354_m1	Mouse

Table 1: TaqMan Gene Expression Assays

8.1.7 Solutions and buffers

8.1.7.1 General

1x PBS (pH 7.4)	140 mM NaCl
	2.7 mM KCl
	10 mM KH2PO4

8.1.7.2 Gel electrophoresis

50x TAE	2 M TRIS
	0.05 M EDTA pH 8.0
	57.1 ml glacial acetic acid (96%)
5x TBE	0.45 M TRIS
	0.01 M EDTA pH 8.0
	0.04 M Boric Acid
10x Orange G	0.006 % (w/v) Orange G

	50% Glycerol 50% MP-Water
Ethidium bromide	0.5 µg/ml 100 ml 1x TAE
Lysis buffer	0.1 M Tris-Cl (pH 8.5) 5 mM EDTA (pH 8.0) 0.2% (w/v) SDS 0.2 M NaCl 100 µg/ml Proteinase K

8.1.7.3 Scaninng Electron Microscopy

Fixation buffers	2.5% (v/v) Glutaraldehyde 0.1 M PIPES (pH 7.4) 1% (v/v) OsO4
Washing buffer	0.15 M PIPES (pH 7.4)

8.1.7.3.1 Immunohistochemistry

Blocking buffer	1% (v/v) BSA 5% (v/v) NGS 0.25% (v/v) TritonX-100
Washing solutions	1x PBS

8.1.8 Histology

8.1.8.1 General Reagents

Aqua-Poly/Mount	Polysciences Europe, Eppelheim, Germany
Aquatex	Merck
Entellan	Merck
Immune Edge Pen	Vector Laboratories Inc, Burlingame
Paraplast-Plus	Roth, Karlsruhe
Roti-Liquid Barrier Marker	Roth, Karlsruhe
Triton X-100	Roth, Karlsruhe
Tween-20	Roth, Karlsruhe

8.1.8.2 Fluorescent Immunohistochemistry

8.1.8.2.1 Sera

Bovine serum albumine	Roth, Karlsruhe
Native goat serum	Roth, Karlsruhe

8.1.8.2.2 Dyes

DAPI	Sigma-Aldrich

8.1.8.2.3 Fixatives

4% PFA (pH 7.4)	Sigma-Aldrich 4% (w/v) PFA 2 N NaOH 1x PBS
2% Glutaraldehyde	2% (v/v) Glutaraldehyde 1x PBS

8.1.8.2.4 Primary Antibodies

Primary Antibodies	Description	Dilution	Source
γ-tubulin	mouse, clone GTU-88	1:1000	Sigma-Aldrich
acetylated α-tubulin	mouse, monoclonal	1:1000	Sigma-Aldrich
Arl13b	rabbit, monoclonal	1:1500	Tamara Caspary, Emory University Atlanta, USA
Adenylyl Cyclase III	rabbit, monoclonal	1:1500	Santa Cruz Biotechnology
Nestin	rat-401 clone, monoclonal	1:1000	EMD Millipore
Brain Lipid Binding Protein	rabbit, monoclonal	1:1000	EMD Millipore
IFT88	rabbit, monoclonal	1:500	Gislene Perreira Heidelberg Uni
IFT88	guinea pig, monoclonal	1:200	Gislene Perreira

Table 2: Primary Antibodies

8.1.8.2.5 Secondary Antibodies

Secondary Antibodies	Dilution	Source
Donkey anti-rabbit Alexa 488	1:500	Life Technologies
Goat anti-mouse Alexa Fluor 488	1:1000	Invitrogen
Goat anti-mouse Alexa Fluor 546	1:1000	Invitrogen
Goat anti-rabbit Alexa Fluor 546	1:1000	Life Technologies
Goat anti-guinea pig Alexa Fluor 546	1:1000	Life Technologies

Table 3: Secondary Antibodies

8.2 Methods

8.2.1 Animal handling of transgenic mice

All experiments were conducted according to the guidelines of the state of Baden-Württemberg and the University of Heidelberg.
The mice colonies used in this study have been kept at the animal facility**,** Interfakultäre Biomedizinische Forschungseinrichtung **(**IBF), of the University of Heidelberg. The software 4D Client (Tierbase) was daily used for the administration of the colonies, to access comments from the animal care takers and to set up matings. Usually, matings were set up on Mondays and female animals were then controlled for vaginal plug early every morning from Tuesday to Friday by the animal care takers. Noon of the day of the vaginal plug was assigned as the date embryonic day 0.5 (E0.5). Once a plug was detected, the animals were separated.

Mouse embryos of the following lines were used for the experimental design in order to achieve the aim of this project.

8.2.1.1 Kif3a^{flox}

Kif3a^{flox} (Marszalek et al., 2000) allele was generated as described in the IBF at the University of Heidelberg and mice were crossed in order to generate embryos with genotype *Kif3a*$^{flox/flox}$. *Kif3a* conditional mice were then mated to En1::CRE mice in order to achieve conditional knock-out of *Kif3a* in the embryonic midbrain.

8.2.1.2 En1::CRE

En1Cre (Kimmel et al., 2000) allele was generated as described and mice genotyped positive for *En1Cre* were then crossed with other mouse lines such as *Kif3a* or *Ift88* conditional mice.

8.2.1.3 Ift88^{flox}

The mouse line Ift88^{flox} (Haycraft *et al*., 2007) was kindly given to us from the lab of Professor Badley K. Yoder of the University of Alabama, Birmingham, USA. Once the line

was re-derived at the IBF, mice could be crossed between them to result in *Ift88*$^{flox/flox}$ litters or crossed to mice of CRE lines already present in the IBF according to the brain area we were interested in.

8.2.1.4 R26^{SmoM2}

R26SmoM2 {{Jeong:2004bx}allele was generated as described and was used in this study to generate conditional knock-out mice or mice in which the Shh signaling receptor Smo was conditionally activated (ca). For this purposes *En1Cre* mice were crossed with mice bearing floxed alleles (genotypes in brackets) such as: *Ift88* cko (*En1Cre, Ift88*$^{flox/flox}$), *Kif3a* cko (*En1Cre, Kif3a*$^{flox/flox}$), Smo ca (*En1Cre, SmoM2*$^{flox/+)}$ and *Ift88* cko; Smo ca (*En1Cre, Ift88*$^{flox/flox}$*, SmoM2*$^{flox/+)}$.

8.2.2 Molecular Biology

8.2.2.1 Genomic DNA extraction from embryonic and adult tissue

In this study, the protocol from Laird et al., 1991 was slightly modified and used for the isolation of genomic DNA from both embryonic and adult tissue.

Both embryonic and adult tissue biopsies (usually tail samples) were placed in 500µl of lysis buffer containing 100µg/ml Proteinase K and placed in overnight (o/N) at 5˚C under agitation. Next day, 500µl Isopropanol were added to each sample, mixed thoroughly and placed at -80˚C for 30 minutes, followed by centrifugation at 13.000rpm at 4˚C for 20 minutes. After centrifugation, the supernatant of each sample was discarded. The remaining pellets were then washed in 300µl of 70% Ethanol with another centrifugation step, this time at room temperature (RT) at 13.000rpm for 20 minutes. Following centrifugation, the 70% ethanol was carefully removed by aspiration and the DNA pellets were air dried. Subsequently, the DNA pellets were dissolved in 60-80µl of water or 10mM Tris- HCL, pH 8.5, o/N at 55˚C under agitation.

8.2.2.2 Polymerase Chain Reaction (PCR)

In order to genotype both adult mice and embryos, DNA fragments were amplified using Taq-Polymerase enzyme and specific primers (see above 3.1.6.1) were used for each reaction.

Standard PCR Mastermix Protocol for 1x

16.2 µl	H2O
2.0 µl	10x PCR reaction buffer
0.4 µl	10 µM Primer F
0.4 µl	10 µM Primer R
0.4 µl	10 mM dNTPs
0.5 µl	DNA (50-300ng)

The PCR was carried out in a Biometra T personal cycler according to the following standard program:

95 °C	5 min	
95 °C	30 sec	40 cycles
60 °C	30 sec	
72 °C	37 sec	
72 °C	10 min	

8.2.2.3 Gel Electrophoresis

Gel electrophoresis was used to identify the correct DNA size of PCR products, hence the genotypes of the mice. 2% agarose gels were used for the separation of DNA fragments of PCR products prepared using 1x TAE buffer and 0,5µg/ml ethidium bromide. DNA samples were supplemented with a 10x Orange G loading dye to a final concentration of 1x. Gels were run at 130 V at RT for about 30-40 minutes. After separation, DNA samples were visualized on a UV table and the bands were photographed.

8.2.2.4 RNA isolation

Total RNA was manually isolated from E11.5 microdissected midbrain tissue. The tissue was dissected in a petri dish with cold 1xPBS and was collected in Eppedorf tubes. The tubes were then quickly placed in a mixture of liquid nitrogen and dry ice. RNA was extracted using RNeasy Mini Kit (74104 Qiagen) according to the manufacturer's instructions.

8.2.2.5 cDNA synthesis

1-5µg of RNA were then transcribed into cDNA using oligo$(dT)_{12–18}$ (0,5 µg/µl, Invitrogen), random hexamers (50 mM, Applied Biosystems, Darmstadt, Germany) and SuperScript II RNase H reverse transcriptase (Invitrogen).

Reaction setup used for 1 – 5 µg of total RNA for cDNA synthesis

1 µl	random hexamer primers (100 µM, Fermentas)
1 µl	oligo$(dT)_{18}$ primer (0.5 mg/ml, Fermentas)
1 µl	dNTP-Mixture
2 µg	RNA (volume 13 µl, if needed could be diluted with Millipore water)

This mixture was first incubated at 65 °C for 5 minutes on a Biorad iCycler thermocycler and was then subsequently placed on ice. Then, via a centrifugation step the liquid at the bottom of the tube was collected, the following reagents were added to it:

5.00 µl	5x First Strand buffer (Invitrogen)
2.50 µl	0.1 M DTT
1.25 µl	Ribolock RNase Inhibitor (Fermentas, 40u/µl)

The reagents were mixed by gently pipetting up and down and were incubated for 2 minutes at 42 °C. Subsequently, 1 µl Super Script II reverse transcriptase was added and the reaction was again mixed carefully before being incubated for 1.5 hours at 42 °C. The cDNA was diluted 1:5 before being used for real time RT-PCR.

8.2.2.5.1 GAPDH-PCR to test cDNA quality

The quality of the cDNA was assessed by PCR with specific primers for *GAPDH* (3.1.6.2) Primers for testing of the cDNA-Quality). *Gapdh* is a housekeeping gene; therefore equal amounts of its PCR product (expected size 500 bp) were expected in each cDNA preparation.

Mastermix used for 1 sample

H_20	16.1 µl
10x PCR buffer	2.0 µl
10 mM dNTPs	0.4 µl
GAPDH 3' primer	0.4 µl
GAPDH 5' primer	0.4 µl
Taq polymerase	0.2 µl
Total volume	19.5 µl

Then, 0.5 µl DNA were added per sample to the mastermix. The PCR reaction was performed according to the following program on a Biometra PCR Cycler TPersonal.

Temperature	**Time**	**# cycles**
94 °C	5 min	1
94 °C	30 s	32
60 °C	30 s	
72 °C	30 s	
72 °C	10 min	1

The PCR products were then ran on an 1% agarose gel at 100 V for about 30 min and once separated they were visualized with ethidium bromide under UV light. If all samples used showed the same amount of Gapdh PCR product, the cDNA could be used for quantitative real time RT-PCR.

8.2.2.5.2 Real Time Quantitative PCR

Quantitative real time PCR reactions were performed using the ABI Prism 7000 Detection System (Applied Biosystems) using TaqMan Gene Expression Assays (2.1.1.6.4 Primers for real time RT-PCR) (Applied Biosystems). Equal amounts of cDNA (1 – 5 µg) of each sample were diluted in water to a final volume of 13.5 µl. The reaction mix was prepared by mixing 15 µl TagMan Master Mix per sample with 1.5 µl of the respective TaqMan Gene Expression Assay. This mixture was then pipetted into the relevant wells of a 96 well reaction plate and the cDNA dilution added. Each sample was assayed in triplets. The plate was sealed with an adhesive cover and centrifuged for 2 min at 1500 rpm, before placed in the cycler, to remove bubbles from the reaction volumes and collect the liquid at the bottom of the tubes. Sterile-filtered water (Sigma) was used as negative control. The standard quantification protocol was applied with the following cycles: 2 min at 50.0° C, 10 min at 95.0° C, followed by 45 cycles: 15 seconds at 95.0° C and 1 min at 60.0°C. Each individual reaction was performed in triplicate. GAPDH primers (Mm99999915_g1) were used to normalize results.
Statistical analysis was performed as follows: Relative expression (RE) levels were calculated with the function ($RE = 2^{-\Delta\Delta Ct}$), where ΔΔCt is the normalized difference in threshold cycle (Ct) number between wild type and cko samples, calculated from the mean Ct value of triplicate replicates of any given condition. Statistical significance between wild type to cko was evaluated by application of Student's *t* test.

8.2.3 Histology

8.2.3.1 Dissection of embryonic brain

Pregnant female mice were sacrificed by cervical dislocation 9.5, 10.5 or 12.5 days post coitum (p.c.). The embryos were carefully dissected out and rinsed in 1xPBS solution. Embryonic samples from both the mother and the embryos were collected separately for DNA extraction and genotyping. In the case that the embryos would be used for immunostainings, they were put in 4% PFA on the shaker at 4° C overnight. The following day, they were rinsed in 1x PBS, two times for 20minutes. In case the brains would be used

for mRNA extraction, they were quickly frozen down after dissection and stored at -80 degrees.

8.2.3.2 Embedding of embryos for cryosections

Serial steps of 10%, 20% and 30% Sucrose in 1x PBS were undertaken o/N at 4°C under agitation.
The last day of the sucrose serial steps, the embryos were placed in small "Peel-Away" mounting moulds that had been before half-way filled with mounting medium (tissue-tek). After 1 hour of incubation at RT in the mounting medium the embryos were orientated as desired and the bottom of the mould was quickly frozen in liquid nitrogen, to fix the embryos in position. The moulds were placed afterwards on dry ice for 10 to 20 min to freeze the mounting medium completely and stored at -80°C.

8.2.3.3 Cryosectioning

The embryos embedded in mounting medium inside the 'Peel-Away' mounting moulds were then used for cryosections on a Leica cryostat. The standard conditions used for cutting cryosections were the following: chamber temperature: -21°C, object temperature: -19°C. The moulds were orientated as to allow sectioning of the desired anatomical plane. 10-12 µm thick sections were collected on microscope slides superfrost ultra plus, dried for one to two hours at RT and subsequently frozen away at -80°C.

8.2.3.4 Immunofluorescent stainings

8.2.3.4.1 Staining on cryosections

Slides were removed from -80°C and sections were left to thaw for 10-15 min at RT. Roti-Liquid Barriere marker was then used to surround the sections on the slide in order to contain later the liquid placed on the sections. After the Roti-Liquid Barriere marker had dried the sections were rehydrated by placing the slides into 1x PBS for 15 min at RT. Excessive 1x PBS was carefully removed with a Kimwipe and 200 µl of blocking buffer with TritonX-100 was added on each slide. The sections were incubated for 1 hour at RT in a wet chamber. Subsequently the blocking buffer was removed and 200 µl of blocking buffer without

TritonX-100 but with the appropriate dilution of primary antibodies was added to the slides. The sections were then incubated with the primary antibody in a wet chamber o/N at 4°C. The next day the primary antibody was removed and the sections were washed for at least 4x 10 min with 1x PBS at RT. After the washing steps the appropriate secondary antibodies diluted in blocking buffer without TritonX-100 were added to the slides and incubated in a wet chamber that was then covered with aluminium foil for one hour at RT. Afterwards, the sections were washed 1x with DAPI in 1xPBS for 10 min at RT, followed with at least 3x 1xPBS washing for 10 min at RT. Before mounting the slides were shortly dumped into water and excess liquid was carefully removed with a Kimwipe. The sections were then mounted with coverslips using Aqua Poly/Mount and stored at 4°C in the dark until usage.

8.2.3.5 *In situ* hybridization

Radioactive *in situ* hybridization was performed as previously described (Brodski et al., 2003). Embryonic mice were fixed by immersion with 4% paraformaldehyde (PFA) and then embedded in paraffin. Antisense mRNA probes were transcribed from plasmids containing fragments of the murine tyrosine hydroxylase (*Th*) gene (base pairs 1–760; GenBank accession number M69200). Transcripts were radiolabelled by *in vitro* transcription with 35S-UTP. For the hybridization, sections were dewaxed, pre-treated, and pre-hybridized. Subsequently, they were hybridized overnight at 57°C and washed at 65°C. The hybridized slides were dipped in autoradiographic emulsion (type NTB2; Eastman Kodak, Rochester, NY), developed after 6 weeks, and counterstained with cresyl violet.

Non-radioactive RNA *in situ* hybridization was essentially performed as previously described (Blaess et al., 2011). Frozen sections were fixed in 4% PFA and washed in PBS. Paraffin sections were de-paraffinized, rehydrated, treated with Proteinase K (Roche, Penzberg, Germany) and then acetylated. After washing in H2O, frozen and paraffin sections were dehydrated in different concentrations of ethanol (70%, 80%, 95% and 100%) and incubated in chloroform to de-fat the sections. After hybridization 1 with the cRNA probes and immunodetection of digoxigenin with alkaline phosphatase conjugated antibody (Roche, Penzberg, Germany), sections were incubated with BM purple (Roche, Penzberg, Germany). The colour reaction was stopped in Tris-EDTA buffer (Gazea M., Tasouri E. et al., under review).

8.2.4 Microscopy

8.2.4.1 Confocal microscopy

Confocal microscopy: Confocal microscopy was performed with a Nikon A1R microscope (Nikon Imaging Center, University of Heidelberg) using a 60x objective (NA 1.4) with oil immersion. Scans were taken at a 500 nm interval at a resolution of 1024 x 1024 pixels, using scan lines of 405, 491, and 561 nm.

8.2.4.2 Scanning electron microscopy (SEM)

Embryonic heads were fixed overnight (o/N) at 4°C in 2.5% glutaraldehyde/ 0.1 M PIPES, pH 7.4, and subsequently washed three times in 0.15 M PIPES, pH 7.4, at 4°C. The fixed samples were then embedded in 3% agarose and cut into 300 µm coronal slices in 1x PBS using a D.S.K. Microslicer. The slices were treated for one hour at room temperature (RT) with 1% OsO_4, washed three times with 0.15 M PIPES pH 7.4, and subsequently dehydrated in a ascending ethanol dilution series (50%, 70%, 90%, 100%). The specimens were dried in a CPC 030 critical point dryer, using CO2 as a transitional medium, followed by sputter coating of a 20 nm Gold film. For scanning electron microscopy (SEM), a LEO 1530 field emission scanning electron microscope with a Schottky cathode was used (LEO Elektronmikroskopie, Oberkochen, Germany).

8.2.5 Quantification

ImageJ software package 1.48v (http://rsb.info.nih.gov/ij/ <http://rsb.info.nih.gov/ij/>) was used to measure the perimeter of Lmx1a- and FoxA2-positive domains in E10.5 old embryonic midbrains ($n \geq 3$). The domains were then normalized to the inner perimeter of the ventricle in each embryonic midbrain separately. Quantification of FoxA2- and TH-expressing mDA neurons at E13.5 and E18.5, was done using at least three embryos per genotype. For E13.5 embryos, one intermediate section per embryo was counted that contained both, SN and VTA. For E18.5 embryos an anterior, intermediate and posterior section was counted for each embryo. For E18.5, numbers were normalized to wild-type (i.e. wild-type set at 100%). For the quantification of mDA neurons in E18.5 *Ift88* and *Kif3a* cko

brains (controls: frozen sections) was performed using 12 μm frozen sections. Counting was performed using the cell counter plugin in ImageJ (Gazea M., Tasouri E. et al., under review).

8.2.6 Statistical analysis

Statistical analysis of histological data was performed using an unpaired two-sided Student‘s *t-test* and parametric analysis of variance (ANOVA) (Prism 6, Graphad). Statistical significance levels were set at $p<0.05$ (*$p<0.05$, **$p<0.01$ ***$p<0.001$). The values are represented as mean ± SD. (Gazea M., Tasouri E. et al., under review).

9 RESULTS

9.1 Primary cilia are present on radial glial-like precursors in the ventricular zone of the ventral midbrain

Previous work both from our laboratory (Willaredt et al., 2008) but also of others (Lancaster et al., 2011) have shown that primary cilia are present in the mouse embryonic midbrain. However, what has not been addressed is the identity of the cells bearing the primary cilia. To determine this antibody staining for proteins known to be expressed by the radial glia-like midbrain dopaminergic neurons precursors was used, namely for nestin and brain lipid binding protein (BLBP) shown in Fig.8A and 8B respectively (Bonilla et al, 2008; Tang et al., 2009). Antibody staining against nestin and BLBP was combined with antibody staining against the protein ADP-ribosylation factor like 13B (Arl13b) which labels the axoneme of the primary cilia (Caspary et al., 2007; Kang et al., 2010). Using confocal microscopy Z-stacks of each E12.5 midbrain section that was stained was imaged. Projection of the Z-stacks showed that cells in the midbrain VZ bearing primary cilia were positive for either nestin or BLBP (Fig.8A, 8B).

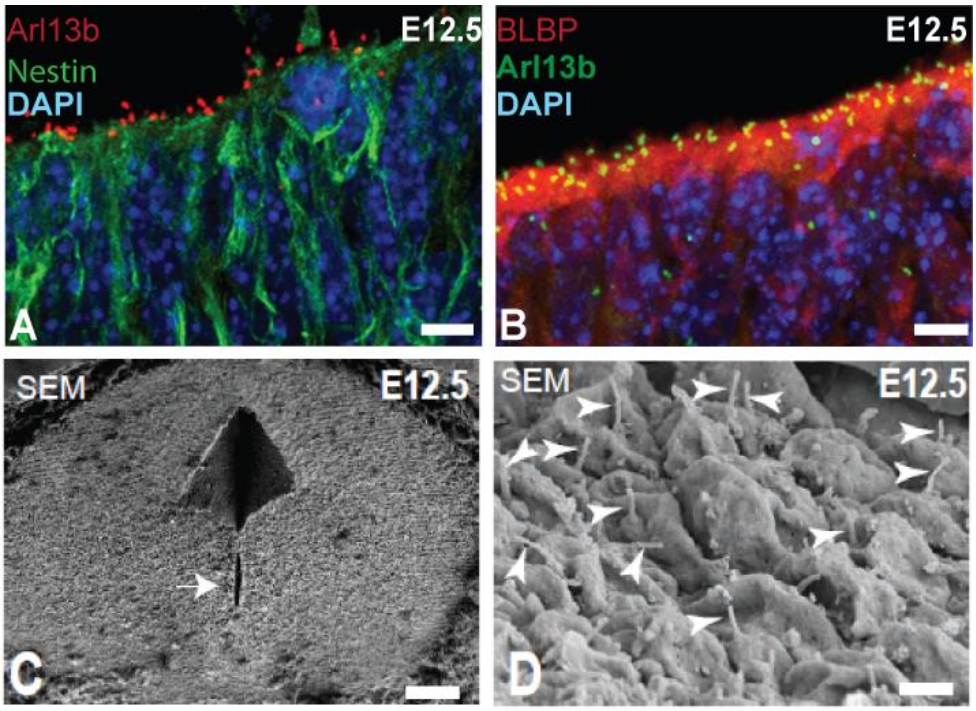

Figure 8. Primary cilia are present on radial glial-like precursors in the ventricular zone of the ventral midbrain. Immunofluoresence (***A, B***) and SEM (***C, D***) images of primary cilia protruding of the cell membrane of cells at the ventral mesencephalon of wild-type E12.5 embryos. ***A, B***, Primary

cilia were labelled using an antibody against Arl13b staining their axonemal structure (***A*:** red) (***B*:** green). Midbrain dopaminergic neural precursors were detected using antibodies against nestin (***A***: green) or BLBP (***B*:** red). DAPI was used to label the nuclei in blue. C, D: arrow (left panel) indicates the ventral ventricular surface of the midbrain; arrowheads (right panels) indicate primary cilia. Scale bars: ***A,B***, 10 μm; ***C***, 500 μm; ***D***, 1 μm.

In addition, SEM was also employed, with the guidance of Dr. Christian Gojak, for an independent analysis of primary cilia in the brain of E12.5 embryos. Analysis of the area of the diencephalon in forebrain displayed several primary cilia, of about 1 μm long, projecting from the cell membrane as seen in the panels C and D of Fig.8.

9.2 Generation of *Ift88* cko by conditional inactivation of *Ift88* in the ventral midbrain using En1::Cre

As the aim of this project was to investigate how primary cilia affect midbrain dopaminergic neuron precursors and therefore the consequences that this may have on mature midbrain neurons, a conditional inactivation approach was employed where *Ift88* expression would be eliminated specifically in the area of interest.

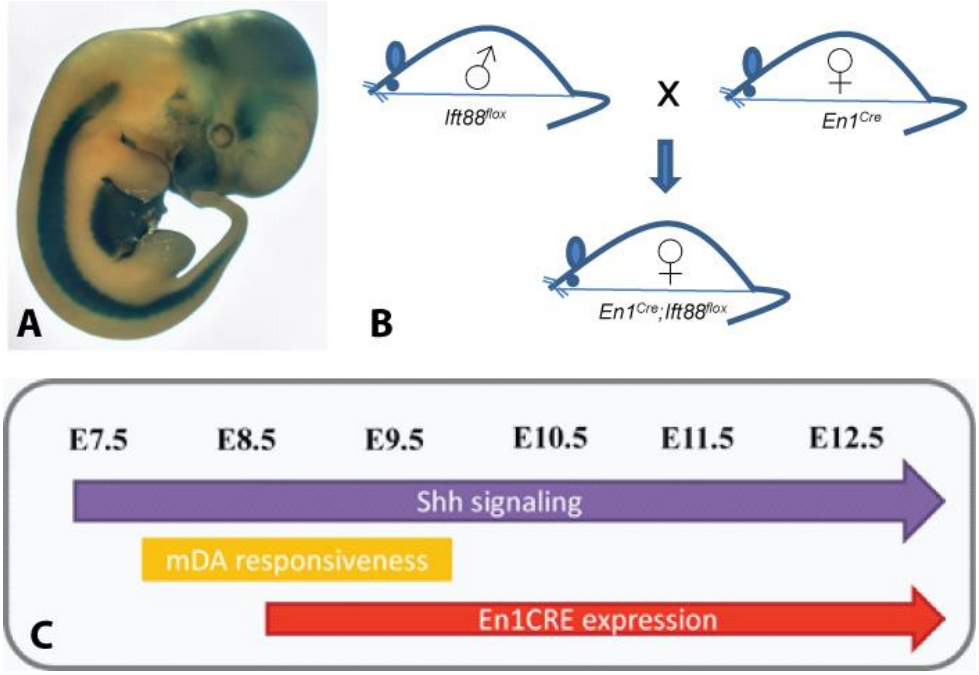

Figure 9. En1-induced *Ift88* knock-out mouse model. *A*, E12.5 embryo showing expression of En1::CRE under the lac-Z promoter. Detection of *En1::CRE* expression is shown in blue. The

following regions are labelled: spinal cord V1 interneurons, the embryonic mesencephalon and rhombomere 1, the ventral ectoderm of the limbs, a subset of somite cells, and some mesoderm-derived tissues. ***B***, Schematic representation demonstrating the cross generating $En1^{CRE}$; $Ift88^{flox}$ mice used in this study. **C**, Illustration depicting the timeline of conditional gene inactivation using En1::CRE in relation to the timeline of Shh signalling and mDA responsiveness.

Ift88 was conditionally inactivated in the midbrain and anterior hindbrain, as seen in Fig.9A, by crossing a floxed allele of *Ift88* gene to a mouse with a knock-in of the CRE recombinase into the Engrailed 1 (*En1)* locus (Fig.9B). *En1::Cre* expression begins at around embryonic day E8.5; hence *Ift88* inactivation occurs at this time point in *Ift88* cko embryos as illustrated in the time line at Fig.9C.

9.3 Conditional inactivation of *Ift88* in the ventral midbrain leads to loss of primary cilia and defects in ventral midbrain

To investigate whether but also when primary cilia were lost in the midbrain of *Ift88* cko embryos, different developmental stages were examined. Primary cilia were co-labelled with an antibody against Arl13b, a protein localized at the ciliary axoneme, and with an antibody against γ- tubulin recognizing the basal body.

The progressive examination of developmental stages began at E9.5, where a significant loss of primary cilia projecting into the ventricle in *Ift88* cko midbrains was already observed (Fig.10A and B). As a result of this observation, the next stage chosen to examine was one day later at E10.5. Through the same double labelling approach, complete loss of primary cilia was observed at E10.5 (Fig.10F). In addition to this observation, co-labelling of γ-tubulin and an antibody against Ift88, demonstrated a dramatic loss of Ift88-positive cilia at the ventricle of E10.5 embryos (Fig.10D). In order to examine whether these findings were consistent, a later developmental stage was also examined which led to the observation that also at E12.5 midbrains of *Ift88* cko embryos completely lack primary cilia (Fig.10H). SEM was also employed as an independent approach in order to add more confidence to the previous findings regarding the absence of primary cilia in the midbrain of *Ift88* cko. In the E12.5 control embryos (Fig.11A), primary cilia of about 1 μm long were detected projecting into the ventricle as observed in Fig.11C, whereas at the same age SEM images revealed a complete loss of primary cilia in *Ift88* cko embryos (Fig.11D).

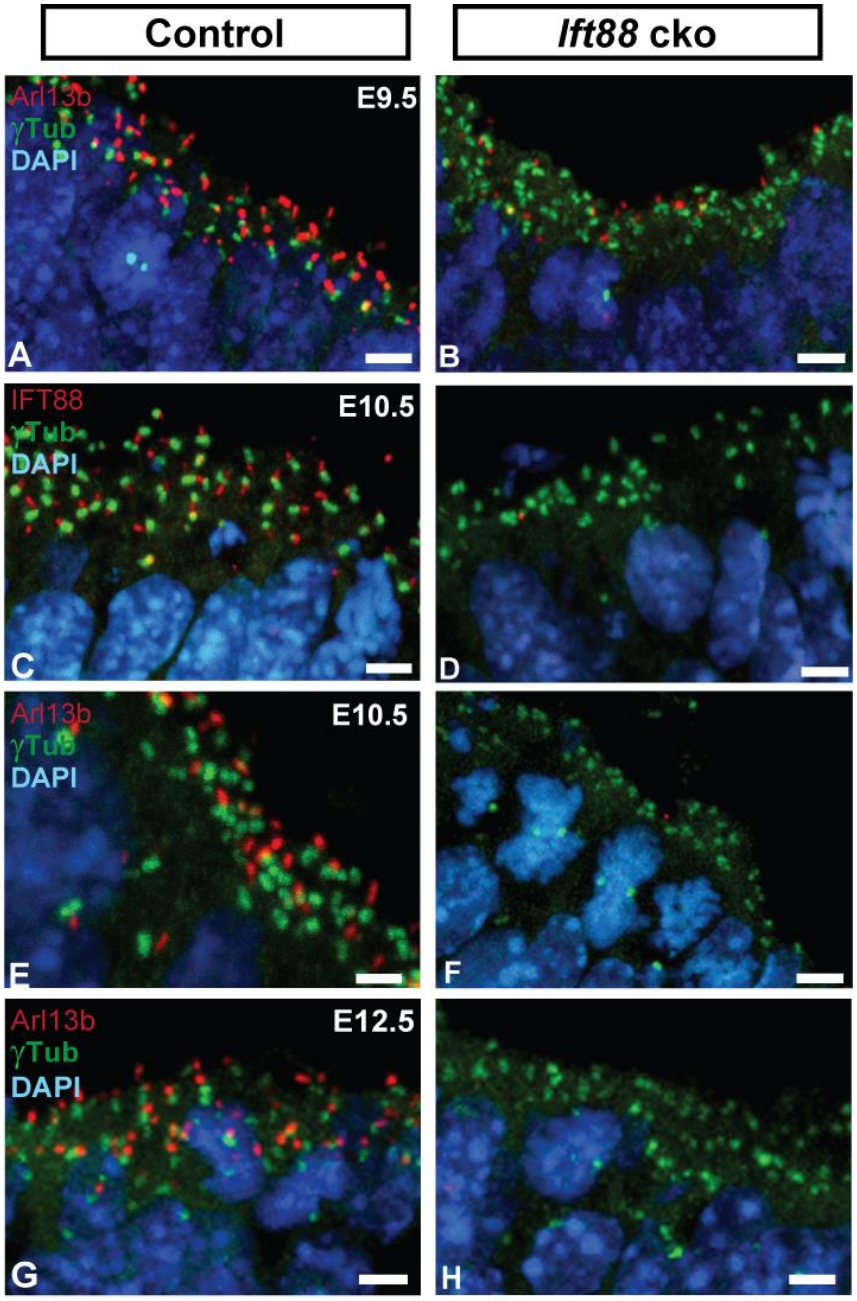

Figure 10. Conditional inactivation of *Ift88* in the ventral midbrain leads to loss of primary cilia and defects in ventral midbrain. Immunofluorescent staining against ciliary marker Arl13b (***A, B, E-H***, red), γ-tubulin (***A-H,*** green) and Ift88 (***C, D***, red) detecting primary cilia at the ventricular surface of the ventral midbrain of control (***A, C, E, G***) and *Ift88* cko (***B, D, F, H***) at E9.5 (***A, B***), E10.5 (***C-F***) and E12.5 (***G, H***) embryos. Blue, DAPI-labelled nuclei. In *Ift88* cko embryos, primary cilia start to disappear at E9.5 and are lost completely at E10.5. Scale bars: **A-H**, 10μm

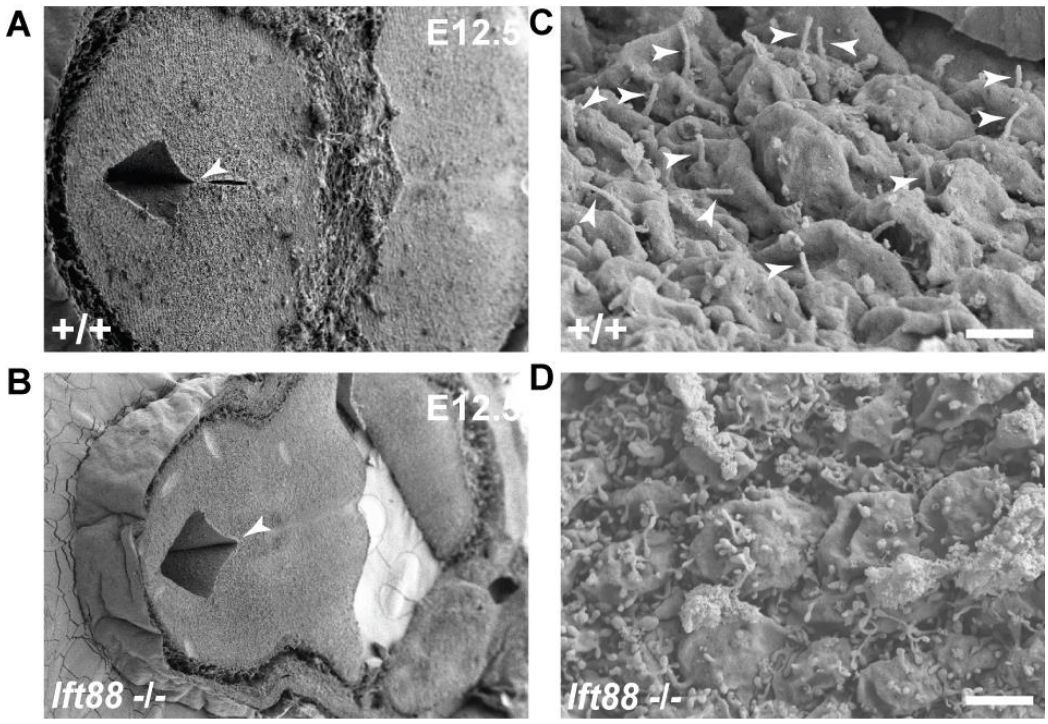

Figure 11. Conditional inactivation of *Ift88* results in a loss of primary cilia in the ventral midbrain. SEM images of the ventral midbrain of E12.5 control (**A, C**) and *Ift88* cko (***B, D***) embryos. Arrowheads in A and B indicate the area imaged in C and D, respectively. Arrowheads in C point to primary cilia projecting into the ventricle, whereas in D primary cilia are lost. Scale bars: ***A, B*** 500 μm; ***C, D***, 1 μm.

As Shh signalling is dependent on primary cilia, we next examined together with our colleague PD Dr. Sandra Blaess of University of Bonn, whether the signaling was affected in the *Ift88* cko mutants. Investigation was done on both E9.5 and E10.5 *Ift88* cko mutants by *in situ* hybridisations for probes *Gli1* and *Gli3* (Fig.12). *Gli1* expression is a readout for high levels of Shh signaling, while *Gli3* expression is downregulated upon high levels of Shh signaling. *Gli1* expression was completely abolished in both time-points (Fig.12B, D) and *Gli3* expression was expanded towards the ventral midbrain (Fig.12F, H) compared to the controls (Fig.12E, G). Both observations taken together, show that indeed Shh signalling is abolished in the ventral midbrain of *Ift88* cko mutants.

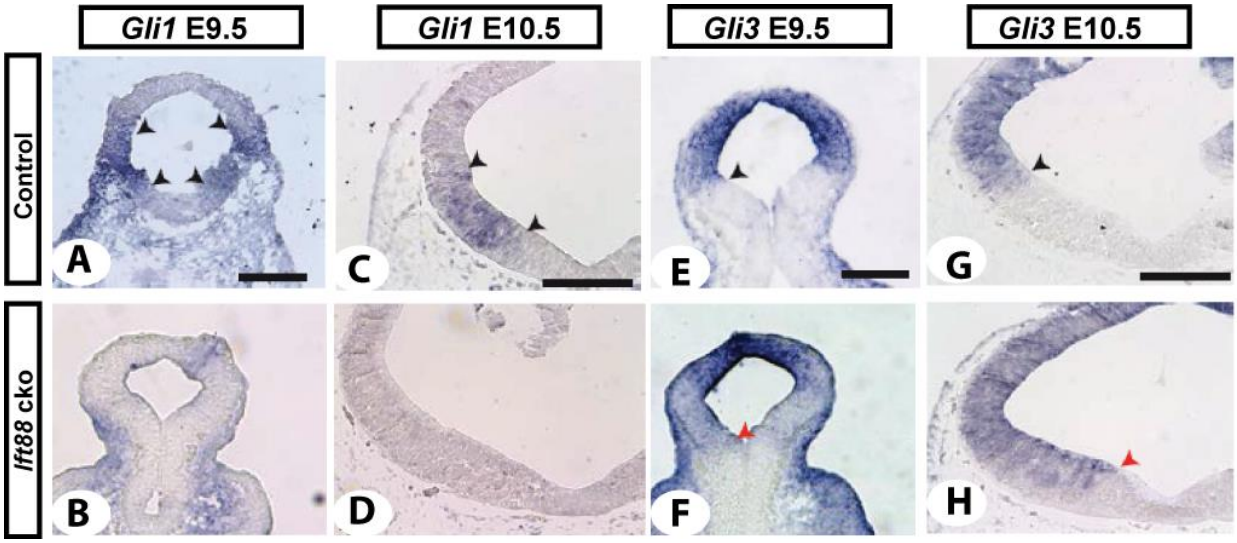

Figure 12. Loss of primary cilia in *Ift88* cko leads to impaired Shh signalling. RNA *in situ* hybridisation for *Gli1* (**A-D**) and *Gli3* (**E-H**) at E9.5 (**A, B, E, F**) and E10.5 (**C, D, G, H**) on control and *Ift88* cko embryos. Black arrowheads indicate the expression domain of each probe in the control, red arrowheads indicate the changes in the expression domains in the *Ift88* cko embryos. Scale bars: ***A-H,*** 200 μm. ISH performed by PD Dr. Blaess and her colleagues at University of Bonn. (Gazea M., Tasouri E. et al., manuscript under review).

9.4 Dopaminergic neuron-generating ventral precursor domain is reduced in *Ift88* cko mutant embryos

As it is already known that Shh signalling is crucial for the development of the ventral midbrain, the next step for our project was to study whether and in what way the lack of primary cilia from E8.5 onwards and the consequent inactivation of Shh signalling affects midbrain development. To assess these questions, we performed *in situ* hybridization for Shh and immunostaining for FoxA2, a transcription factor induced by Shh expression.

At E10.5 a broad Shh expression at the ventral midbrain of the control was observed (Fig.13A) that was significantly reduced in the *Ift88* cko (Fig.13B). Expression of floor plate marker FoxA2 at the same age showed similar reduction pattern in *Ift88* cko (Fig.13D) as the Shh domain. Moreover, expression domains of Lmx1a- a transcription factor induced by Wnt signaling, and Corin, a cell surface protease that is expressed in the medial aspects of the mDA precursor area, were also shown through *in situ* hybridization and immunostaining respectively, to be reduced in *Ift88* cko compared to control (Fig.13F, H).

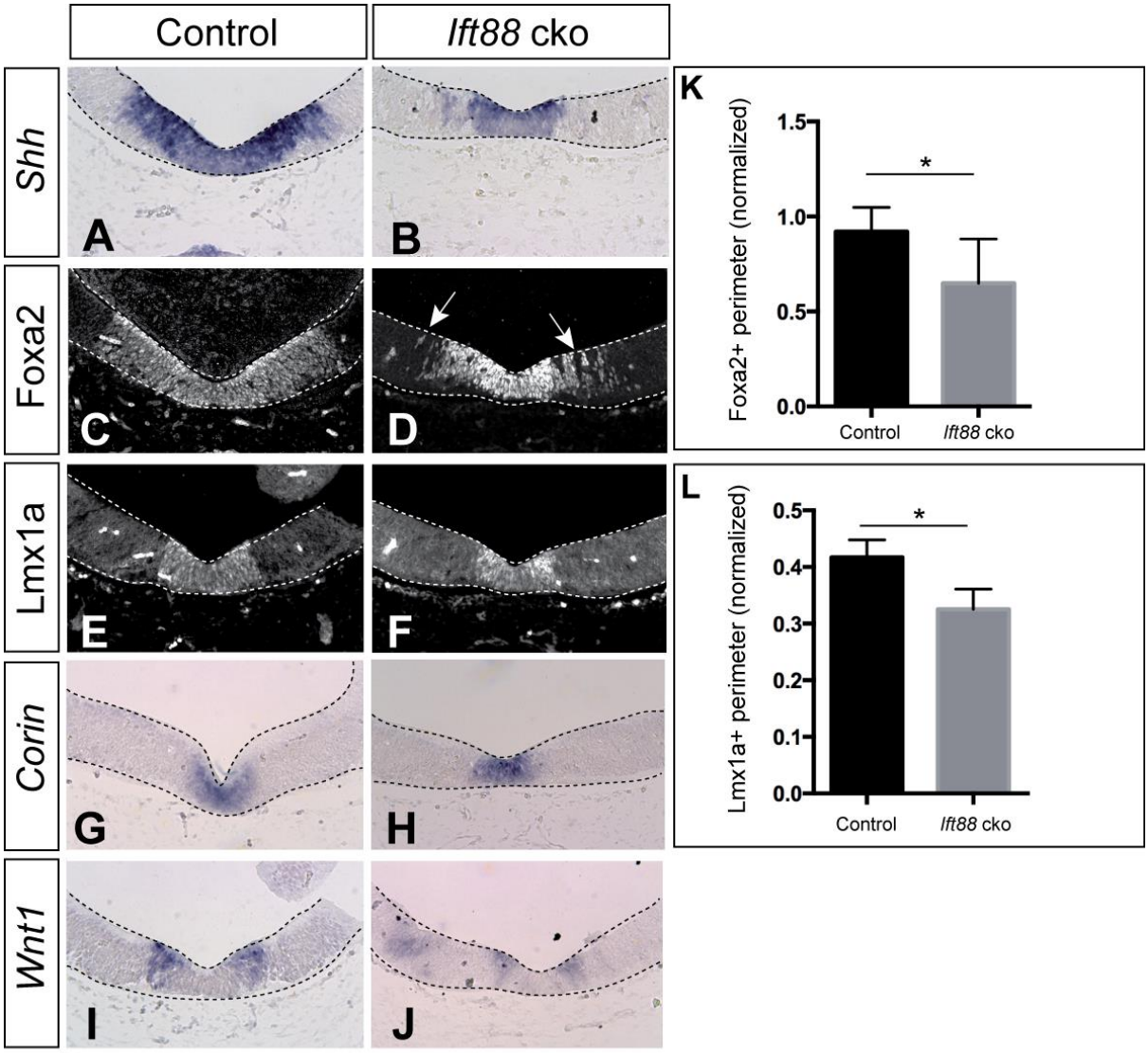

Figure 13. Dopaminergic neuron-generating ventral precursor domain is reduced in size in *Ift88* cko mutants at E10.5. (*A, B, G-J*) RNA *in situ* hybridization on sections of the ventral midbrain of E10.5 wild-type and *Ift88* cko for *Shh* (***A, B***), *Corin* (***G, H***) and *Wnt1* (***I, J***) and (***C-F***) immunostainings of FoxA2 (***C, D***) and Lmx1a (***E, F***). The VZ is outlined in all images (***A-J***). **(*L, M*)** Quantification of the size of the FoxA2 (***L***) and Lmx1a (***M***) expression domains in control and *Ift88* cko at E10.5. Values are means ± SD. The perimeter of the Lmx1a or Foxa2 positive domain was measured and normalized for the perimeter of the ventricle. ANOVA with Tukey's multiple comparison test. n≥3. Foxa2: $F(2,13) = 12.63$, Lmx1a: $F(2,8) = 8.67$, * $p < 0.05$. ***A-J***. Scale bars: 100 μm. ISH, immunostainings and quantification performed by PD Dr. Blaess and her colleagues at University of Bonn. (Gazea M., Tasouri E. et al., manuscript under review).

Quantification of the size of FoxA2 and Lmx1a expression domains revealed a significant reduction of the domains in Ift88 cko ventral midbrains ad compared to the controls (Fig.13K, L).

Nkx6-1 domain, lateral to the Lmx1a domain, was also examined but was not shown to be altered (data not shown). However, as the FoxA2 domain was significantly reduced in size, the FoxA2/Nkx6-1-double positive domain was almost completely not obvious in the *Ift88* cko embryos compared to the controls. These data reveal that after E9.0 *Ift88* expression is necessary for the broad expression of the Shh/FoxA2 positive domain. Nevertheless, they also suggest that at the same time *Ift88* is indeed important in regulating the size of the mDA precursor domain but not critical for its induction.

9.5 Wnt expression and signalling is reduced in the midbrain of *Ift88* cko embryos

In addition to these four markers, Wnt1 was also used as it is expressed laterally in the mDA precursor domain and undoubtedly has a major role in the proliferation and differentiation of the mDA precursor population (Yang et al., 2013). Wnt1 domain was still present in *Ift88* cko embryos at E10.5; however its expression levels had decreased (Fig.13I, J). Furthermore, the expression levels of other canonical and non-canonical Wnt signaling factors were also examined at the mRNA level.

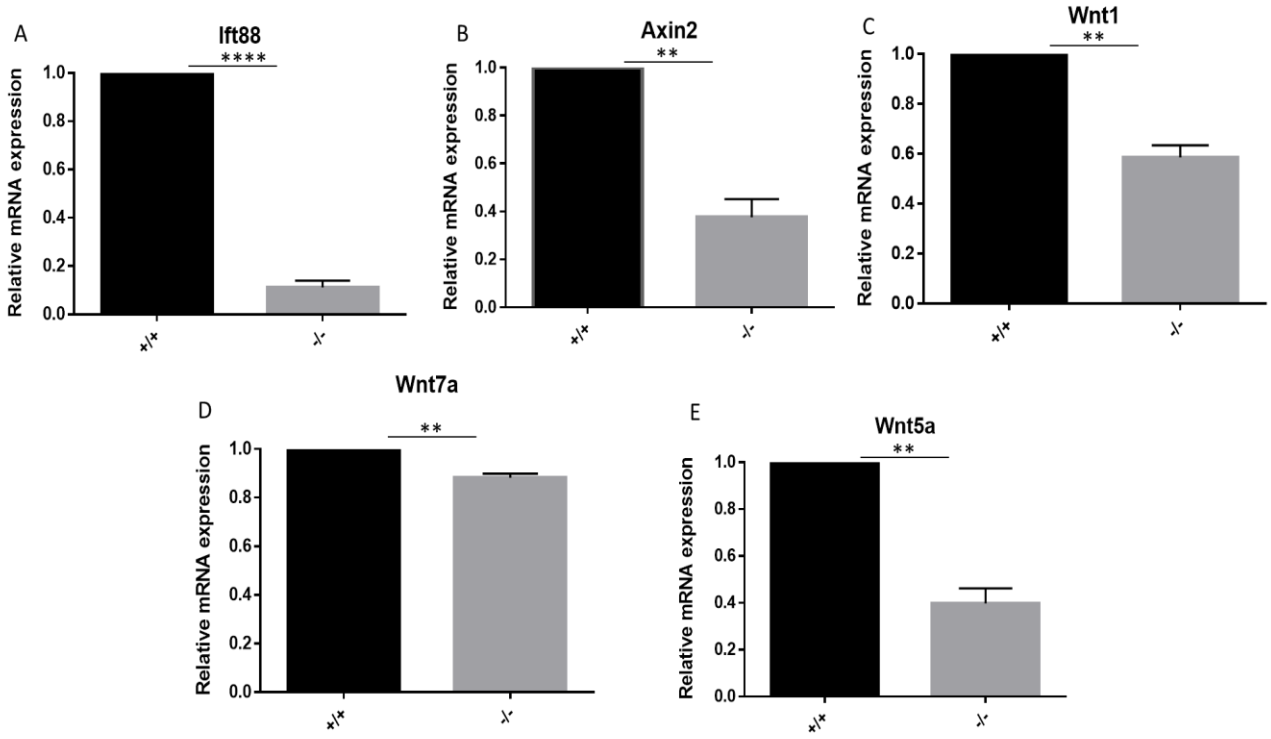

Figure 14. Wnt expression and signaling is reduced in the ventral midbrain of *Ift88* cko at E11.5 embryos. A-E Quantification of the expression of Ift88 and of canonical and non-canonical Wnt

signaling pathway components in the midbrain of *Ift88* cko embryos compared to control littermates, as resulted from qPCR experiments. **A**, Ift88 expression; **B**, Axin2 (Wnt signaling readout) expression; **C**, Wnt1 expression; **D**, Wnt7a expression; **E**, Wnt5a expression. Values are given as mean percentage ± SEM. Student's t-test used for all: n=4, ** p< 0.01, **** p <0.0001.

Manually microdissected midbrain tissue of E11.5 *Ift88* cko embryos was used to assess the mRNA levels of *Wnt1, Wnt5a, Wnt7a and Axin2* through real-time quantitative PCR. Littermates of the *Ift88* cko embryos were used as controls. The mRNA levels of *Ift88* in both control and *Ift88* cko embryos were also examined in order to evaluate the effectiveness of the $En1^{CRE}$-mediated knockout but also the specificity of the microdissection.
In case tissue surrounding the midbrain was also used for RT qPCR then the results of this experiment would be compromised as Ift88 levels in *Ift88* cko embryos would not be significantly reduced. Expression of *Ift88* mRNA levels was reduced by 88.8% ± 2.7% ($p < 0.0001$) demonstrating that the knockout was indeed effective and very importantly that the microdissection was a reliable tool (Fig. 15A). Expression of *Axin2*, a readout of Wnt signalling, was reduced by 62.4% ± 7.5% ($p = 0.0037$) compared to wild-type controls (Fig.15B). Likewise, expression of both *Wnt1* and *Wnt5a* was also significantly reduced by 41.45% ± 4.8% ($p = 0.0033$) and 60.2% ± 6.4% ($p = 0.0026$), respectively (Fig.15C, E). Finally, *Wnt7a* expression levels were also decreased by 11.78% ± 1.6% ($p = 0.0054$) (Fig.15D). For all comparisons Student's t-test was used.

9.6 Tyrosine hydroxylase-positive midbrain dopaminergic neurons are reduced in *Ift88* cko embryos

Since we observed that the mDA progenitor domain in *Ift88* cko embryos is reduced, the inevitable question regarding the effect that this would have on mDA neurons arose. By E13.5, most mDA neurons have already been differentiated and therefore are TH-positive. At this age, antibody staining for TH in control and *Ift88* cko embryos demonstrated a significant loss of TH-positive neurons in the ventral midbrain of the latter (data not shown, WT: 928.8 ± 64.1 cells, *Ift88* cko: 627.5 ± 21.7 cells, n = 4, Student's t-test: $p = 0.0043$). More specifically *Ift88* cko embryos seem to be missing the medially located dopaminergic neurons. Co-labelling for TH and FoxA2 showed that these TH-positive neurons that were still present in the *Ift88* cko embryos were also positive for FoxA2. This observation demonstrates that despite the loss of a large population of TH-positive neurons, the ones still

present in the midbrain of *Ift88* cko display the proper mDA neuronal phenotype. In order to assess whether this phenotype is still present or not at later embryonic stages, E18.5 midbrains of control and *Ift88* cko embryos were co-stained with antibodies against TH and FoxA2 as previously (data not shown). Quantification of TH-positive cells in the ventral midbrains at E18.5 revealed that the number of TH-positive cells was significantly reduced in *Ift88* cko in comparison to the control midbrains. This shows that the phenotype persists in later stages as well and also in nuclei such as VTA and the laterally located SN, TH- and FoxA2-positive mDA neurons, even though still present, are less dense compared to the controls (data not shown).

In order to confirm what these results suggest regarding the correct neuronal phenotype that the surviving mDA neurons show at E13.5, dopamine transporter (DAT) and transcription factors Nurr1 and Pitx3 were used (Blaess and Ang, 2014). As a result, the same neurons that were positive for TH were also expressing the three other markers used (Fig.15). Previous studies have shown that the FoxA2/Shh/Nkx6-1 triple-positive domain possibly is the precursor domain for neurons later localized in the red nucleus (Prakash et al., 2009; Blaess et al., 2011). Due to the significantly reduced in size Shh and FoxA2 domain in E10.5 *Ift88* cko embryos, we assumed that the neurons in the red nucleus would not form at later stages in the mutant embryos.

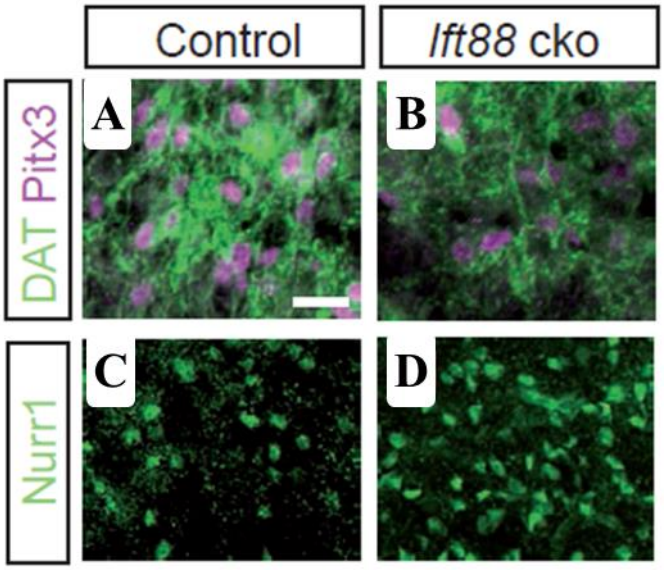

Figure 15. mDA neurons still present in *Ift88* cko at E18.5 retain their appropriate neuronal identity. Immunofluorescent stainings against antibodies for DAT (green) and Pitx3 (magenta) (**A, B**) and for Nurr1 (green) (**C, D**) on ventral midbrains of control and *Ift88* cko at E18.5. Immunostainings performed by PD Dr. Blaess and her colleagues at University of Bonn. (Gazea M., Tasouri E. et al., manuscript under review).

9.7 Expression of a constitutively-active Shh receptor, Smoothened, results in the ventralization of the embryonic midbrain

The midbrain phenotype observed in the *Ift88* cko mutants is strongly comparable to the midbrain phenotype seen in the *Gli2/Gli3* double cko mutants by our collaborator Dr. S. Blaess. Conditional inactivation of *Gli2* and *Gli3* transcription factors using $En1^{Cre}$ led to the abolishment of *Gli1* expression at both E9.5 and E10.5, as seen in the *Ift88* cko mutants, reflecting the inactivation of Shh signalling. Examination of the ventral midbrain precursor domain using markers similar to the ones used in this study in *Ift88* cko such as Shh, FoxA2, Lmx1a and Corin revealed a dramatic reduction in size of the precursor domain. As a consequence of this, the population of TH-positive mDA neurons was reduced at both E12.5 and E18.5 (Gazea M., Tasouri E. et al., 2015, in revision). The similar midbrain phenotype observed in *Gli2/Gli3* and *Ift88* cko mutants suggests that the main cause of the reduced size of the mDA precursor domain in the latter is the inactivation of Shh signalling due to the loss of primary cilia. In order to pinpoint at what level of the Shh signalling pathway the loss of cilia interferes, a constitutively-active *Smo* mutant construct (Fig.16) was expressed in the midbrain of *Ift88* cko mice after E8.0 when $En1^{Cre}$ begins its expression.

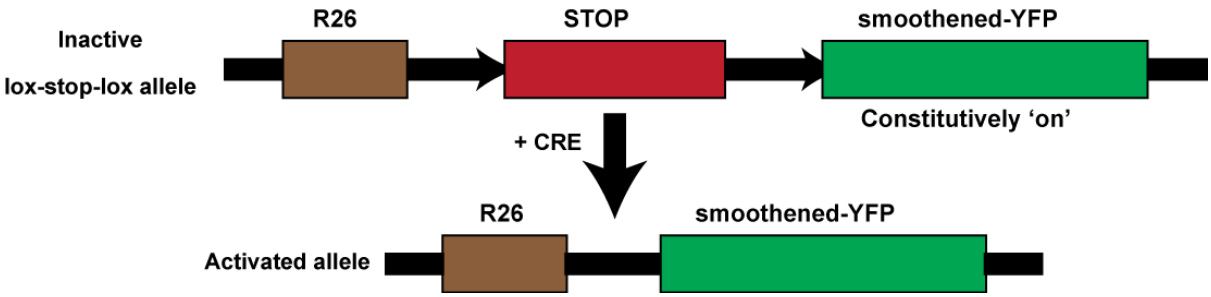

Figure 16 . An explanatory scheme on how conditional activation of *Smo* gene occurs through Cre-mediated removal of a transcription stop cassette. Once the Cre is introduced into the system, the stop cassette is removed and *Smo* becomes constitutively active.

This could demonstrate whether the cilia loss affects the formation of Gli1 activator and repressor, and thus leading to the midbrain phenotype observed in *Ift88* cko embryos. The mutant mice generated from this cross ($En1^{Cre/+;}$ $R26^{SmoM/+;}$ $Ift88^{flox/flox}$ termed *SmoM2/Ift88 cko*) were compared to the one in which the constitutively-active form of Smo was expressed in a wild-type background (($En1^{Cre/+;}$ $R26^{SmoM/+}$ termed *SmoM2* ca).

E12.5 *SmoM2* ca embryos had a midbrain overgrowth phenotype visible during dissection (Fig.17A). On the other hand, littermates that were *SmoM2/Ift88* cko showed normal brain size during dissection. Examination of the *SmoM2* ca and *SmoM2/Ift88* cko E12.5 embryos for primary cilia, using Arl13b to stain the ciliary axoneme and γ-tubulin to detect the basal body, revealed that primary cilia were still present as expected in the *SmoM2* ca and absent in the *SmoM2/Ift88* cko embryos (Fig.17B).

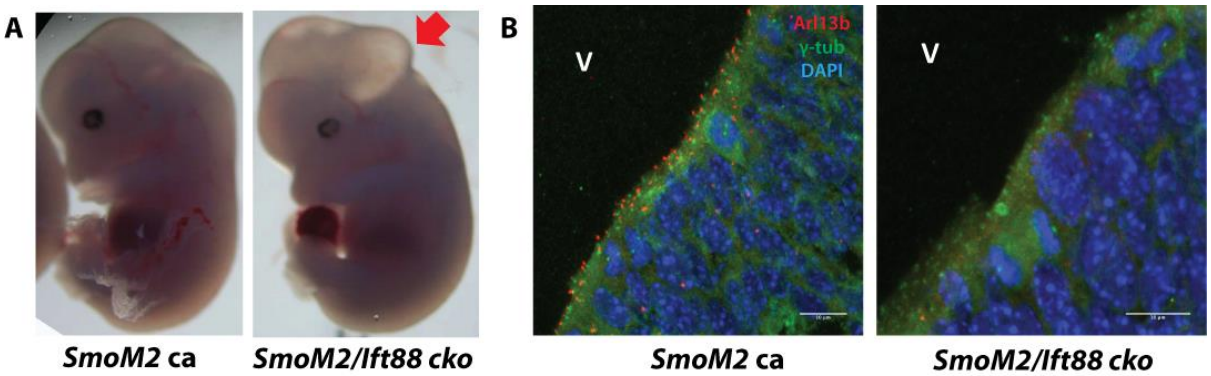

C

M2 -SMO	En1^{Cre}	Ift88	Overgrowth
+	+	flox/wt or wt/wt	13
+	+	flox /flox	0

Figure 17. Constitutive activation of Smo gene results in a midbrain overgrowth in *Ift88* cko.
A, E12.5 embryos in which the left one has been genotyped as *SmoM2* ca., therefore the constitutively-active form of *Smo* is expressed in a wild-type *Ift88* background and the right embryo has been genotyped as *SmoM2/Ift88* cko. A midbrain overgrowth is observed in the right embryo. **B**, Immunofluorescent staining for Arl13b (red) and γ-tubulin (green) on the ventral midbrain of E12.5 *SmoM2* ca. and *SmoM2/Ift88* cko embryos. DAPI-labelled nuclei in blue. Primary cilia are present in *SmoM2* ca. but absent in *SmoM2/Ift88* cko. **C**, Table listing the numbers of embryos demonstrating a midbrain overgrowth phenotype and their respective phenotypes among the collected embryos.

From all the E12.5 embryos collected from this particular cross, thirteen that were genotyped as *SmoM2* ca exhibited the midbrain overgrowth phenotype, whereas none from the ones genotyped as *SmoM2/Ift88* cko shared this type of overgrowth as listed in the table in Fig.17C.

In situ hybridization for *FoxA2* (Fig. 18F) and *Shh* (Fig.18D) on E10.5 *SmoM2* ca embryos revealed that their domain was dorsally expanded. In addition to this result, *Gli1*-positive domain had also shifted dorsally in the midbrain of E10.5 *En1*$^{Cre/+}$; *R26*$^{SmoM/+}$ embryos

(Fig.18A) compared to control (Fig.18B) demonstrating that indeed Shh expression was expanded dorsally. Conversely, *Lmx1a* domain was found to still be restricted to the ventral midbrain (Fig.18H) but when compared to the control (Fig.18G) it was shown to be larger in size. The same increase in size was also true for the *Wnt1*-positive domain (Fig.18J). However, in the *SmoM2/Ift88* cko mutants, where cilia were no longer present, the *Shh* and *FoxA2* expression domain remained restricted to the ventral midbrain (Fig.18C, E) while *Lmx1a* and *Wnt1* expression was restrained to the medial ventral midline (Fig.18G, I) as in the *Ift88* cko (Fig.13 F, J). *Gli1* expression was not detected in the midbrain of *SmoM2/Ift88* cko embryos (Fig.18A) which falls into line with the absence of cilia. Furthermore, the scattered appearance of *FoxA2*-positive cells in the lateral edges of the *FoxA2* domain (Fig.18E) and the sizes of *FoxA2* and *Lmx1a* domains (Fig.18E, G) in the midbrain of *SmoM2/Ift88* cko embryos resembled the phenotypes observed in *Ift88* cko mutants (Fig.13D, F).

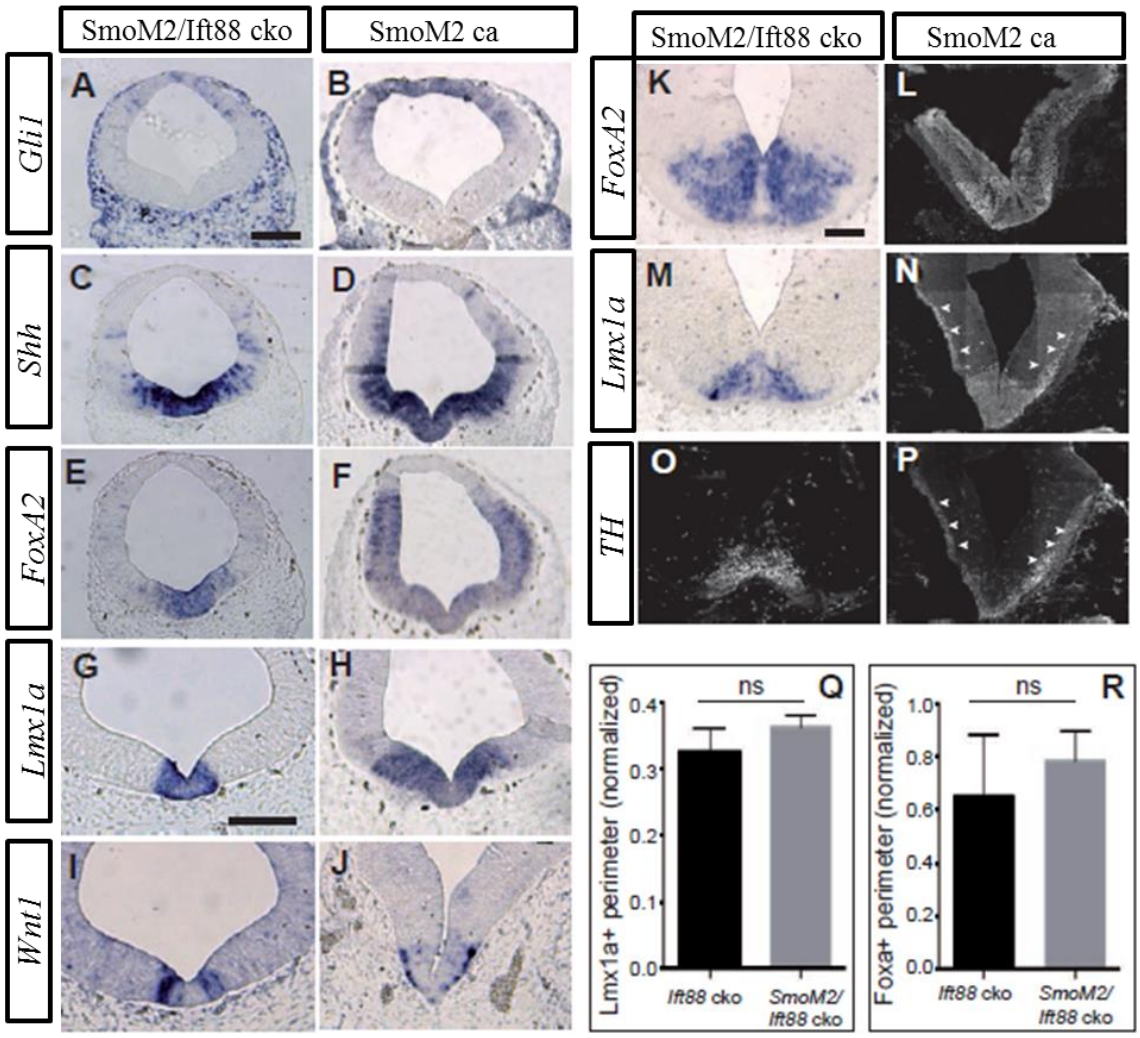

Figure 18. Primary cilia are crucial for the activation of Shh signaling pathway, downstream of Smo. A-K, **M** RNA *in situ* hybridization for *Gli1* (**A, B**), *Shh* (**C, D**), *FoxA2* (**E, F,K**), *Lmx1a* (**G, H**,

M) and *Wnt1* (**I, J**) on *SmoM2/Ift88* cko and *SmoM2* ca mutant embryos at E10.5 (**A-J**) and E12.5 (**K-P**). **L**, **N-P**, Immunofluorescent staining using antibodies against FoxA2 (**L**), Lmx1a (**N**) and TH (**O, P**) on *SmoM2/Ift88* cko and *SmoM2* ca mutant embryos at E12.5. **Q, R** Quantification of the size of Lmx1a- (**Q**) FoxA2- (**R**) domains in E10.5 *Ift88* cko and *SmoM2/Ift88* cko. The perimeter of each domain was measured and normalized to the perimeter of the ventricle. Values are means ±SD. Student's t-test. For both domains n≥ 3. Constitutive activation of the Shh pathway in *SmoM2* ca mutant embryos, where primary cilia are still present hence Shh signaling is still active, leads to a ventralization of the midbrain and to the abnormal distribution of mDA precursors and neurons. On the other hand, conditional activation of *Ift88* in the *SmoM2* background mirrored the phenotype observed in *Ift88* cko embryos. These observations indicate that activation of the Shh pathway downstream of Smo is dependent on the presence of primary cilia. Scale bars: **A-J**, 200 μm; **K-P**, 100 μm. ISH, immunostainings and quantification performed by PD Dr. Blaess and her colleagues at University of Bonn. (Gazea M., Tasouri E. et al., manuscript under review).

However, analysis of FoxA2-positive domain in the midbrain of E12.5 *SmoM2* ca embryos showed FoxA2 expression in its dorsal-lateral level (Fig.18L). Examination of TH- and Lmx1a-positive mDA neurons revealed abnormal distribution in *SmoM2* ca (Fig.18N, P) compared to the control. Yet, analysis of FoxA2, Lmx1a and TH in the S*moM2/Ift88* cko mutants found that their domains were restricted in the ventral midbrain as normal (Fig.18K, M, O). All the data collected from this set of experiment involving the expression of a constitutively-active Shh receptor, Smoothened, lead to the conclusion that the loss of cilia in *Ift88* cko results in the abolishment of all Shh signaling downstream Smo.

9.8 Conditional inactivation of *Kif3a* in the ventral midbrain leads to a delayed loss of primary cilia and only subtle defects in mDA neuron development

In order to exclude the possibility that the phenotype observed in mDA neurons in *Ift88* cko mice is due to a non-ciliary function of Ift88 itself, another ciliary mutant was employed for an Ift88-independent approach. *Kif3a* was conditional inactivated in the embryonic midbrain using the same *En1::CRE* approach previously used in this study ($En1^{Cre/+}$, $Kif3a^{flox/flox}$, which will be referred to as *Kif3a* cko). *Kif3a* encodes a component of the kinesin-2 motor that is necessary for the maintenance of the primary cilium as it is involved in the anterograde transport of protein cargo along the axoneme of the primary cilium but also for ciliogenesis (Pedersen and Rosenbaum, 2008).

Detection of primary cilia in *Kif3a* cko embryos in a progressive developmental manner, i.e. at E9.5, E10.5 and E12.5, was done by double labelling primary cilia using Arl13b and γ-tubulin (Fig.19) as described previously in this thesis.

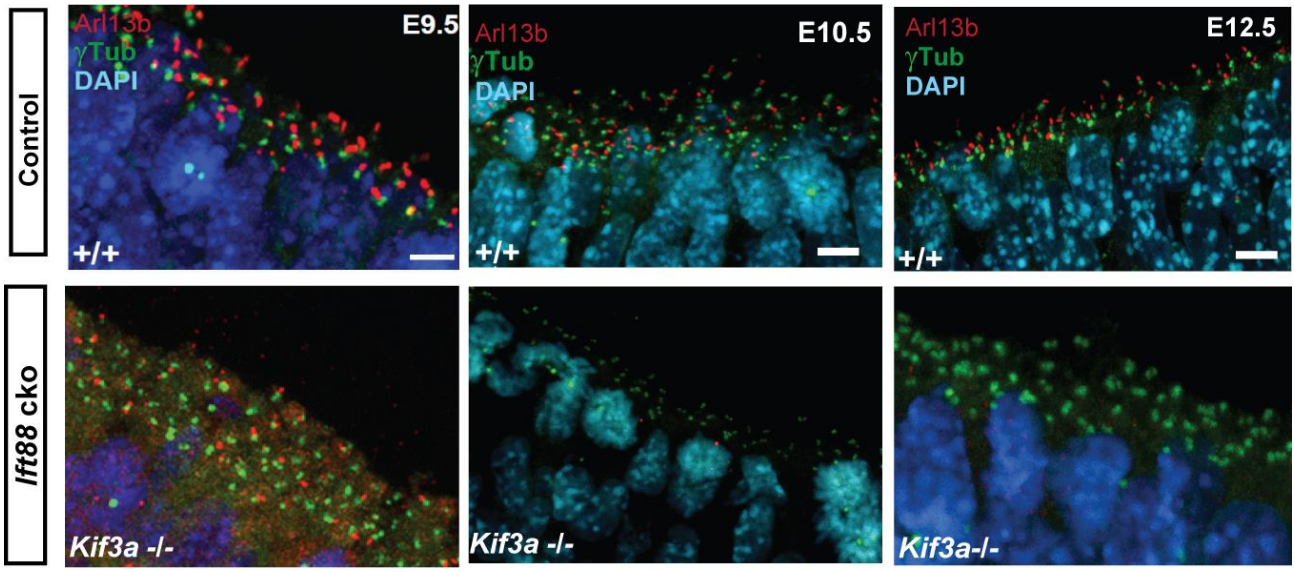

Figure 19. Conditional inactivation of *Kif3a* in the ventral midbrain leads to a relative late loss of primary cilia. Immunofluorescent staining against ciliary marker Arl13b (red), γ-tubulin (green) on the ventral midbrain of control and *Kif3a* cko at E9.5, E10.5 and E12.5. DAPI-labelled nuclei in blue. Top panel shows the presence of primary cilia in the ventral midbrain of E9.5, E10.5 and E12.5 control embryos, whereas the lower panel clearly shows the gradual decrease of the number of primary cilia in the midbrain of E9.5, E10.5 and E12.5 *Kif3a* cko embryos.

Analysis of E9.5 *Kif3a* cko embryos demonstrated only a partial loss of primary cilia projecting into the ventricle, in contrast to *Ift88* cko embryos (Fig. 19). One day later in development, at E10.5, a total loss of primary cilia was observed as seen in *Ift88* cko mutants. An additional time-point was also examined, E12.5, where, as expected, primary cilia were absent in *Kif3a* cko.

In order to check whether this slightly delayed in comparison to *Ift88* cko cilia loss would have any effects on Shh signaling pathway, *in situ* hybridization for *Gli1* and *Gli3* were performed. *Gli1* expression was still detected in the midbrain of E9.5 *Kif3a* cko embryos (Fig.20B) indicating that the Shh signaling was not completely inactivated yet. However, by E10.5 *Gli1* was no longer detected in *Kif3a* cko midbrain (Fig.20E) similarly as in *Ift88* cko mutants (Fig.12D). Another indication proving that Shh signaling was not fully inactivated in

Kif3a cko midbrain was the *Gli3* expression at E9.5 (Fig.20C), which was restrained in the dorsal midbrain, unlike in *Ift88* cko midbrain (Fig.12F) where it was expanded ventrally.

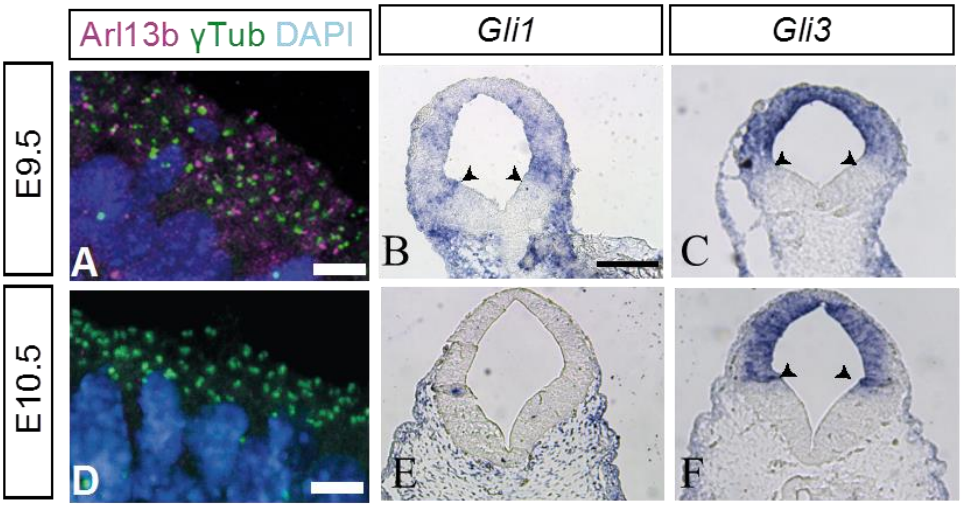

Figure 20. Relatively late loss of primary cilia in *Kif3a* cko results in delayed inactivation of Shh pathway. A, B Immunofluorescent staining for Arl13b (magenta) and γ-tubulin (green) on the ventral midbrain of *Kif3a* cko at E9.5 (**A**) and E10.5 (**B**) showing that conditional inactivation of *Kif3a* leads to a later loss of primary cilia than in *Ift88* cko embryos. **B, C, E, F** RNA *in situ* hybridizations in *Kif3a* cko embryos for *Gli1* (**B, E**) and *Gli3* (**C, F**) showing that Shh pathway is still active at E9.5 and its inactivation occurs one day later than in *Ift88* cko, at E10.5. Scale bars **A, D**, 10 μm; **B, C, E, F**, 200 μm. ISH performed by PD Dr. Blaess and her colleagues at University of Bonn. (Gazea M., Tasouri E. et al., manuscript under review)

E10.5 *Kif3a* cko embryos were also studied to assess expression of *FoxA2*, *Lmx1a* and *Corin* domains (data not shown) in order to compare them to the observations made in *Ift88* cko mutants (Fig.13D, F, H respectively). All three domains were reduced in comparison to the controls. Quantification of FoxA2- and Lmx1a-positive domains at E10.5 showed significant reduction of both domains in *Kif3a* cko compared to E10.5 controls.

Interestingly, investigation of TH-positive mDA neurons in both E13.5 and E18.5 *Kif3a* cko midbrains showed no reduction in their number compared to the control as was also seen by the quantification of TH-positive cells at E18.5 (data not shown). Moreover, the mDA neurons detected by TH also expressed other mDA neuronal markers such as Lmx1a and FoxA2 at E13.5 and Pitx3, Nurr1 and DAT at E18.5 (data not shown).

Taken together, conditional inactivation of *Kif3a* displayed a slightly later disappearance of primary cilia projecting into the ventricular zone of the ventral midbrain and more subtle

defects in the development of ventral midbrain as proven by the normal number of TH-positive mDA neurons compared to the *Ift88* cko mutants.

10 Discussion

10.1 Primary cilia and Shh in midbrain mDA development

The first unclear spot in current literature that this project embarked to lighten was the simple question regarding the identity of cells bearing primary cilia in the ventricular zone of the ventral midbrain. A report focusing on the ciliopathy Joubert syndrome, published only few years ago, clearly showed that primary cilia are present in the midbrain of control mouse embryos at E11.5 using the ciliary marker Arl13b (Lancaster et al., 2011). However, as the identity of the cells from which the primary cilia were projecting into the ventricular zone was not mentioned in the current literature I performed two set of stainings, against nestin and against BLBP- both being radial glial markers- in order to determine it. The stainings as seen in Fig.1A and Fig.1B showed that primary cilia, detected using Arl13b, are projecting into the midbrain ventricle from radial glial-like precursors present in the ventricular zone.
Furthermore, previous studies have shown that Shh is important for the induction of many neuronal subtypes as it is expressed at the floor plate of the neural tube during development (Briscoe and Ericson, 2001). In addition to this literature knowledge, more recent publications revealed the significant role that primary cilia have in the patterning of spinal cord. Mouse mutants in proteins involved in ciliary function such as Ift172 (Huangfu et al., 2003), Ift57 (Houde et al., 2005), Ift52 (Liu et al., 2005), Dync2h1 (Huangfu and Anderson, 2005), Ftm (Vierkotten et al., 2007), Ift 144 (Liem et al.., 2012), Ift25 (Keady et al., 2012) but also of our protein of interest Ift88 (Huangfu et al., 2003). The results demonstrated in the previous chapter of this thesis show similar outcome with the findings from all these mutants mentioned above. Many of these mutants were characterized by a loss of floor plate marker but also of low or no expression of Shh at the floor plate. Another common feature of these mutants is the display of a loss of Shh signaling. This finding was demonstrated in these studies by the reduced expression of downstream targets of Shh pathway, such as *Ptch1* and *Gli1* and by defects in neuronal determination. In addition to these three results, neuronal subtypes, such as V3 interneurons and motor neurons, which are normally located ventrally at the spinal cord, were lost in these mutants. Our results demonstrate that in the ventral midbrain of the conditional *Ift88* knock-out, the domains of floor plate markers FoxA2, Lmx1a and Corin are significantly reduced in size in comparison to the control. Also, in line with literature findings of the mutants mentioned above, Shh floor plate expression in *Ift88*

cko already at E10.5, about two days after inactivation of *Ift88*, is severely reduced. As seen from the results of the *in situ* hybridization for *Gli1*, its expression is completely absent therefore Shh signaling is inactivated in *Ift88* cko. Importantly, we also observed in the ventral midbrain of *Ift88* cko the loss of a neuronal population, in this case, the mDA neuronal population. These observations seem to be the consequences of the loss of primary cilia in the midbrain, due to the inactivation of *Ift88*, which as it has been shown in the results section, begins already at E9.5, just one day after En1::CRE expression starts, and is completed one day later at E10.5. Also, the use of another ciliary mutant in our study, namely the *Kif3a* cko, and the similar outcome that cilia loss presented in the midbrain of this mutant regarding the reduced size of Lmx1a and FoxA2 expression domains, further strengthens the argument that indeed this particular phenotype can be attributed to the absence of primary cilia. However, it was indeed surprising that later investigation of the mDA neuronal population in the two mutants, *Ift88* and *Kif3a* cko, presented two different outcomes, as only *Ift88* cko mutants displayed a reduction in the number of mDA.

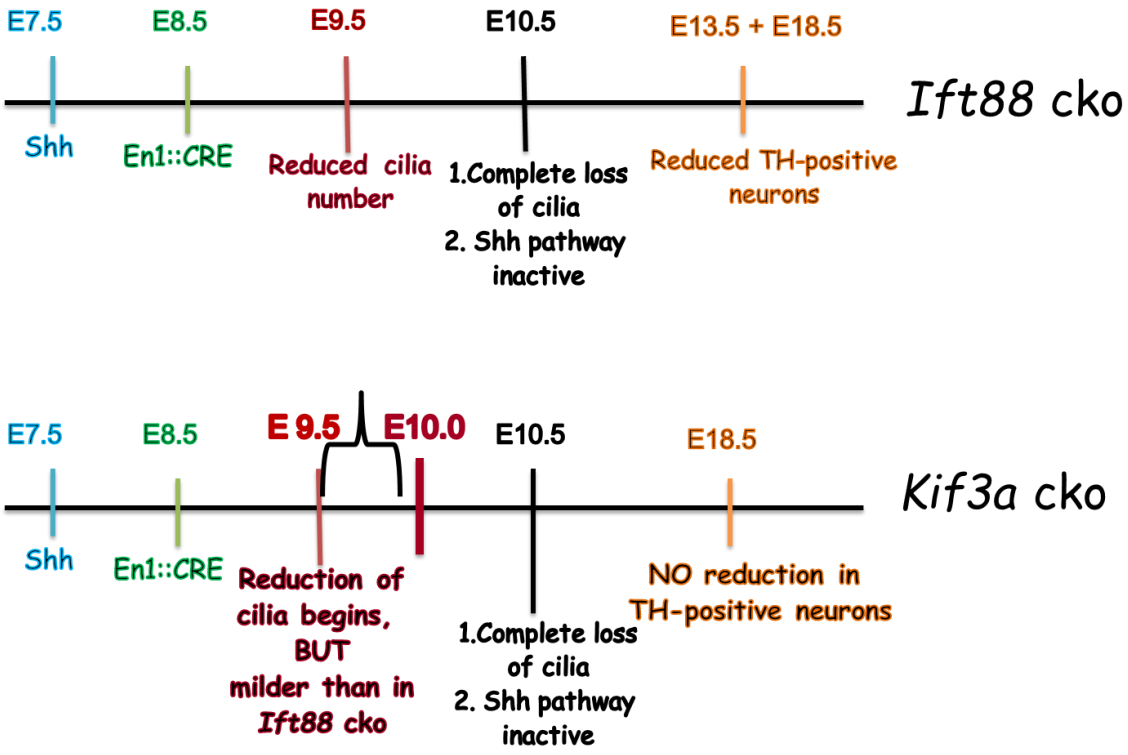

Figure 21. Timeline showing the different timing of cilia loss in *Ift88* and *Kif3a* cko and the resulting effect on the development of mDA neurons. Top timeline shows that strong reduction of cilia in *Ift88* cko occurs already at E9.5 and is completed by E10.5. This leads in inactivation of Shh

pathway and in a significant reduction of TH-positive neurons at E13.5 and E18.5. **Lower timeline (Fig.21)** demonstrates that the delayed loss of primary cilia in *Kif3a* cko might be the reason for the very subtle phenotypes observed regarding mDA neurons at later stages.

Investigation regarding mDA neurons in *Kif3a* cko mutants at E18.5 revealed neither loss of this neuronal population nor any disorganization in their distribution. This difference between the two ciliary mutants used in this study is potentially explained by the slightly different timing of primary cilia loss in the two cko (Fig.21). As shown in *Ift88* cko mutants, the number of primary cilia is already drastically reduced at E9.5, with their loss being completed by E10.5. On the other hand, at E9.5 primary cilia are still present and only a slight reduction in their number is observed in the midbrain of *Kif3a* cko mutants. However, also in *Kif3a* cko mutants primary cilia are entirely absent at E10.5.

Since primary cilia loss is undoubtedly associated with Shh inactivation, it is possible that the short window between the timing of cilia loss in *Ift88* cko and *Kif3a* cko is critical for the later generation of mDA neurons. It seems that inactivation of *Ift88* and by extension inactivation of *Shh* before E9.5 is the key factor that causes the difference between the two mutants. Inactivation of Shh in *Kif3a* cko mutants occurs after E9.5 and as it was shown by staining against TH at E13.5 and E18.5, it only led to a short-lived effect on the generation of mDA precursors and neurons. In support of this explanation of our results, recently published data demonstrate merely a temporary reduction in the size of the mDA precursor domain and later at the number of mDA neurons when inactivation of Shh signaling occurs around E9.5 (Hayes et al., 2013). Moreover another study showed that if Shh signaling is ectopically activated in the floor plate, the number of mDA progenitors is transiently increased (Tang et al., 2013). Therefore the data presented in this thesis regarding the absence of primary cilia and the effect that this has on mDA neurons indicate that functional primary cilia are essential for mDA precursors before E9.5.

A number of studies have examined the role of Shh signaling in the development of not only the mDA neurons but also of other neuronal populations such as the cerebellar granule cells. Recent publications looking into the development of the cerebellum showed that Shh signaling is important for the expansion of the precursor pool which would then give rise to cerebellar granule cells (Corrales et al., 2004; Corrales et al., 2006; Lewis et al., 2004). More publications in the same field also showed that primary cilia are required for cerebellar development and for the expansion of the cerebellar granule cell precursors. Conditional inactivation of *Kif3a* led to the removal of primary cilia from the surface of cerebellar granule

cell precursors and the disruption of cerebellar development. The observed cerebellar defects and the loss of cerebellar granule neurons were caused by the inactivation of Shh signaling (Spassky et al., 2008). In addition to this study, it had been previously shown that loss of either *Ift88* or *Kif3a* through a CNS-specific ablation caused cerebellar hypoplasia and foliation. This was attributed to the effect that cilia loss had in the expansion of the progenitor pool (Chizhikov et al., 2007). In one of the studies, *Smo* was conditionally inactivated from the cerebellar granule cell precursors and its loss basically mimics the phenotype seen in the *Kif3a* mutants, but with an even stronger hypofoliation (Spassky et al., 2008). The more severe defects observed in the cerebellar development of conditional Smo mutants advocated that Shh signaling was still active despite the ablation of primary cilia. Construction of a *Kif3a* and *Smo* double conditional mutant resulted in a phenotype closer to the one seen in *Kif3a* and not *Smo,* therefore the authors concluded that *Kif3a* must be epistatic to the Smo receptor (Spassky et al., 2008). This outcome agrees with the phenotype seen in the *SmoM2/Ift88* cko in the results section, where it was obvious that this double mutant resembled the phenotype, such as the reduced size of FoxA2 and Lmx1a expression domains, observed in the *Ift88* cko. Hence, *Ift88* acts downstream Smo receptor.

Studies on the role of Shh signaling in the maintenance of progenitor cells in the telencephalon showed that even though its removal caused only minor defects in patterning, it dramatically affected the number of neural progenitors in the postnatal subventricular zone as well as in the hippocampus (Machold et al., 2003). Further analysis demonstrated that inactivation of Shh signaling led to abnormalities in the dentate gyrus and olfactory bulb but also that stimulation of the pathway in the mature brain reversed the increase in programmed cell death and caused increased proliferation in telencephalic progenitors (Machold et al., 2003). Additionally, *Stumpy* mutants – a protein localized to primary cilia- were shown to have defects in the proliferation and neurogenesis of neuronal precursor (Breunig et al., 2008). The authors showed that lack of cilia in these mutants and the following alteration of Shh signaling led to abnormal hippocampal morphogenesis (Breunig et al., 2008). Furthermore, another study looking into the mechanisms through which embryonic neural progenitors transform into postnatal neural stem cells demonstrated that conditional ablation of ciliary genes such as *Kif3a* or *Smo* resulted in the loss of primary cilia in precursors but subsequently in failure of neurogenesis in the postnatal dentate and in a hypotrophic dentate gyrus (Han et al., 2008). The authors employed the same system we used in our study namely the expression of a constitutively active Smo allele in a try to rescue neurogenesis, in their case, in the *Kif3a* mutant. Double mutants resulting from crossing SmoM2 to the *Kif3a*

mutants were analyzed and expression of SmoM2 allele in a wild type *Kif3a* background, suggesting that cilia were still present and Shh signaling still active, led in hyperplasia of the dentate gyrus. However, expression of SmoM2 allele in *Kif3a* mutant background was shown to be unable to rescue neurogenesis. The hyperplasia of the dentate gyrus photographs the observation done in the *SmoM2 ca* where there was an obvious growth in the embryonic midbrain. Similarly to the Han et al. results, expression of *SmoM2* in *Ift88* cko in the project presented in this thesis did not manage to rescue neurogenesis, in particular the generation of mDA neurons as this was the neuronal population of our interest. Ours but also the results from Han et al. mentioned above using the same model system, direct to the notion that regardless the type of Smo proteins, wild type or mutant, they depend on functional primary cilia to propagate their biological function hence they are epistatic to primary cilia.

10.2 The controversial role of primary cilia in Wnt signaling

Primary cilia, even though so small and -as thought- unimportant for so long, are now considered signalling hubs as they have been involved in the recent years in a variety of signalling cascades. As discussed above, primary cilia or primary cilia-associated proteins are essential for the transduction of Hh signalling as supported by an extensive amount of results using different models and mutants (Eggenschwiler and Anderson, 2007; Goetz and Anderson, 2010). Although the function of primary cilia in Hh signalling is well understood, their exact role in other pathways such as Wnt or Fgf signalling still remains elusive. However, as protein members of not only the Hh signalling but also of Wnt and Fgf signalling have been implicated in the formation of mDA neurons, one can logically hypothesize that primary cilia could possibly mediate effects of Wnt and/or Fgf. It has been shown that induction and expansion of mDA neurons from the floor plate requires Shh (Blaess et al., 2006), and needs FGF8 from the isthmic organizer (Ye et al., 1998). Furthermore, analysis done in FGFR mutants indicated that FGF signalling is crucial for the development of ventral midbrain and regulates neuronal differentiation of the midbrain dopaminergic precursor domain (Lahti et al., 2012). In addition, current literature agrees that besides FGF, Wnt signalling is important for the neurogenesis but also promotes the proliferation of the mDA progenitor pool (Joksimovic et al., 2009, Tang et al., 2009). These findings indicate that Wnt signalling antagonizes Shh and that the interplay between these

two signalling pathways could control the neurogenic potential of structures such as the floor plate (Jokismovic et al., 2009).

In this thesis, analysis of Wnt factors by *in situ* hybridization or real time quantitative PCR revealed a reduced expression. In the ventral midbrain of E10.5 *Ift88* cko embryos Wnt1 domain was still present but clearly the level of expression of decreased as was shown by *in situ* hybridization. The expression of Wnt1, Wnt5a, Wnt7a and Axin2 - a read out for Wnt signaling - at the mRNA level was examined in real time quantitative PCR and all of the factors demonstrated a reduced expression. This finding comes as a surprise, as studies in zebra fish and in cell culture in the current literature report opposite results. Loss or disruption of primary cilia was shown to be accompanied by an increase in canonical Wnt signaling and/or also characterized by disrupted non-canonical Wnt signaling processes (Ross et al., 2005; Simons et al., 2005; Corbit et al., 2008). However, the IFT mutants showing elevated Wnt signalling mentioned in the literature did not demonstrate any defects associated with abnormal activation of Wnt pathway such as axis duplication (Chazaud et al., 2006; Corbit et al., 2008), whereas the *Ift88* cko mutants examined in this thesis showed defects in early patterning that could be associated with reduced canonical Wnt signaling.

As the relationship between primary cilia and Wnt signaling still remains controversial in current literature, it is worth mentioning that other studies suggest a link between Wnt signaling and the basal body of primary cilium. Mice lacking genes associated with the basal body of the primary cilium, such as *Bbs1*, *Bbs4* or *Bbs6* exhibit phenotypes observed in Bardet-Biedl patients such as retinal degeneration and kidney defects, but also display Wnt/PCP mutant phenotypes such as neural tube closure defects (Ross et al., 2005; Eichers et al., 2006). Studies determining genetic interaction between *Bbs* genes and core PCP genes such as *vang-like 2* (*Vangl2*), both in mice and zebra fish, showed that removal of *Bbs1* and *Vangl2* led to significant embryonic lethality and hair bundle defects. These observations were not seen in mice double heterozygous for Bbs1 and Vangl2, indicating that lack of certain basal body proteins is associated with dysfunctional Wnt/PCP signaling (van Amerongen and Nusse, 2009). However, our data regarding Wnt expression and signaling in the midbrain of *Ift88* cko embryos question this finding as the basal bodies are still present and lack of Ift88 leads to the absence of the axoneme. In any case, more investigation needs to be done; examining the same Wnt ligands looked at using RT-PCR with *in situ* hybridization. Moreover, it would also be useful to examine non-canonical Wnt components, e.g. Vangl2, and their expression in the midbrain of *Ift88* cko. More insight into this direction

could give a clearer answer regarding the role of primary cilia in canonical and non-canonical Wnt signalling.

10.3 Midbrain defects in ciliopathies

As the data presented in this thesis show that primary cilia are essential for the appropriate patterning of mDA neurons in the ventral midbrain of the mouse and particularly important for DA neuron progenitor cells at an early stage, it is interesting to know whether midbrain defects have ever been reported in patients of ciliopathies.

Recently, a study looking into neuroimaging findings in patients of Joubert syndrome and related disorders (JSRD) was published and reported a wide spectrum of morphological defects observed which supports the heterogeneity of these disorders. Among the characteristic 'molar tooth sign' and vermis hypoplasia that are usually the hallmarks of JSRD, the patients also exhibited defects in midbrain structures such as failure of the superior cerebellar peduncles to decussate (Poretti et al., 2011). In addition to this report, another publication comparing neuropathologic findings from five JS patients also reported nondecussation of superior cerebellar peduncles and abnormalities in the substantia nigra (Juric-Sekhar et al., 2012). However, it is not stated whether these anomalies observed in the substantia nigra of these patients could be attributed to defective dopaminergic neurogenesis.

Even in mouse models of ciliopathies there has not been a detailed investigation of midbrain defects. Importantly, Gorivodsky et al. had reported already some years ago that loss of function mutation of *Ift172*, which encodes a protein component of the IFTA complex involved in the retrograde transport of protein cargo across the ciliary axoneme, led to defective midbrain-hindbrain boundary due to Fgf8 dysregulation (Gorivodsky et al., 2009). A more recent report studying a mouse mutant for *Tmem67*, which encodes meckelin - a protein that is found to be defective in patients with JS or Meckel syndrome, observed midbrain defects such as occasional midbrain exensephaly and a shorter rostral-caudal midbrain tegmentum axis (Abdelhamed et al., 2013).

Therefore, the data presented in this thesis are the first to investigate and report the role of ciliary protein in the development of mDA neurons. These findings will hopefully also trigger more detailed analyses of patients suffering from ciliopathies, such as JS, in order to see if they display any defects in mDA neurons. At the moment, colleagues have generated mice in which Ift88 is specifically depleted in dopaminergic neurons using DAT-CRE recombinase.

The DAT-CRE; *Ift88* cko mice are being characterized, firstly by investigating the cilia loss and the population of TH-positive neurons at one, three and six months old. It is of great interest to study whether this DAT-specific absence of primary cilia could induce any motor, mild or severe, impairment that could link primary cilia to diseases such as Parkinson's disease.

10.4 Conclusions

The work presented in this thesis addresses the role of primary cilium in the development of mDA neurons. In collaboration with the laboratory of PD Dr. Sandra Blaess in Bonn, we have shown, using two mouse mutants defective in ciliary gene *Ift88* or *Kif3a*, that ablation of primary cilia in the midbrain has direct effects on the Shh activity in the ventral midbrain and to the dopaminergic precursor domains. Even though it has been already known that generation of mDA in the ventral midbrain is dependent upon functional Shh signalling, we are the first to show that primary cilia are required for appropriate patterning of the ventral midbrain. Additionally, conditional activation of *Ift88* under the En1 promoter allowed us to also uncover the timing at which cilia-mediated Shh signalling is most crucial for the induction of DA progenitor cells. Furthermore, our data clearly show that primary cilium acts in an epistatic fashion to Smo in regulating mDA neuron development; hence Smo activity is dependent upon functional primary cilia. Although the relationship between primary cilia and Shh-mediated neurogenesis in the midbrain is now clear, our data regarding the role of primary cilia in Wnt signalling further add to the existing literature controversy. Therefore, future analysis is required to see whether Wnt signalling is dependent upon primary cilia function and whether this relationship could have any effect on the development of mDA neurons. Hopefully, future research on post-mortem tissues of patients suffering from ciliopathies will also add to the current knowledge regarding the role of primary cilia in the development of midbrain neuronal populations. In addition to this, as our work clearly states the relationship between primary cilia and mDA neurons it is of great interest to look into animal models of Parkinson's and see if primary cilia are still present at different time points of the disease and whether they have any effect on disease progression.

The primary cilium is a fascinating tiny organelle and as the last decades have proven there is a lot of uncovered ground to discover regarding its relationship with signalling pathways and its involvement in a broad spectrum of diseases.

11 References

Abdelhamed, Z. A., et al. (2013). "Variable expressivity of ciliopathy neurological phenotypes that encompass Meckel-Gruber syndrome and Joubert syndrome is caused by complex de-regulated ciliogenesis, Shh and Wnt signalling defects." Hum Mol Genet **22**(7): 1358-1372.

Acampora, D., et al. (1995). "Forebrain and midbrain regions are deleted in Otx2-/- mutants due to a defective anterior neuroectoderm specification during gastrulation." Development **121**(10): 3279-3290.

Adams, K. A., et al. (2000). "The transcription factor Lmx1b maintains Wnt1 expression within the isthmic organizer." Development **127**(9): 1857-1867.

Alavian, K. N., et al. (2008). "Transcriptional regulation of mesencephalic dopaminergic neurons: the full circle of life and death." Mov Disord **23**(3): 319-328.

Albrecht-Buehler, G. (1977). "Phagokinetic tracks of 3T3 cells: parallels between the orientation of track segments and of cellular structures which contain actin or tubulin." Cell **12**(2): 333-339.

Alves dos Santos, M. T. and M. P. Smidt. (2011). "En1 and Wnt signaling in midbrain dopaminergic neuronal development." Neural Dev **6:** 23

Andersson, E., et al. (2006). "Identification of intrinsic determinants of midbrain dopamine neurons." Cell **124**(2): 393-405.

Andersson, E. R., et al. (2008). "Wnt5a regulates ventral midbrain morphogenesis and the development of A9-A10 dopaminergic cells in vivo." PLoS One **3**(10): e3517.

Ang, S. L., et al. (1996). "A targeted mouse Otx2 mutation leads to severe defects in gastrulation and formation of axial mesoderm and to deletion of rostral brain." Development **122**(1): 243-252.

Ang, S. L. and J. Rossant (1994). "HNF-3 beta is essential for node and notochord formation in mouse development." Cell **78**(4): 561-574.

Angers, S. and R. T. Moon (2009). "Proximal events in Wnt signal transduction." Nat Rev Mol Cell Biol **10**(7): 468-477.

Backman, C., et al. (1999). "A selective group of dopaminergic neurons express Nurr1 in the adult mouse brain." Brain Res **851**(1-2): 125-132.

Badano, J. L., et al. (2006). "The ciliopathies: an emerging class of human genetic disorders." Annu Rev Genomics Hum Genet **7**: 125-148.

Baek, J. H., et al. (2006). "Persistent and high levels of Hes1 expression regulate boundary formation in the developing central nervous system." Development **133**(13): 2467-2476.

Barrow, J. R., et al. (2007). "Wnt3 signaling in the epiblast is required for proper orientation of the anteroposterior axis." Dev Biol **312**(1): 312-320.

Bayly, R. D., et al. (2012). "A novel role for FOXA2 and SHH in organizing midbrain signaling centers." Dev Biol **369**(1): 32-42.

Benzing, T., et al. (2007). "Wnt signaling in polycystic kidney disease." J Am Soc Nephrol **18**(5): 1389-1398.

Betarbet, R., et al. (2000). "Chronic systemic pesticide exposure reproduces features of Parkinson's disease." Nat Neurosci **3**(12): 1301-1306.

Bjorklund, A. and S. B. Dunnett (2007). "Dopamine neuron systems in the brain: an update." Trends Neurosci **30**(5): 194-202.

Blaess, S., et al. (2011). "Temporal-spatial changes in Sonic Hedgehog expression and signaling reveal different potentials of ventral mesencephalic progenitors to populate distinct ventral midbrain nuclei." Neural Dev **6**: 29.

Blaess, S., et al. (2006). "Sonic hedgehog regulates Gli activator and repressor functions with spatial and temporal precision in the mid/hindbrain region." Development **133**(9): 1799-1809.

Bonilla, S., et al. (2008). "Identification of midbrain floor plate radial glia-like cells as dopaminergic progenitors." Glia **56**(8): 809-820.

Brancati, F., et al. (2009). "MKS3/TMEM67 mutations are a major cause of COACH Syndrome, a Joubert Syndrome related disorder with liver involvement." Hum Mutat **30**(2): E432-442.

Breunig, J. J., et al. (2008). "Primary cilia regulate hippocampal neurogenesis by mediating sonic hedgehog signaling." Proc Natl Acad Sci U S A **105**(35): 13127-13132.

Briscoe, J. and J. Ericson (2001). "Specification of neuronal fates in the ventral neural tube." Curr Opin Neurobiol **11**(1): 43-49.

Brodski, C., et al. (2003). "Location and size of dopaminergic and serotonergic cell populations are controlled by the position of the midbrain-hindbrain organizer." J Neurosci **23**(10): 4199-4207.

Cajanek, L., et al. (2013). "Tiam1 regulates the Wnt/Dvl/Rac1 signaling pathway and the differentiation of midbrain dopaminergic neurons." Mol Cell Biol **33**(1): 59-70.

Caspary, T., et al. (2007). "The graded response to Sonic Hedgehog depends on cilia architecture." Dev Cell **12**(5): 767-778.

Castelo-Branco, G., et al. (2010). "Delayed dopaminergic neuron differentiation in Lrp6 mutant mice." Dev Dyn **239**(1): 211-221.

Castelo-Branco, G., et al. (2004). "GSK-3beta inhibition/beta-catenin stabilization in ventral midbrain precursors increases differentiation into dopamine neurons." J Cell Sci **117**(Pt 24): 5731-5737.

Castelo-Branco, G., et al. (2006). "Ventral midbrain glia express region-specific transcription factors and regulate dopaminergic neurogenesis through Wnt-5a secretion." Mol Cell Neurosci **31**(2): 251-262.

Castelo-Branco, G., et al. (2003). "Differential regulation of midbrain dopaminergic neuron development by Wnt-1, Wnt-3a, and Wnt-5a." Proc Natl Acad Sci U S A **100**(22): 12747-12752.

Chazaud, C. and J. Rossant (2006). "Disruption of early proximodistal patterning and AVE formation in Apc mutants." Development **133**(17): 3379-3387.

Chi, C. L., et al. (2003). "The isthmic organizer signal FGF8 is required for cell survival in the prospective midbrain and cerebellum." Development **130**(12): 2633-2644.

Chiang, C., et al. (1996). "Cyclopia and defective axial patterning in mice lacking Sonic hedgehog gene function." Nature **383**(6599): 407-413.

Chilov, D., et al. (2010). "beta-Catenin regulates intercellular signalling networks and cell-type specific transcription in the developing mouse midbrain-rhombomere 1 region." PLoS One **5**(6): e10881.

Chizhikov, V. V., et al. (2007). "Cilia proteins control cerebellar morphogenesis by promoting expansion of the granule progenitor pool." J Neurosci **27**(36): 9780-9789.

Chung, S., et al. (2009). "Wnt1-lmx1a forms a novel autoregulatory loop and controls midbrain dopaminergic differentiation synergistically with the SHH-FoxA2 pathway." Cell Stem Cell **5**(6): 646-658.

Cooper, O., et al. (2010). "Differentiation of human ES and Parkinson's disease iPS cells into ventral midbrain dopaminergic neurons requires a high activity form of SHH, FGF8a and specific regionalization by retinoic acid." Mol Cell Neurosci **45**(3): 258-266.

Corbit, K. C., et al. (2008). "Kif3a constrains beta-catenin-dependent Wnt signalling through dual ciliary and non-ciliary mechanisms." Nat Cell Biol **10**(1): 70-76.

Corrales, J. D., et al. (2006). "The level of sonic hedgehog signaling regulates the complexity of cerebellar foliation." Development **133**(9): 1811-1821.

Corrales, J. D., et al. (2004). "Spatial pattern of sonic hedgehog signaling through Gli genes during cerebellum development." Development **131**(22): 5581-5590.

Crossley, P. H. and G. R. Martin (1995). "The mouse Fgf8 gene encodes a family of polypeptides and is expressed in regions that direct outgrowth and patterning in the developing embryo." Development **121**(2): 439-451.

Crossley, P. H., et al. (1996). "Midbrain development induced by FGF8 in the chick embryo." Nature **380**(6569): 66-68.

Curtin, J. A., et al. (2003). "Mutation of Celsr1 disrupts planar polarity of inner ear hair cells and causes severe neural tube defects in the mouse." Curr Biol **13**(13): 1129-1133.

Dahlstrom, A. and K. Fuxe (1964). "Localization of monoamines in the lower brain stem." Experientia **20**(7): 398-399.

Danielian, P. S. and A. P. McMahon (1996). "Engrailed-1 as a target of the Wnt-1 signalling pathway in vertebrate midbrain development." Nature **383**(6598): 332-334.

Danilov, A. I., et al. (2009). "Ultrastructural and antigenic properties of neural stem cells and their progeny in adult rat subventricular zone." Glia **57**(2): 136-152.

Davenport, J. R. and B. K. Yoder (2005). "An incredible decade for the primary cilium: a look at a once-forgotten organelle." Am J Physiol Renal Physiol **289**(6): F1159-1169.

Davis, C. A. and A. L. Joyner (1988). "Expression patterns of the homeo box-containing genes En-1 and En-2 and the proto-oncogene int-1 diverge during mouse development." Genes Dev **2**(12B): 1736-1744.

Davis, E. E., et al. (2006). "The emerging complexity of the vertebrate cilium: new functional roles for an ancient organelle." Dev Cell **11**(1): 9-19.

Dessaud, E., et al. (2008). "Pattern formation in the vertebrate neural tube: a sonic hedgehog morphogen-regulated transcriptional network." Development **135**(15): 2489-2503.

Echelard, Y., et al. (1993). "Sonic hedgehog, a member of a family of putative signaling molecules, is implicated in the regulation of CNS polarity." Cell **75**(7): 1417-1430.

Eggenschwiler, J. T. and K. V. Anderson (2007). "Cilia and developmental signaling." Annu Rev Cell Dev Biol **23**: 345-373.

Eichers, E. R., et al. (2006). "Phenotypic characterization of Bbs4 null mice reveals age-dependent penetrance and variable expressivity." Hum Genet **120**(2): 211-226.

Essner, J. J., et al. (2005). "Kupffer's vesicle is a ciliated organ of asymmetry in the zebrafish embryo that initiates left-right development of the brain, heart and gut." Development **132**(6): 1247-1260.

Essner, J. J., et al. (2002). "Conserved function for embryonic nodal cilia." Nature **418**(6893): 37-38.

Ferri, A. L., et al. (2007). "Foxa1 and Foxa2 regulate multiple phases of midbrain dopaminergic neuron development in a dosage-dependent manner." Development **134**(15): 2761-2769.

Follit, J. A., et al. (2006). "The intraflagellar transport protein IFT20 is associated with the Golgi complex and is required for cilia assembly." Mol Biol Cell **17**(9): 3781-3792.

Follit, J. A., et al. (2009). "Characterization of mouse IFT complex B." Cell Motil Cytoskeleton **66**(8): 457-468.

Gale, E. and M. Li (2008). "Midbrain dopaminergic neuron fate specification: Of mice and embryonic stem cells." Mol Brain **1**: 8.

Garcia-Gonzalo, F. R., et al. (2011). "A transition zone complex regulates mammalian ciliogenesis and ciliary membrane composition." Nat Genet **43**(8): 776-784.

Gerdes, J. M., et al. (2009). "The vertebrate primary cilium in development, homeostasis, and disease." Cell **137**(1): 32-45.

Gerdes, J. M., et al. (2007). "Disruption of the basal body compromises proteasomal function and perturbs intracellular Wnt response." Nat Genet **39**(11): 1350-1360.

German, D. C., et al. (1983). "Three-dimensional computer reconstruction of midbrain dopaminergic neuronal populations: from mouse to man." J Neural Transm **57**(4): 243-254.

Gill, P. S. and N. D. Rosenblum (2006). "Control of murine kidney development by sonic hedgehog and its GLI effectors." Cell Cycle **5**(13): 1426-1430.

Goetz, S. C. and K. V. Anderson (2010). "The primary cilium: a signalling centre during vertebrate development." Nat Rev Genet **11**(5): 331-344.

Gorivodsky, M., et al. (2009). "Intraflagellar transport protein 172 is essential for primary cilia formation and plays a vital role in patterning the mammalian brain." Dev Biol **325**(1): 24-32.

Gray, R. S., et al. (2009). "The planar cell polarity effector Fuz is essential for targeted membrane trafficking, ciliogenesis and mouse embryonic development." Nat Cell Biol **11**(10): 1225-1232.

Greene, N. D., et al. (1998). "Abnormalities of floor plate, notochord and somite differentiation in the loop-tail (Lp) mouse: a model of severe neural tube defects." Mech Dev **73**(1): 59-72.

Hammond, R., et al. (2009). "Sonic hedgehog is a chemoattractant for midbrain dopaminergic axons." PLoS One **4**(9): e7007.

Han, Y. G., et al. (2008). "Hedgehog signaling and primary cilia are required for the formation of adult neural stem cells." Nat Neurosci **11**(3): 277-284.

Harland, R. (2000). "Neural induction." Curr Opin Genet Dev **10**(4): 357-362.

Haycraft, C. J., et al. (2007). "Intraflagellar transport is essential for endochondral bone formation." Development **134**(2): 307-316.

Hayes, L., et al. (2013). "Duration of Shh signaling contributes to mDA neuron diversity." Dev Biol **374**(1): 115-126.

Hebsgaard, J. B., et al. (2009). "Dopamine neuron precursors within the developing human mesencephalon show radial glial characteristics." Glia **57**(15): 1648-1658.

Hegarty, S. V., et al. (2013). "Midbrain dopaminergic neurons: a review of the molecular circuitry that regulates their development". Dev Biol **379** (2): 123-138

Hemmati-Brivanlou, A. and D. Melton (1997). "Vertebrate neural induction." Annu Rev Neurosci **20**: 43-60.

Heydeck, W., et al. (2009). "Planar cell polarity effector gene Fuzzy regulates cilia formation and Hedgehog signal transduction in mouse." Dev Dyn **238**(12): 3035-3042.

Hu, M. C., et al. (2006). "GLI3-dependent transcriptional repression of Gli1, Gli2 and kidney patterning genes disrupts renal morphogenesis." Development **133**(3): 569-578.

Huang, P. and A. F. Schier (2009). "Dampened Hedgehog signaling but normal Wnt signaling in zebrafish without cilia." Development **136**(18): 3089-3098.

Huangfu, D. and K. V. Anderson (2005). "Cilia and Hedgehog responsiveness in the mouse." Proc Natl Acad Sci U S A **102**(32): 11325-11330.

Huangfu, D., et al. (2003). "Hedgehog signalling in the mouse requires intraflagellar transport proteins." Nature **426**(6962): 83-87.

Hui, C. C. and S. Angers (2011). "Gli proteins in development and disease." Annu Rev Cell Dev Biol **27**: 513-537.

Hwang, D. Y., et al. (2003). "Selective loss of dopaminergic neurons in the substantia nigra of Pitx3-deficient aphakia mice." Brain Res Mol Brain Res **114**(2): 123-131.

Hwang, D. Y., et al. (2009). "Vesicular monoamine transporter 2 and dopamine transporter are molecular targets of Pitx3 in the ventral midbrain dopamine neurons." J Neurochem **111**(5): 1202-1212.

Hynes, M., et al. (1995). "Induction of midbrain dopaminergic neurons by Sonic hedgehog." Neuron **15**(1): 35-44.

Hynes, M., et al. (1995). "Control of neuronal diversity by the floor plate: contact-mediated induction of midbrain dopaminergic neurons." Cell **80**(1): 95-101.

Jacobs, F. M., et al. (2009). "Identification of Dlk1, Ptpru and Klhl1 as novel Nurr1 target genes in meso-diencephalic dopamine neurons." Development **136**(14): 2363-2373.

Jacobs, F. M., et al. (2009). "Pitx3 potentiates Nurr1 in dopamine neuron terminal differentiation through release of SMRT-mediated repression." Development **136**(4): 531-540.

Jessell, T. M. (2000). "Neuronal specification in the spinal cord: inductive signals and transcriptional codes." Nat Rev Genet **1**(1): 20-29.

Joksimovic, M., et al. (2009). "Spatiotemporally separable Shh domains in the midbrain define distinct dopaminergic progenitor pools." Proc Natl Acad Sci U S A **106**(45): 19185-19190.

Joksimovic, M., et al. (2009). "Wnt antagonism of Shh facilitates midbrain floor plate neurogenesis." Nat Neurosci **12**(2): 125-131.

Jones, C., et al. (2008). "Ciliary proteins link basal body polarization to planar cell polarity regulation." Nat Genet **40**(1): 69-77.

Joyner, A. L., et al. (2000). "Otx2, Gbx2 and Fgf8 interact to position and maintain a mid-hindbrain organizer." Curr Opin Cell Biol **12**(6): 736-741.

Juric-Sekhar, G., et al. (2012). "Joubert syndrome: brain and spinal cord malformations in genotyped cases and implications for neurodevelopmental functions of primary cilia." Acta Neuropathol **123**(5): 695-709.

Kameda, Y., et al. (2011). "Hes1 regulates the number and anterior-posterior patterning of mesencephalic dopaminergic neurons at the mid/hindbrain boundary (isthmus)." Dev Biol **358**(1): 91-101.

Kang, W. Y., et al. (2010). "Migratory defect of mesencephalic dopaminergic neurons in developing reeler mice." Anat Cell Biol **43**(3): 241-251.

Keady, B. T., et al. (2012). "IFT25 links the signal-dependent movement of Hedgehog components to intraflagellar transport." Dev Cell **22**(5): 940-951.

Kele, J., et al. (2006). "Neurogenin 2 is required for the development of ventral midbrain dopaminergic neurons." Development **133**(3): 495-505.

Tucker, K. L. and Caspary T. (2013) Cilia and nervous system development and function. Springer

Kim, H. J. (2011). "Stem cell potential in Parkinson's disease and molecular factors for the generation of dopamine neurons." Biochim Biophys Acta **1812**(1): 1-11.

Kim, H. J., et al. (2007). "Control of neurogenesis and tyrosine hydroxylase expression in neural progenitor cells through bHLH proteins and Nurr1." Exp Neurol **203**(2): 394-405.

Kimmel, R. A., et al. (2000). "Two lineage boundaries coordinate vertebrate apical ectodermal ridge formation." Genes Dev **14**(11): 1377-1389.

Kitagawa, H., et al. (2007). "A regulatory circuit mediating convergence between Nurr1 transcriptional regulation and Wnt signaling." Mol Cell Biol **27**(21): 7486-7496.

Klinghoffer, R. A., et al. (2002). "An allelic series at the PDGFalphaR locus indicates unequal contributions of distinct signaling pathways during development." Dev Cell **2**(1): 103-113.

Korotkova, T. M., et al. (2005). "Differential expression of the homeobox gene Pitx3 in midbrain dopaminergic neurons." Eur J Neurosci **22**(6): 1287-1293.

Krauss, S., et al. (1993). "A functionally conserved homolog of the Drosophila segment polarity gene hh is expressed in tissues with polarizing activity in zebrafish embryos." Cell **75**(7): 1431-1444.

Kriegstein, A. and A. Alvarez-Buylla (2009). "The glial nature of embryonic and adult neural stem cells." Annu Rev Neurosci **32**: 149-184.

Lahti, L., et al. (2012). "Cell-autonomous FGF signaling regulates anteroposterior patterning and neuronal differentiation in the mesodiencephalic dopaminergic progenitor domain." Development **139**(5): 894-905.

Lancaster, M. A., et al. (2009). "Impaired Wnt-beta-catenin signaling disrupts adult renal homeostasis and leads to cystic kidney ciliopathy." Nat Med **15**(9): 1046-1054.

Lancaster, M. A., et al. (2011). "Subcellular spatial regulation of canonical Wnt signalling at the primary cilium." Nat Cell Biol **13**(6): 700-707.

Law, S. W., et al. (1992). "Identification of a new brain-specific transcription factor, NURR1." Mol Endocrinol **6**(12): 2129-2135.

Lee, J. E., et al. (2012). "CEP41 is mutated in Joubert syndrome and is required for tubulin glutamylation at the cilium." Nat Genet **44**(2): 193-199.

Lees, A. J., et al. (2009). "Parkinson's disease." Lancet **373**(9680): 2055-2066.

Lewis, P. M., et al. (2004). "Sonic hedgehog signaling is required for expansion of granule neuron precursors and patterning of the mouse cerebellum." Dev Biol **270**(2): 393-410.

Le Pen, G., et al. (2008). "Progressive loss of dopaminergic neurons in the ventral midbrain of adult mice heterozygote for Engrailed1: a new genetic model for Parkinson's disease?" Parkinsonism Relat Disord **14** Suppl 2: S107-11.

Liem, K. F., Jr., et al. (2012). "The IFT-A complex regulates Shh signaling through cilia structure and membrane protein trafficking." J Cell Biol **197**(6): 789-800.

Lin, F., et al. (2003). "Kidney-specific inactivation of the KIF3A subunit of kinesin-II inhibits renal ciliogenesis and produces polycystic kidney disease." Proc Natl Acad Sci U S A **100**(9): 5286-5291.

Lin, W., et al. (2009). "Foxa1 and Foxa2 function both upstream of and cooperatively with Lmx1a and Lmx1b in a feedforward loop promoting mesodiencephalic dopaminergic neuron development." Dev Biol **333**(2): 386-396.

Liu, A. and A. L. Joyner (2001). "EN and GBX2 play essential roles downstream of FGF8 in patterning the mouse mid/hindbrain region." Development **128**(2): 181-191.

Liu, A. and L. A. Niswander (2005). "Bone morphogenetic protein signalling and vertebrate nervous system development." Nat Rev Neurosci **6**(12): 945-954.

Liu, A., et al. (2005). "Mouse intraflagellar transport proteins regulate both the activator and repressor functions of Gli transcription factors." Development **132**(13): 3103-3111.

Louie, C. M. and J. G. Gleeson (2005). "Genetic basis of Joubert syndrome and related disorders of cerebellar development." Hum Mol Genet **14 Spec No. 2**: R235-242.

Lu, W., et al. (1997). "Perinatal lethality with kidney and pancreas defects in mice with a targetted Pkd1 mutation." Nat Genet **17**(2): 179-181.

Machold, R., et al. (2003). "Sonic hedgehog is required for progenitor cell maintenance in telencephalic stem cell niches." Neuron **39**(6): 937-950.

Marchand, R. and L. J. Poirier (1983). "Isthmic origin of neurons of the rat substantia nigra." Neuroscience **9**(2): 373-381.

Marin, F., et al. (2005). "Ontogeny of tyrosine hydroxylase mRNA expression in mid- and forebrain: neuromeric pattern and novel positive regions." Dev Dyn **234** (3): 709-17

Marszalek, J. R., et al. (2000). "Genetic evidence for selective transport of opsin and arrestin by kinesin-II in mammalian photoreceptors." Cell **102**(2): 175-187.

Martinez-Barbera, J. P., et al. (2001). "Regionalisation of anterior neuroectoderm and its competence in responding to forebrain and midbrain inducing activities depend on mutual antagonism between OTX2 and GBX2." Development **128**(23): 4789-4800.

Martinez, S. (2001). "The isthmic organizer and brain regionalization." Int J Dev Biol **45**(1): 367-371.

Mavromatakis, Y. E., et al. (2011). "Foxa1 and Foxa2 positively and negatively regulate Shh signalling to specify ventral midbrain progenitor identity." Mech Dev **128**(1-2): 90-103.

Maxwell, S. L., et al. (2005). "Pitx3 regulates tyrosine hydroxylase expression in the substantia nigra and identifies a subgroup of mesencephalic dopaminergic progenitor neurons during mouse development." Dev Biol **282**(2): 467-479.

McGrath, J., et al. (2003). "Two populations of node monocilia initiate left-right asymmetry in the mouse." Cell **114**(1): 61-73.

McMahon, A. P. and A. Bradley (1990). "The Wnt-1 (int-1) proto-oncogene is required for development of a large region of the mouse brain." Cell **62**(6): 1073-1085.

McMahon, A. P., et al. (1992). "The midbrain-hindbrain phenotype of Wnt-1-/Wnt-1- mice results from stepwise deletion of engrailed-expressing cells by 9.5 days postcoitum." Cell **69**(4): 581-595.

McNaught, K. S., et al. (2004). "Systemic exposure to proteasome inhibitors causes a progressive model of Parkinson's disease." Ann Neurol **56**(1): 149-162.

Meyer-Lindenberg, A., et al. (2002). "Reduced prefrontal activity predicts exaggerated striatal dopaminergic function in schizophrenia." Nat Neurosci **5**(3): 267-271.

Montcouquiol, M., et al. (2003). "Identification of Vangl2 and Scrb1 as planar polarity genes in mammals." Nature **423**(6936): 173-177.

Morizane, A., et al. (2008). "From bench to bed: the potential of stem cells for the treatment of Parkinson's disease." Cell Tissue Res **331**(1): 323-336.

Nakatani, T., et al. (2010). "Lmx1a and Lmx1b cooperate with Foxa2 to coordinate the specification of dopaminergic neurons and control of floor plate cell differentiation in the developing mesencephalon." Dev Biol **339**(1): 101-113.

Nonaka, S., et al. (1998). "Randomization of left-right asymmetry due to loss of nodal cilia generating leftward flow of extraembryonic fluid in mice lacking KIF3B motor protein." Cell **95**(6): 829-837.

Novarino, G., et al. (2011). "Modeling human disease in humans: the ciliopathies." Cell **147**(1): 70-79.

Nunes, I., et al. (2003). "Pitx3 is required for development of substantia nigra dopaminergic neurons." Proc Natl Acad Sci U S A **100**(7): 4245-4250.

Ocbina, P. J. and K. V. Anderson (2008). "Intraflagellar transport, cilia, and mammalian Hedgehog signaling: analysis in mouse embryonic fibroblasts." Dev Dyn **237**(8): 2030-2038.

Ocbina, P. J., et al. (2009). "Primary cilia are not required for normal canonical Wnt signaling in the mouse embryo." PLoS One **4**(8): e6839.

Olanow, C. W. and W. G. Tatton (1999). "Etiology and pathogenesis of Parkinson's disease." Annu Rev Neurosci **22**: 123-144.

Omodei, D., et al. (2008). "Anterior-posterior graded response to Otx2 controls proliferation and differentiation of dopaminergic progenitors in the ventral mesencephalon." Development **135**(20): 3459-3470.

Ono, Y., et al. (2010). "The basic helix-loop-helix transcription factor Nato3 controls neurogenic activity in mesencephalic floor plate cells." Development **137**(11): 1897-1906.

Ono, Y., et al. (2007). "Differences in neurogenic potential in floor plate cells along an anteroposterior location: midbrain dopaminergic neurons originate from mesencephalic floor plate cells." Development **134**(17): 3213-3225.

Otto, E. A., et al. (2003). "Mutations in INVS encoding inversin cause nephronophthisis type 2, linking renal cystic disease to the function of primary cilia and left-right axis determination." Nat Genet **34**(4): 413-420.

Pakkenberg, B., et al. (1991). "The absolute number of nerve cells in substantia nigra in normal subjects and in patients with Parkinson's disease estimated with an unbiased stereological method." J Neurol Neurosurg Psychiatry **54**(1): 30-33.

Pan, J. and W. Snell (2007). "The primary cilium: keeper of the key to cell division." Cell **129**(7): 1255-1257.

Pang, Z. P., et al. (2011). "Induction of human neuronal cells by defined transcription factors." Nature **476**(7359): 220-223.

Panhuysen, M., et al. (2004). "Effects of Wnt1 signaling on proliferation in the developing mid-/hindbrain region." Mol Cell Neurosci **26**(1): 101-111.

Pankratz, N., et al. (2009). "Alpha-synuclein and familial Parkinson's disease." Mov Disord **24**(8): 1125-1131.

Park, H. L., et al. (2000). "Mouse Gli1 mutants are viable but have defects in SHH signaling in combination with a Gli2 mutation." Development **127**(8): 1593-1605.

Park, T. J., et al. (2006). "Ciliogenesis defects in embryos lacking inturned or fuzzy function are associated with failure of planar cell polarity and Hedgehog signaling." Nat Genet **38**(3): 303-311.

Park, T. J., et al. (2008). "Dishevelled controls apical docking and planar polarization of basal bodies in ciliated epithelial cells." Nat Genet **40**(7): 871-879.

Pedersen, L. B. and J. L. Rosenbaum (2008). "Intraflagellar transport (IFT) role in ciliary assembly, resorption and signalling." Curr Top Dev Biol **85**: 23-61.

Peng, C., et al. (2011). "Pitx3 is a critical mediator of GDNF-induced BDNF expression in nigrostriatal dopaminergic neurons." J Neurosci **31**(36): 12802-12815.

Phillips, C. L., et al. (2004). "Renal cysts of inv/inv mice resemble early infantile nephronophthisis." J Am Soc Nephrol **15**(7): 1744-1755.

Pinson, K. I., et al. (2000). "An LDL-receptor-related protein mediates Wnt signalling in mice." Nature **407**(6803): 535-538.

Piontek, K., et al. (2007). "A critical developmental switch defines the kinetics of kidney cyst formation after loss of Pkd1." Nat Med **13**(12): 1490-1495.

Placzek, M. and J. Briscoe (2005). "The floor plate: multiple cells, multiple signals." Nat Rev Neurosci **6**(3): 230-240.

Poretti, A., et al. (2011). "Joubert syndrome and related disorders: spectrum of neuroimaging findings in 75 patients." AJNR Am J Neuroradiol **32**(8): 1459-1463.

Prakash, N., et al. (2009). "Nkx6-1 controls the identity and fate of red nucleus and oculomotor neurons in the mouse midbrain." Development **136**(15): 2545-2555.

Prakash, N. and W. Wurst (2006). "Development of dopaminergic neurons in the mammalian brain." Cell Mol Life Sci **63**(2): 187-206.

Puelles, L. (2001). "Brain segmentation and forebrain development in amniotes." Brain Res Bull **55**(6): 695-710.

Pugacheva, E. N., et al. (2007). "HEF1-dependent Aurora A activation induces disassembly of the primary cilium." Cell **129**(7): 1351-1363.

Rawal, N., et al. (2006). "Dynamic temporal and cell type-specific expression of Wnt signaling components in the developing midbrain." Exp Cell Res **312**(9): 1626-1636.

Rhinn, M. and M. Brand (2001). "The midbrain--hindbrain boundary organizer." Curr Opin Neurobiol **11**(1): 34-42.

Robinson, T. E. and K. C. Berridge (1993). "The neural basis of drug craving: an incentive-sensitization theory of addiction." Brain Res Brain Res Rev **18**(3): 247-291.

Roelink, H., et al. (1994). "Floor plate and motor neuron induction by vhh-1, a vertebrate homolog of hedgehog expressed by the notochord." Cell **76**(4): 761-775.

Roelink, H., et al. (1995). "Floor plate and motor neuron induction by different concentrations of the amino-terminal cleavage product of sonic hedgehog autoproteolysis." Cell **81**(3): 445-455.

Ross, A. J., et al. (2005). "Disruption of Bardet-Biedl syndrome ciliary proteins perturbs planar cell polarity in vertebrates." Nat Genet **37**(10): 1135-1140.

Saadi-Kheddouci, S., et al. (2001). "Early development of polycystic kidney disease in transgenic mice expressing an activated mutant of the beta-catenin gene." Oncogene **20**(42): 5972-5981.

Sakurada, K., et al. (1999). "Nurr1, an orphan nuclear receptor, is a transcriptional activator of endogenous tyrosine hydroxylase in neural progenitor cells derived from the adult brain." Development **126**(18): 4017-4026.

Sasaki, H. and B. L. Hogan (1994). "HNF-3 beta as a regulator of floor plate development." Cell **76**(1): 103-115.

Sattar, S. and J. G. Gleeson (2011). "The ciliopathies in neuronal development: a clinical approach to investigation of Joubert syndrome and Joubert syndrome-related disorders." Dev Med Child Neurol **53**(9): 793-798.

Schneider, L., et al. (2010). "Directional cell migration and chemotaxis in wound healing response to PDGF-AA are coordinated by the primary cilium in fibroblasts." Cell Physiol Biochem **25**(2-3): 279-292.

Schneider, L., et al. (2005). "PDGFRalphaalpha signaling is regulated through the primary cilium in fibroblasts." Curr Biol **15**(20): 1861-1866.

Scholey, J. M. (1996). "Kinesin-II, a membrane traffic motor in axons, axonemes, and spindles." J Cell Biol **133**(1): 1-4.

Scholey, J. M. (2003). "Intraflagellar transport." Annu Rev Cell Dev Biol **19**: 423-443.

Schwarz, M., et al. (1997). "Conserved biological function between Pax-2 and Pax-5 in midbrain and cerebellum development: evidence from targeted mutations." Proc Natl Acad Sci U S A **94**(26): 14518-14523.

Simon, H., et al. (1995). "Independent assignment of antero-posterior and dorso-ventral positional values in the developing chick hindbrain." Curr Biol **5**(2): 205-214.

Simon, H. H., et al. (2001). "Fate of midbrain dopaminergic neurons controlled by the engrailed genes." J Neurosci **21**(9): 3126-3134.

Simons, M., et al. (2005). "Inversin, the gene product mutated in nephronophthisis type II, functions as a molecular switch between Wnt signaling pathways." Nat Genet **37**(5): 537-543.

Simons, M. and M. Mlodzik (2008). "Planar cell polarity signaling: from fly development to human disease." Annu Rev Genet **42**: 517-540.

Smidt, M. P., et al. (2000). "A second independent pathway for development of mesencephalic dopaminergic neurons requires Lmx1b." Nat Neurosci **3**(4): 337-341.

Smidt, M. P., et al. (2004). "Early developmental failure of substantia nigra dopamine neurons in mice lacking the homeodomain gene Pitx3." Development **131**(5): 1145-1155.

Smidt, M. P., et al. (1997). "A homeodomain gene Ptx3 has highly restricted brain expression in mesencephalic dopaminergic neurons." Proc Natl Acad Sci U S A **94**(24): 13305-13310.

Soriano, P. (1997). "The PDGF alpha receptor is required for neural crest cell development and for normal patterning of the somites." Development **124**(14): 2691-2700.

Sousa, K. M., et al. (2010). "Wnt2 regulates progenitor proliferation in the developing ventral midbrain." J Biol Chem **285**(10): 7246-7253.

Spassky, N., et al. (2008). "Primary cilia are required for cerebellar development and Shh-dependent expansion of progenitor pool." Dev Biol **317**(1): 246-259.

Spektor, A., et al. (2007). "Cep97 and CP110 suppress a cilia assembly program." Cell **130**(4): 678-690.

Stottmann, R. W., et al. (2009). "Ttc21b is required to restrict sonic hedgehog activity in the developing mouse forebrain." Dev Biol **335**(1): 166-178.

Stuebner, S., et al. (2010). "Fzd3 and Fzd6 deficiency results in a severe midbrain morphogenesis defect." Dev Dyn **239**(1): 246-260.

Tang, M., et al. (2013). "Temporal and spatial requirements of Smoothened in ventral midbrain neuronal development." Neural Dev **8**: 8.

Tang, M., et al. (2009). "Multiple roles of beta-catenin in controlling the neurogenic niche for midbrain dopamine neurons." Development **136**(12): 2027-2038.

Tang, M., et al. (2010). "Interactions of Wnt/beta-catenin signaling and sonic hedgehog regulate the neurogenesis of ventral midbrain dopamine neurons." J Neurosci **30**(27): 9280-9291.

Tasouri, E. and K. L. Tucker (2011). "Primary cilia and organogenesis: is Hedgehog the only sculptor?" Cell Tissue Res **345**(1): 21-40.

Tissir, F. and A. M. Goffinet (2010). "Planar cell polarity signaling in neural development." Curr Opin Neurobiol **20**(5): 572-577.

Toulouse, A. and A. M. Sullivan (2008). "Progress in Parkinson's disease-where do we stand?" Prog Neurobiol **85**(4): 376-392.

Tzschentke, T. M. and W. J. Schmidt (2000). "Functional relationship among medial prefrontal cortex, nucleus accumbens, and ventral tegmental area in locomotion and reward." Crit Rev Neurobiol **14**(2): 131-142.

Urbanek, P., et al. (1997). "Cooperation of Pax2 and Pax5 in midbrain and cerebellum development." Proc Natl Acad Sci U S A **94**(11): 5703-5708.

Vallstedt, A., et al. (2001). "Different levels of repressor activity assign redundant and specific roles to Nkx6 genes in motor neuron and interneuron specification." Neuron **31**(5): 743-755.

van Amerongen, R. and R. Nusse (2009). "Towards an integrated view of Wnt signaling in development." Development **136**(19): 3205-3214.

Vernay, B., et al. (2005). "Otx2 regulates subtype specification and neurogenesis in the midbrain." J Neurosci **25**(19): 4856-4867.

Vierkotten, J., et al. (2007). "Ftm is a novel basal body protein of cilia involved in Shh signalling." Development **134**(14): 2569-2577.

Volpicelli, F., et al. (2007). "Bdnf gene is a downstream target of Nurr1 transcription factor in rat midbrain neurons in vitro." J Neurochem **102**(2): 441-453.

Wallen, A. and T. Perlmann (2003). "Transcriptional control of dopamine neuron development." Ann N Y Acad Sci **991**: 48-60.

Wallen, A., et al. (1999). "Fate of mesencephalic AHD2-expressing dopamine progenitor cells in NURR1 mutant mice." Exp Cell Res **253**(2): 737-746.

Wang, J., et al. (2005). "Regulation of polarized extension and planar cell polarity in the cochlea by the vertebrate PCP pathway." Nat Genet **37**(9): 980-985.

Wang, Y., et al. (2006). "The role of Frizzled3 and Frizzled6 in neural tube closure and in the planar polarity of inner-ear sensory hair cells." J Neurosci **26**(8): 2147-2156.

Watanabe, D., et al. (2003). "The left-right determinant Inversin is a component of node monocilia and other 9+0 cilia." Development **130**(9): 1725-1734.

Wiens, C. J., et al. (2010). "Bardet-Biedl syndrome-associated small GTPase ARL6 (BBS3) functions at or near the ciliary gate and modulates Wnt signaling." J Biol Chem **285**(21): 16218-16230.

Wilkinson, D. G., et al. (1987). "Expression of the proto-oncogene int-1 is restricted to specific neural cells in the developing mouse embryo." Cell **50**(1): 79-88.

Willaredt, M. A., et al. (2008). "A crucial role for primary cilia in cortical morphogenesis." J Neurosci **28**(48): 12887-12900.

Wurst, W. and L. Bally-Cuif (2001). "Neural plate patterning: upstream and downstream of the isthmic organizer." Nat Rev Neurosci **2**(2): 99-108.

Yan, C. H., et al. (2011). "Lmx1a and lmx1b function cooperatively to regulate proliferation, specification, and differentiation of midbrain dopaminergic progenitors." J Neurosci **31**(35): 12413-12425.

Ye, W., et al. (2001). "Distinct regulators control the expression of the mid-hindbrain organizer signal FGF8." Nat Neurosci **4**(12): 1175-1181.

Ye, W., et al. (1998). "FGF and Shh signals control dopaminergic and serotonergic cell fate in the anterior neural plate." Cell **93**(5): 755-766.

Yu, J., et al. (2002). "Sonic hedgehog regulates proliferation and differentiation of mesenchymal cells in the mouse metanephric kidney." Development **129**(22): 5301-5312.

Zetterstrom, R. H., et al. (1996). "Cellular expression of the immediate early transcription factors Nurr1 and NGFI-B suggests a gene regulatory role in several brain regions including the nigrostriatal dopamine system." Brain Res Mol Brain Res **41**(1-2): 111-120.

Zhang, X. M., et al. (2001). "Smoothened mutants reveal redundant roles for Shh and Ihh signaling including regulation of L/R symmetry by the mouse node." Cell **106**(2): 781-792.

Zou, H. L., et al. (2009). "Expression of the LIM-homeodomain gene Lmx1a in the postnatal mouse central nervous system." Brain Res Bull **78**(6): 306-312.

Eidesstattliche Erklärung

Hiermit erkläre ich an Eides statt, dass ich die vorliegende Dissertation selbstständig und ohne unerlaubte Hilfsmittel durchgeführt habe.

Heidelberg, den _____

Evangelia Tasouri